

Accelerated Evaluation of Automated Vehicles

by

Ding Zhao

A dissertation submitted in partial fulfillment
of the requirements for the degree of
Doctor of Philosophy
(Mechanical Engineering)
in The University of Michigan
2016

Doctoral Committee:

Professor Huei Peng, Chair
Assistant Professor Kwai Hung Henry Lam
Associate Research Scientist David J. LeBlanc
Assistant Professor Necmiye Ozay
Professor Noel C. Perkins

© Ding Zhao

2016

*Dedicated to my parents Jingchun Zhao and Hui Su,
and my wife Ting Su.*

ACKNOWLEDGEMENTS

Five years have passed since my flight landed at DTW to follow my dream of pursuing a Ph.D. degree. Since then, it has been a journey full of passion, learning, and intellectual growth. As I stand at the end of this road, I would like to thank those who are an indispensable part of this wonderful journey.

First I would like to thank my advisor, Professor Huei Peng, who walked with me along this road. Among a myriad of things Professor Peng taught me, four are the most valuable: 1) How to think as a researcher; 3) How to contribute to a research team; 3) How to get things organized and keep a vigorous state physically and mentally; 4) How to balance career success and family happiness. His inspiration and influence on me are beyond what this dissertation reflects, which I will benefit from for a lifelong time.

Second I would like to thank my committee members: Professor Henry Lam, Dr. David Leblanc, Professor Necmiye Ozay, and Professor Noel Perkins. Without their help, I could not reach the point where I stand now. They help me to think about the problem deeply and are always ready to help. Their broad knowledge opens my eyes to the frontier of the knowledge and links my research to real-world impacts. These inputs keep me enthusiastic and proud of my work.

I would like to thank my colleagues at the University of Michigan Transportation Research Institute (UMTRI), Shan, Scott, Carol, Jim, Bob, Nobu, Dan, Jingwen, Steve, and Paul. Thanks for all their unreserved help. They provide me with a warm family-like environment. I would like to show great gratitudes to the engineers in Ford Motor Company who gives me a lot of help and mentoring: Eric Tseng, Greg Stevens, Jianbo Lu, Douglas Blue, Saeed Barbat, Tom Pilutti, Mike Dong, and Hamid Ossareh. I would like to give thanks to our excellent collaborators in Denso Corporation: Rajesh Malhan, Joseph Lull,

Zhe Huang, and Jeff White. Their professional attitudes and great supports always encourage me to improve my work and become a better engineer.

I would like to thank my brothers and sisters in the VDL. Byung-Joo, Sean, Chiao-Ting, Changsun, Jong-Hwa, Xiaowu, Xiaosong, Shengbo, William, Zhengzhong, Weichao, Tianyou, Yuxiao, Xiaobing, Baojin, Xianan, Ziheng, Su-Yang, Geunsoab, Junlong, Tingting, Daofei, and Lang, without you guys, life in Ann Arbor will never be so colorful.

I want to thank all my family for their unconditional support and love. My father 赵景春 and my mom 苏辉 have always been my best friends and models in my life. Lastly, I would like to close this acknowledgment with a line from a poem I wrote to my wife 苏婷 in 2011, during my first final season in the U.S., when we were separated by the ocean:

裸婚为布， 血誓为染；

比翼共绘， 最美夕阳.

TABLE OF CONTENTS

DEDICATION	ii
ACKNOWLEDGEMENTS	iii
LIST OF FIGURES	viii
LIST OF TABLES	xii
LIST OF APPENDICES	xiii
LIST OF MATHEMATICAL NOTATIONS	xiv
LIST OF ABBREVIATIONS	xvi
LIST OF SYMBOLS	xviii
ABSTRACT	xxi
CHAPTER 1 Introduction.....	1
1.1 Motivation	1
1.2 Naturalistic Field Operational Tests.....	4
1.3 Literature Review on Evaluation Approaches of Automated Vehicle.....	7
1.3.1 Test Matrix evaluation	7
1.3.2 Worst-case scenario evaluation.....	13
1.3.3 Monte Carlo simulations	14
1.3.4 Summary	14
1.4 Objective, Approaches, and Scope of the Study	15
1.5 Contributions.....	17
1.6 Outline of the Dissertation	19
CHAPTER 2 Accelerated Evaluation based on Likelihood Analysis	20
2.1 Introduction	20
2.2 The Three-car Car-following Model.....	20
2.2.1 Stochastic lead vehicle model	21
2.2.2 Trailing vehicle model	26
2.3 Accelerated Evaluation based on Likelihood Analysis.....	31
2.4 Simulation Analysis	34

2.4.1 Automated vehicle models	34
2.4.2 Evaluation metrics.....	37
2.4.1 Simulation results.....	38
2.4.2 Benefits and limitations of the proposed method.....	41
2.5 Summary	42
CHAPTER 3 Accelerated Evaluation based on Importance Sampling Techniques.....	43
3.1 Introduction	43
3.2 Importance Sampling Techniques	43
3.2.1 Limitations of the Monte Carlo approach	43
3.2.2 Importance Sampling techniques	45
3.3 Evaluation of AV in Lane Change Scenario using Importance Sampling	48
3.3.1 Extraction of lane changes events from the naturalistic driving database	48
3.3.2 Lane changes model.....	50
3.3.3 Accelerated Evaluation of AV in the lane change scenario	54
3.4 Simulation Analysis	55
3.4.1 Analysis of crash events.....	56
3.4.2 Analysis of injury events.....	59
3.5 Summary	62
CHAPTER 4 Adaptive Accelerated Evaluation	63
4.1 Introduction	63
4.2 The Adaptive Accelerated Evaluation	64
4.2.1 The zero-variance distribution	64
4.2.2 The Cross Entropy method	65
4.3 Adaptive Accelerated Evaluation in the Lane Change Scenario	66
4.4 Simulation Analysis	72
4.4.1 Evaluation with the non-optimized AE distributions.....	72
4.4.2 Evaluation with the Adaptive Accelerated Evaluation	75
4.5 Summary	80
CHAPTER 5 Accelerated Evaluation with Dynamic Interactions in the Car-following Scenario	81
5.1 Introduction	81

5.2 Model of Dynamic Interactions in Car-following Scenario.....	81
5.2.1 Extraction of naturalistic car-following events	81
5.2.2 Lead human controlled vehicle	83
5.2.3 Automated vehicle model	85
5.3 The Optimal Mean Shift Approach.....	88
5.3.1 State space form of the car-following model	89
5.3.2 Accelerated Evaluation	91
5.4 Simulation Analysis	100
5.4.1 Simulation results with baseline accelerated methods	100
5.4.2 Simulation results with proposed accelerated evaluation method	103
5.4.3 Sensitivity analysis of the human-controlled vehicle model.....	109
5.5 Summary	110
CHAPTER 6 Conclusions and Future Work	112
6.1 Conclusions	112
6.2 Future Research Directions	113
6.2.1 Improvement of the HV model accuracy	114
6.2.2 Accelerated Evaluation of other AV scenarios	114
6.2.3 Accelerated Evaluation of other systems	116
APPENDICES	117
BIBLIOGRAPHY	120

LIST OF FIGURES

Figure 1.1 States with enacted automated vehicle legislation [13].....	2
Figure 1.2 Google driverless car took a man with vision disability [39].....	6
Figure 1.3 Test Matrix evaluation flowchart [46].....	7
Figure 1.4 CAMP surrogate target vehicle [52] in a field test.....	8
Figure 1.5 Urban simulator environment in HASTE [58]	9
Figure 1.6 Pre-crash scenarios defined by NHTSA [75]	10
Figure 1.7 Five priority scenario groups in vehicle to vehicle crashes [75]	11
Figure 1.8 Concept of the Accelerated Evaluation method	16
Figure 2.1 The three car-following simulation scenario.....	20
Figure 2.2 Lead vehicle speed profiles used in the EURO-NCAP AEB test	21
Figure 2.3 Speed queried from the SAVEME database with Time To Collision < 11 s [96]	22
Figure 2.4 Light vehicle trips in the IVBSS database [32]	23
Figure 2.5 Data extracted from the IVBSS database	24
Figure 2.6 Histogram of the lead HV with speed between 40 mph and 41 mph	24
Figure 2.7 Lead HV statistics modeled by the Gaussian Mixture Model.....	26
Figure 2.8 Concept of the errorable driver model.....	28
Figure 2.9 Comparison results of the trailing HV model [111]	29
Figure 2.10 Structure of the Michigan errorable car-following model (based on [111]) .	30
Figure 2.11 One crash example of the <i>Michigan model</i>	31
Figure 2.12 Empirical distribution of the naturalistic driving in logarithmic scale for data at vehicle speed between 40 mph and 41 mph.....	32
Figure 2.13 GMM fitted lead vehicle model in the logarithmic scale for data with vehicle speed between 40 mph and 41 mph	32
Figure 2.14 Procedure to generate accelerated transition matrix.....	33
Figure 2.15 A comparison of the velocity profiles of the lead human controlled vehicle in accelerated and non-accelerated (naturalistic) tests	33

Figure 2.16 Layout of the AV control model	34
Figure 2.17 AEB triggering threshold dependent on the vehicle speed	36
Figure 2.18 Acceleration profiles of the AEB designs	36
Figure 2.19 Estimated crash rate.....	39
Figure 2.20 Status of AV controller when rear crashes happen	40
Figure 2.21 Estimation of relative velocity during crash.....	41
Figure 2.22 Simulation layout for human controlled vehicles.....	41
Figure 3.1 Procedure of the Accelerated Evaluation method based on Importance Sampling techniques	46
Figure 3.2 Lane change scenarios that may cause frontal crashes.....	49
Figure 3.3 Recorded lane change events in the SPMD database	50
Figure 3.4 Distribution of vehicle speed of the cut-in vehicle in the lane change scenario	51
Figure 3.5 Distributions of the reciprocal of the range at the lane change moment	51
Figure 3.6 Distribution of the reciprocal of range fitted with the Pareto distribution	52
Figure 3.7 Distributions of the reciprocal of the Time To Collision at the lane change moment	52
Figure 3.8 Interpolation/extrapolation of the parameters of Time To Collision at different velocities	53
Figure 3.9 Distribution of Time To Collision in different range intervals	53
Figure 3.10 Lane change scenario for AV evaluation	54
Figure 3.11 Estimation of crash rate in the lane change scenario.....	57
Figure 3.12 Convergence of crash rate estimation in the lane change scenario	57
Figure 3.13 Influence of the confidence level on the relative error and test number at convergence	59
Figure 3.14 Moderate-to-fatal injury model for forward collisions.....	60
Figure 3.15 Estimation of injury rate in the lane change scenario.....	60
Figure 3.16 Convergence of injury rate estimation in the lane change scenario	61
Figure 4.1 Procedure of the Adaptive Accelerated Evaluation.....	63
Figure 4.2 Definition of the conflict event.....	73

Figure 4.3 Estimation of the conflict rate in the lane change scenario (improper AE distribution).....	74
Figure 4.4 Convergence of conflict rate estimation in the lane change scenario (improper AE distribution)	74
Figure 4.5 Searching for optimal parameters for conflict events with AAE	75
Figure 4.6 Estimation of the conflict rate in the lane change scenario (with AE distribution calculated by AAE)	76
Figure 4.7 Convergence of conflict rate estimation in the lane change scenario (with AE distribution calculated by AAE)	76
Figure 4.8 Searching for optimal parameters for crash events with AAE	77
Figure 4.9 Estimation of the crash rate in the lane change scenario (with AE distribution calculated by AAE)	78
Figure 4.10 Convergence of crash rate estimation in the lane change scenario (with AE distribution calculated by AAE)	78
Figure 4.11 Estimation of the injury rate in the lane change scenario (with AE distribution calculated by AAE)	79
Figure 4.12 Convergence of injury rate estimation in the lane change scenario (with AE distribution calculated by AAE)	79
Figure 5.1 Car-following scenarios that may cause frontal crashes	82
Figure 5.2 Recorded car-following events in the SPMD database	83
Figure 5.3 Estimation of the lead vehicle acceleration	84
Figure 5.4 Automated vehicle model.....	87
Figure 5.5 Procedure to calculate crash rate in the car-following scenario	99
Figure 5.6 Original HV distribution and the uniform AE distribution	101
Figure 5.7 An example maneuver generated by the baseline accelerated evaluation approach with uniform distribution.....	103
Figure 5.8 Estimation of the crash rate using uniform distribution as the AE distribution	103
Figure 5.9 Comparison of lead vehicle speed profiles in accelerated and non-accelerated (naturalistic) driving conditions	104

Figure 5.10 An example maneuver generated by the accelerated evaluation approach leading to a crash	105
Figure 5.11 Estimation of the crash rate in the car-following scenario	105
Figure 5.12 Convergence of crash rate estimation in the car-following scenario	106
Figure 5.13 Estimation of the injury rate in the car-following scenario	107
Figure 5.14 Convergence of injury rate estimation in the car-following scenario	107
Figure 5.15 Estimation of the conflict rate in the car-following scenario	108
Figure 5.16 Convergence of conflict rate estimation in the car-following scenario.....	108
Figure 5.17 Calculation of crash rate using the Accelerated Evaluation approach with the varying HV parameter σ_u	110
Figure 5.18 Crash rate varying with the HV parameter σ_u	110
Figure 6.1 Procedure of the AV evaluation using the Accelerated Evaluation	113
Figure 6.2 Approaches to identify AV evaluation scenarios	115

LIST OF TABLES

Table 1.1 Announced automated vehicle technologies [9], [10]	2
Table 1.2 SAE 6 Levels of Automation Vehicles [14]	3
Table 1.3 Major N-FOT projects in the U.S.	5
Table 1.4 Projects studying the Test Matrix method	12
Table 1.5 Summary of AV evaluation approaches	15
Table 2.1 Deterministic car-following model.....	27
Table 2.2 Parameters the car-following simulation	39
Table 3.1 Accelerated rates of crash and injury events	61
Table 4.1 Summary of performance of the Adaptive Accelerated Evaluation approach in estimating the crash rate, injury rate, and the conflict rate in the lane change scenario	80
Table 5.1 Comparison of between the IVBSS database and the SPMD database	82
Table 5.2 Parameters for the car-following simulations.....	102
Table 5.3 Summary of performance of the Accelerated Evaluation in estimating the crash rate, injury rate, and the conflict rate in the car-following scenario	109

LIST OF APPENDICES

APPENDIX A.....	118
APPENDIX B	119

LIST OF MATHEMATICAL NOTATIONS

Special Typeface

d	Differential like in dx, dt ; to be distinguished from a variable or constant d , or a function $d(x)$
\mathbb{E}, \mathbb{E}_f	Expectation, expectation by sampling through distribution function f
$\widehat{\mathbb{E}}, \widehat{\mathbb{E}}_f$	Empirical expectation, empirical expectation by sampling through distribution function f
$I_{\varepsilon}(x)$	Indicator function
\mathbb{N}	Natural number set $\{0, 1, 2, \dots\}$
$\mathcal{N}(\mu, \sigma^2)$	Normal distribution with mean μ and variance σ^2
\mathbb{P}	Probability
\mathbb{R}	Real set $(-\infty, \infty)$, $\mathbb{R}^{m \times n}$ denotes m by n matrix in \mathbb{R} domain
\mathcal{U}	Uniform distribution
$\mathbb{V}ar$	Variance
\mathbb{Z}	Integer set $\{0, \pm 1, \pm 2, \dots\}$
Φ	Standard normal distribution
Ψ	Logarithmic moment generation function
$\ \cdot\ _2^2$	Euclidean norm
\rightarrow	Convergence
\exists	Exist
\forall	For all

Subscript and Superscript

\mathbf{A}^T	The transpose of \mathbf{A}
x^{Max}, x^{Min}	The maximum and minimum value of x

Miscellaneous Mathematical Notation

Matrices and vectors are most often denoted by bold typeface, \mathbf{C} , $\boldsymbol{\Sigma}$, \mathbf{x} , $\boldsymbol{\vartheta}$ etc.

$x(m:n)$ denotes the column vector $[x(m), x(m+1), \dots, x(n)]^T$

LIST OF ABBREVIATIONS

AAE	Adaptive Accelerated Evaluation
ABS	Anti-lock Braking Systems
ACAS	Automotive Collision Avoidance System
ACC	Adaptive Cruise Control
ADAC	Allgemeiner Deutscher Automobil-Club e.V.
AIDE	Adaptive Integrated Driver-vehicle InterfacE
AE	Accelerated Evaluation
AEB	Autonomous Emergency Braking
APROSYS	Advanced Protection Systems
ASSESS	Assessment of Integrated Vehicle Safety Systems
AV	Automated Vehicles
CARE	Community Road Accident Database
CCIS	Co-operative Crash Injury Study
CDS	Crashworthiness Data System
CIB	Crash Imminent Braking
CICAS	Cooperative Intersection Collision Avoidance System
CMC	Crude Monte Carlo
DBS	Dynamic Brake Support
EDR	Exponential Change of Measure
ECM	Event Data Recorder
ESC	Electronic Stability Control
Euro NCAP	European New Car Assessment Program
FARS	Fatal Accidents Recording System
FCW	Forward Collision Warning
GMM	Gaussian Mixture Model
GES	General Estimates System
GIDAS	German In-depth Accident Study

HASTE	Human Machine Interface And the Safety of Traffic in Europe
HIL	Hardware-in-the-Loop
HMI	Human Machine Interface
HV	Human-controlled Vehicles
ICC	Integrated Chassis Control
interactive	accident avoidance by active intervention for Intelligent Vehicles
IS	Importance Sampling
IVBSS	Integrated Vehicle-Based Safety Systems
IVIS	In-Vehicle Information Systems
KL divergence	Kullback–Leibler divergence
LCV	Lane Change Vehicle
LiDAR	Light Detection And Ranging
LSTO	Lower Speed Thresholds of Operation
MAIS	Maximum Abbreviated Injury Score
NASS	National Automotive Sampling System
N-FOT	Naturalistic-Field Operational Test
NHTSA	National Highway Traffic Safety Administration
NMVCCS	National Motor Vehicle Crash Causation Survey
PI controller	Proportional-Integral controller
RDCW	Road Departure Crash Warning
SAE	Society of Automotive Engineers
SeMiFOT	Sweden-Michigan Naturalistic Field Operational Test
SPMD	Safety Pilot Model Deployment
TRACE	Traffic Accident Causation in Europe
TTC	Time To Collision
UMTRI	The University of Michigan Transportation Research Institute
V2V	Vehicle to Vehicle
VOIESUR	Véhicule Occupant Infrastructure Etudes de la Sécurité des Usagers de la Route
VT	Virginia Tech
WCSE	Worst-Case Scenario Evaluation

LIST OF SYMBOLS

aAEB	Target AEB acceleration [m/s ²]
a_{L_0}, a_0, a_{T_0}	Initial acceleration for lead HV, AV, trailing HV [m/s ²]
A_v	Vehicle frontal area [m ²]
a_L, a, a_T	Initial acceleration for lead HV, AV, trailing HV [m/s ²]
a_d	Desired acceleration of AV [m/s ²]
b_{rr}	Convergence threshold of the relative error [-]
C_d	Aerodynamic drag coefficient [-]
d_n	Distance travelled in test n [m]
D_{nature}, D_{acc}	Test distance needed in N-FOT and in the accelerated tests [m]
f_x, f_x^*	Nominal distribution and AE distribution of random variable x [-]
\tilde{f}_x	A family of AE distributions of random variable x [-]
f_{rr}	Rolling resistance coefficient [-]
f_{zv}^*	Zero-Variance distribution [-]
F_x, F_{x0}, \tilde{F}_x	Longitudinal force, initial value, relative to initial value [N]
g	Gravity constant[m/s ²]
h_0, h_1, h_2	Model parameters of the lead HV [m/s ² , 1, s ⁻¹]
k, K	Step index, total step number [-]
K_p, K_i, K_d	Proportional gain, Integration gain, Derivative gain [-]
$k_{R_L^{-1}}$	Shape parameter of the Pareto distribution of R_L^{-1} [-]
l_α, l_r	Half-width, relative half-width [-]
L	Likelihood ratio [-]
k_T, k_T^*	Termination step, virtual termination step [-]
M	Vehicle mass [kg]
n, N	Test index, total test number [-]
N_{nature}, N_{acc}	Number of tests needed to reach convergence in the naturalistic driving tests, in accelerated tests [-]

r_c	Crash rate [crash/mile]
$R_{\mathcal{E}}$	Critical range for event set \mathcal{E} [m]
R_L, R_T	Range between AV and front HV, range between the AV and trailing HV [m]
R_L^{desire}	Desired range [m]
\dot{R}_L, \dot{R}_T	Range rate between the AV and front HV, range rate between the AV and trailing HV [m/s]
rAEB	AEB acceleration rate limit [m/s ³]
r_{rel}	Relative error [-]
t_{crash}	Crash time [s]
$t_{HW}, t_{HW}^{desire}, t_{HW}^{Err}$	Time headway, desired time headway, time headway error [s]
t_{LC}, T_{LC}	Lane change time, duration of lane change event [s]
T_s	Sampling time [s]
T_{CF}	Duration of the car-following event [s]
TTC_L	Time-To-Collision to the lead HV [s]
TTC_{AEB}	Threshold Time-To-Collision value to activate AEB system [s]
u	Input to the system in the state space form [m/s ²]
u_h	Additive term in calculating the acceleration representing the randomness of human driver behaviors [m/s ²]
v_L, v, v_T	Velocity of the lead HV, AV, and trailing HV [m/s]
v_{L_0}, v_0, v_{L_0}	Initial velocity for lead HV, AV, trailing HV [m/s]
\tilde{v}_L, \tilde{v}	Relative velocity of the lead HV, AV [m/s]
z_α	Quartile of standard normal distribution with significance level α [-]
α	Statistical significance level [-]
β	Convergence threshold of the relative half-width [-]
$\beta_0, \beta_1, \beta_2$	Parameters of the rear-end injury model [-]
γ	Probability of rare event occurring [-]
θ_{rg}	Road grade angle [rad]
$\theta_{TTC_L^{-1}}, \theta_{R_L^{-1}}$	Adjusted parameters for the distributions of TTC_L^{-1} and R_L^{-1} [-]

$\boldsymbol{\vartheta}$	Adjusted parameter vector in the Cross Entropy analysis [-]
$\vartheta_{TTC_L^{-1}}^{ECM}, \vartheta_{R_L^{-1}}^{ECM}$	Adjusted parameters in ECM [-]
$\vartheta_{R_L^{-1}}, \vartheta_{TTC_L^{-1}}$	Adjusted parameters in the accelerated tests [-]
$\lambda_{TTC_L^{-1}}$	Scaling factor of the distribution of TTC_L^{-1} [-]
$\lambda_{R_L^{-1}}$	The scaling factor for the exponential distribution of R_L^{-1} [-]
μ_c	The expectation of the crash rate [crash/mile]
$\boldsymbol{\mu}_i$	Mean vector of the i^{th} component in the GMM lead HV model [-]
μ_u	Expectation of u [m/s ²]
$\mu_{R_L^{-1}}$	Threshold parameter the Pareto distribution of R_L^{-1} [-]
ρ_{air}	Air density [kg/m ³]
σ	Standard deviation [-]
σ_u	Standard deviation of the randomness of the lead HV [m/s ²]
$\sigma_{R_L^{-1}}$	Scale parameter of the Pareto distribution of R_L^{-1} [-]
τ	Time delay [s]
Δv	Relative velocity [m/s]
$\boldsymbol{\Sigma}_i$	Covariance matrix the i^{th} component in the GMM lead HV model [-]
δ	Bias in the AE distribution in the car-following scenario [m/s ²]
\mathcal{E}	Rare event set [-]

ABSTRACT

Automated Vehicles (AVs), which monitor the driving environment and conduct some or all of the driving tasks, must be evaluated thoroughly before their release and deployment. The challenges of AV evaluation stem from two facts. i) Crashes are exceedingly rare events. In the U.S., one needs to drive on average 530 thousand miles to experience a police-reported crash and nearly 100 million miles for a fatal crash. The low exposure to safety-critical scenarios makes the Naturalistic-Field Operational Tests (N-FOT) very time-consuming and expensive to conduct, in which prototype AVs are driven by volunteers or test engineers on public roads. ii) AVs can “cheat” to pass predefined tests. Traditionally, vehicle test protocols and test conditions are pre-defined and fixed. This is not a problem when the vehicle is “dumb”, but becomes a problem when the vehicle is intelligent and can be customized to excel in the predefined tests, and performance in other test conditions receives less attention. An evaluation approach that represents the real world but not as time-consuming as the N-FOT is needed to address the problems mentioned above.

In this research, we propose an “Accelerated Evaluation” concept to accelerate the evaluations of AV by several orders of magnitude. The interactions between the AV and the surrounding Human-controlled Vehicles (HVs) are modeled based on the naturalistic driving data collected by the University of Michigan Transportation Research Institute in the Safety Pilot Model Deployment Program and the Integrated Vehicle-Based Safety Systems Program. Probabilities of conflict, crash, and severe injury are used as the main metrics to assess the safety of AV designs. In general, Accelerated Evaluation consists of six steps. 1) Collect a large quantity of naturalistic driving data. 2) Extract events that have potential multi-vehicle conflicts. 3) Model the conflict driving scenarios using stochastic models. 4) Reduce the non-safety-critical events by skewing the probability density functions. 5) Conduct Monte Carlo simulations with the skewed (accelerated) probability density function, resulting in more intense interactions between the AV and HVs. 6) “Skew back” the simulation results to calculate the performance of AVs under naturalistic driving

conditions. The proposed approach can be used in computer simulations, human-in-the-loop tests with driving simulators, hardware-in-the-loop tests, or vehicle tests.

Four methodologies were developed in this dissertation to form the basis of the Accelerated Evaluation concept. The first method is based on the likelihood analysis of naturalistic driving. The test scenarios are built as a probabilistic model based on time series driving data. The evaluation procedure is accelerated by reducing the relatively safe events that have a high likelihood of occurring. The second method provides a mathematical basis for the “skewing back” mechanism in step 5) based on the Importance Sampling theory, such that the statistical equivalence between the accelerated tests and naturalistic driving tests can be rigorously proved. The third method, the “Adaptive Accelerated Evaluation”, provides a procedure to recursively find the best way to skew the probabilistic density functions of HVs to maximally reduce the evaluation duration. Finally, the Accelerated Evaluation approach to analyzing the dynamic interactions between AVs and HVs was developed based on stochastic optimization techniques.

Simulation results show that the accelerated tests can reduce the evaluation time of crash, injury or conflict events by 300 to 100,000 times. In other words, driving for 1,000 miles can expose the AV with challenging scenarios that take 300 thousand to 100 million miles in the real-world to encounter. This technique thus has the potential to dramatically reduce the development and validation time of AVs.

CHAPTER 1

INTRODUCTION

1.1 Motivation

Automated Vehicle¹ (AV) technologies have the potential to significantly change the future of ground mobility. AVs can save fuel, reduce traffic accidents, ease traffic congestion, and provide better mobility service to the elderly, physically challenged and vision challenged population [1].

Effort is being made to remove the legal obstacles to developing AVs. As of December 2015, six U.S. states (Nevada, Florida, California, and Michigan, Tennessee, North Dakota, and Arizona) and the District of Columbia have passed laws permitting testing of automated cars on public roads. Fourteen other states are considering similar legislations [2], [3] as shown in Figure 1.1. In Europe, the United Kingdom permitted the testing of autonomous cars on public roads starting January 2015 [4] and promise to update the U.K. regulations in 2017 [5]. Some cities in Belgium, France, and Italy are planning to operate transport systems using driverless cars [6], [7]. Gothenburg, Sweden gave the green light to driverless cars, in their current plan 100 Volvo cars will be launched in 2017 [8].

Almost all major car companies have initiated research and development programs for AVs. Table 1.1 shows the announced AV production plans [9], [10]. On October 14, 2015, Tesla activated the Autopilot function on Model S through an over-the-air software update [11] enabling functions such as Adaptive Cruise Control, Lane Keeping, Auto Lane Change, Autopark, and Automatic Emergency Steering [12].

¹ The term “automated” is used instead of “autonomous”, because the former term is more accurate and is more widely adopted [159].

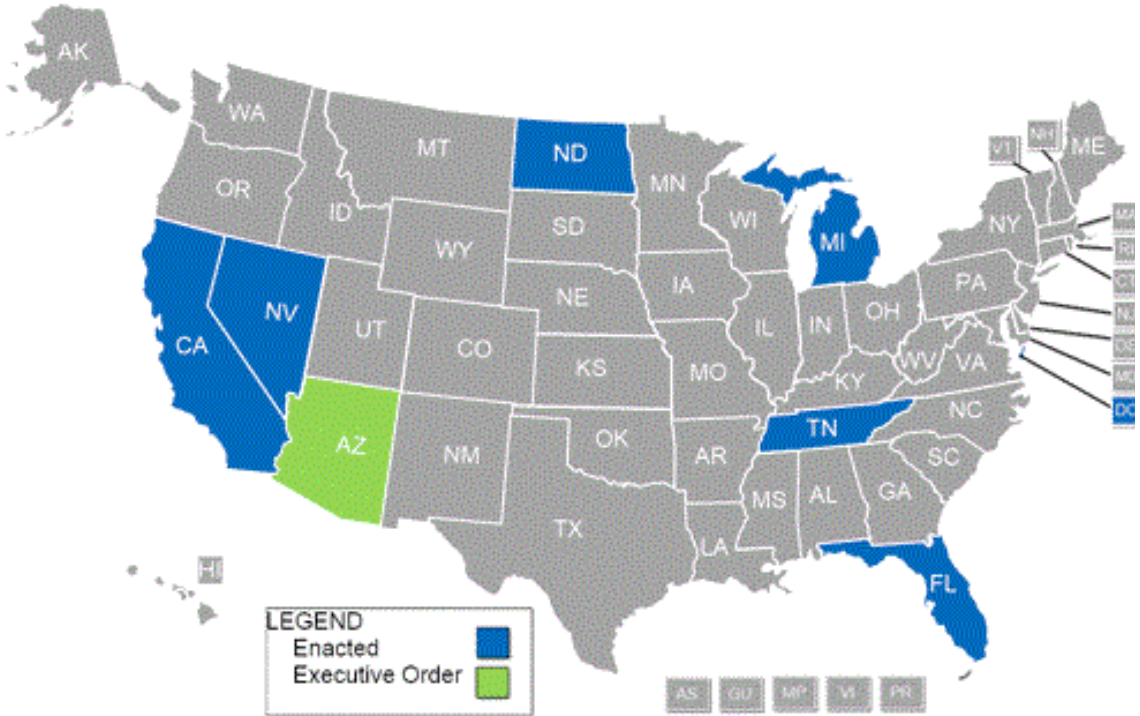


Figure 1.1 States with enacted automated vehicle legislation [13]

Table 1.1 Announced automated vehicle technologies [9], [10]

OEM	Automation Level	Launch Year	First Models	Top Level Functions			Region of Introduction
				TJA	APA	Hwy	
BMW	Semi-Highly	2014 2017	X5 5- / 7-series	✓	✓	✓	Europe & North America
Mercedes Benz	Semi-Highly	2014 2017	E-Class S-Class	✓	✓	✓	Europe, North America, Australia
Audi	Semi-Highly	2016	A8	✓	✗	✓	Europe & North America
Volkswagen	Semi-	2017	Passat	✓	✗	✓	Europe & North America
General Motors (Cadillac)	Semi-Highly-	2018 >2020	SRX, ATS & XTS	✗	✓	✓	North America
Ford	Semi-Highly	2017 2020	Fusion Explorer	✓	✓	✓	Europe & North America
Lexus	Highly	2020	LS	✓	✓	✓	Japan, Europe & North America
Nissan	Highly	2020	Leaf	✓	✓	✓	Europe & North America
Volvo	Semi	2015	XC90	✓	✓	✓	Europe & North America
Google	Fully-	2018	Model / OEM agnostic	✓	✓	✓	North America

TJA – Traffic Jam Assist

APA – Autonomous Parking Assist

Hwy – Automated Highway Driving

The Society of Automotive Engineers (SAE) defined six levels of automated driving in the SAE J3016 Standard [14] as shown in Table 1.2 (details shown in APPENDIX A). “A key distinction is between level 2, where the human driver performs part of the dynamic driving task, and level 3, where the automated driving system performs the entire dynamic driving task.” [15] We are in an era when the industry is moving from level 1 and up, possibly all the way to level 5. Since Electronic Stability Control (ESC) has been mandatory in the U.S. since 2013, all new models of light vehicles can be said to be at least level 1 automation already. However, some argues that ESC really should not be treated as an AV function because it is activated intermittently and is designed for vehicle stability rather than automated driving.

Table 1.2 SAE 6 Levels of Automation Vehicles [14]

Level	Name	Execution of steering and acceleration/ deceleration	Monitoring of driving environment	Fallback performance of dynamic driving task	System capability (driving modes)
<i>Human driver monitors the driving environment</i>					
0	No Automation	Human	Human	Human	n/s
1	Driver Assistance	Human system	Human	Human	Some modes
2	Partial Automation	System	Human	Human	Some modes
<i>Automated driving system monitors the driving environment</i>					
3	Conditional Automation	System	System	Human	Some modes
4	High Automation	System	System	System	Some modes
5	Full Automation	System	System	System	All modes

As the level of automation increases, the AV system will become more complex, making the evaluation of AV more challenging. Today’s high-end cars may have 100 million lines of code while the Boeing 787 only has 6.5 million [16]. It is not practical for either the company’s internal design release team or the evaluation authorities, such as the National Highway Traffic Safety Administration (NHTSA) [17], to check every line of the algorithms. As a result, problems may be found after the product release, which could lead to expensive recalls [18], [19]. It is desirable to evaluate automated driving systems early

in the design process. This is consistent with NHTSA's view for the development of automated driving:

"The main topics that will need to be addressed include ... Development of test and evaluation methods - Based on the real world scenarios (use cases) that map to the functional description of the automated system, develop test track tests and/or simulation approaches that can evaluate the performance of the level 2 or level 3 systems² relative to these use cases. "[20, p. 9]

In this research, we focus on AVs in level 3 to level 5, namely, highly to fully Automated Vehicles. For simplicity, in the remainder of this dissertation, when we talk about evaluating AVs, we mean evaluating levels 3-5 AVs, which monitor the environment and conduct the driving tasks without the help from the human driver.

1.2 Naturalistic Field Operational Tests

Naturalistic Field Operational Tests (N-FOTs) [21] have been used to evaluate AVs. In an N-FOT, data is collected from a number of equipped vehicles driven in naturalistic conditions over an extended period of time [22]. Large-scale N-FOT projects conducted in the U.S. are as shown in Table 1.3. The 100-Car Naturalistic Driving Study was conducted by the Virginia Polytechnic Institute and State University (popularly known as Virginia Tech or VT) to determine the main contributing factors of crashes. Its data had been used to analyze driver performance, behavior, environment, driving context and other factors that were associated with critical incidents, near crashes and crashes [23]–[27]. The Automotive Collision Avoidance System (ACAS) project [28] tested Forward Collision Warning (FCW) and Adaptive Cruise Control (ACC) functions of light vehicles. The Road Departure Crash Warning (RDCW) project [29] developed and assessed a set of technologies intended to warn drivers about lane departure and excessive speed entering a curve. The Sweden-Michigan Naturalistic Field Operational Test (SeMiFOT) [30] is a project that involves 13 organizations from the automotive industry, road authority, and

² The NHTSA has a five level taxonomy of AVs as shown in APPENDIX A. The NHTSA level 2 is the same as SAE level 2. The NHTSA level 3 includes the entire SAE level 3 and partially level 4 and 5.

academia. The test vehicles were equipped with ACC, FCW with Emergency Brake, Lane Departure Warning, Blind Spot Information System, Electronic Stability Control, and Impairment Warning, and were tested by 39 drivers for a total of 106,528 miles. The Integrated Vehicle-Based Safety Systems (IVBSS) [31], [32] project developed and evaluated an integrated system with three crash-warning functions: forward crash, lateral drift, and lane change/merge crash warnings on both light sedans and heavy trucks. More recently, Safety Pilot Model Deployment (SPMD) program [33]–[36] exploited the connected vehicle technologies and tested about 2,800 equipped vehicles in Ann Arbor, Michigan.

Table 1.3 Major N-FOT projects in the U.S.

Name	Conductor	Period	Mileage [mile]	Vehicle	Sensor	Drivers	Research topic
100 Car Naturalistic Driving Study	VT	2001-2009	2,000,000	100 sedans	Camera	109 primary drivers 132 secondary drivers	Rear end collision
ACAS	UM	2004-2005	137,000	11 sedans	Camera Radar	96 drivers	Forward collision warning
RDCW	UM	2005-2006	83,000	11 sedans	Camera Radar	11 drivers	Lane departure warning
SeMiFOT	UM	2008-2009	106,528	10 sedans, 4 trucks	Camera Radars	39 drivers	Forward collision warning, lane departure warning, blind spot information system, electronic stability control, and impairment warning
IVBSS	UM	2010-2011	sedan: 213,309 truck: 601,944	16 sedans 10 heavy trucks	Camera Radar	108 drivers for sedans 18 professional truck drivers	Integrated warning
SPMD	UM	2012-2014	Over 34 million	2,800 various types of vehicles	Camera DSRC	2,700 volunteer drivers and several professional bus and truck drivers	Connected vehicle
Google driverless car	Google	2012-present	1.3 million	At least 50 sedans and SUVs	Lidar Camera Radar	Google technicians and volunteers	Fully self-driven vehicle

Google, instead of testing a specific function, designed several SAE Level 4 AVs [37] and tested them on the public road since 2012. The Google driverless car scans and generates a 3D map of its environment using a Velodyne LiDAR (Light Detection And Ranging) system [38] mounted on the top of the car. On March 28, 2012, Google posted a YouTube video showing Steve Mahan, a Morgan Hill California resident who is ninety-five percent blind. He was taken on a ride in a driverless Toyota Prius [39] as shown in Figure 1.2. In the video, it is noted that the AV takes him from his home to a drive-through restaurant, then to the dry cleaning shop, and finally back home [40]. Up to December 2015, the Google driverless cars have logged nearly 1.3 million miles of autonomous driving [41].



Figure 1.2 Google driverless car took a man with vision disability [39]

Conducting an N-FOT to evaluate an AV involves non-intrusive driving conditions, i.e., the test subjects were told to drive the way they normally did. This test approach suffers from several limitations. An obvious problem is the time needed. Under naturalistic conditions, the probability of exposure to critical events is very low. In the U.S., there were 5.7 million police-reported motor vehicle crashes and 30,057 fatal crashes in 2013, while the vehicles traveled a total of 2.99 trillion miles [42]. This translates to approximately 0.53 million miles for a police-reported crash and 99 million miles for a fatal crash. The latter is almost the same as the distance from Earth to the Sun (93 million miles). Since the average mileage driven annually by licensed drivers is 14,012 miles [42], on average one needs to drive 38 years to experience a police-reported crash and 6,877 years for a fatal crash.

Because of this low exposure rate, the N-FOT projects require a large number of vehicles, long test duration, and a large budget. According to Akamatsu et al. [43], an N-FOT “cannot be conducted with less than \$10,000,000”. A more efficient approach for AV evaluation is needed.

1.3 Literature Review on Evaluation Approaches of Automated Vehicle

The field of automated vehicle has a rich history, with early demonstrations [44] in the 1990s and continuous improvement [45] over the last decade. Meanwhile, methods for AV evaluation have been developed and improved over time. In this section, we reviewed existing approaches that can accelerate the evaluation procedure. We divided the approaches into three categories: Test Matrix approach, Worst-Case Scenario evaluation, and Monte Carlo Simulations.

1.3.1 Test Matrix evaluation

In a Test Matrix evaluation, a series of test scenarios are first defined. The vehicles then go through each test and are assessed objectively or subjectively. An example evaluation process is shown in Figure 1.3.

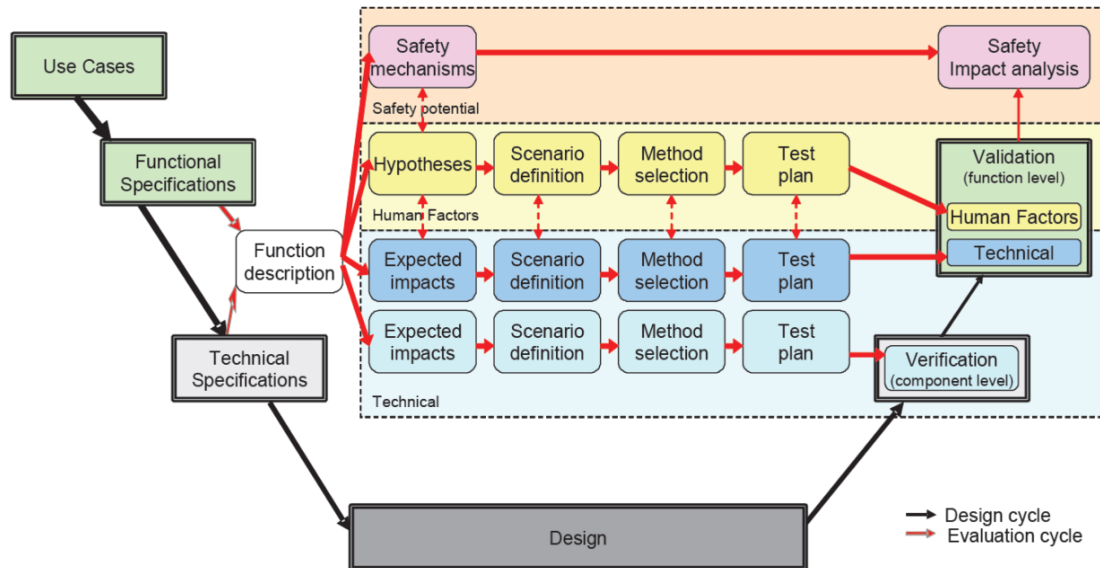


Figure 1.3 Test Matrix evaluation flowchart [46]

Many programs have been launched to develop evaluation procedure using the Test Matrix method. In the U.S., one of the earliest efforts was conducted by the CAMP (Crash Avoidance Metrics Partnership) program [47]–[49]. Twenty-six dynamic, vehicle-level tests were proposed to evaluate Forward Collision Warning system performance. A surrogate target (a mock vehicle) as shown in Figure 1.4 was used. The total test time is two to four weeks (not including initial fabrication, set-up, and surveying of test sites) [50]–[52]. CICAS (Cooperative Intersection Collision Avoidance System) project [53] used a scenario-based field-test approach to evaluating a comprehensive system to reduce the number of crashes at intersections due to violations of traffic control devices [54], [55]. In the “Development of Performance Evaluation Procedures for Active Safety Systems” project [56], eleven scenarios were used to assess the performance of DBS (Dynamic Brake Support) and CIB (Crash Imminent Braking) on two production vehicles sold in the U.S.



Figure 1.4 CAMP surrogate target vehicle [52] in a field test

The European Commission also conducted several projects to develop evaluation procedure using the Test Matrix method. The HASTE (Human Machine Interface And the Safety of Traffic in Europe) project [57] was launched by the European Commission to develop methodologies and guidelines for the assessment of In-Vehicle Information Systems (IVIS). Three levels of road complexities were defined: straight roads, gentle S-shaped roads, and discrete critical events [58]. Both simulator experiments and field trials were used. It was found that visual distraction and cognitive distraction from the use of IVIS have very different impacts on the primary task of driving and static performance [57]. AIDE (Adaptive Integrated Driver-vehicle InterfacE) [59], [60] introduced a 15-scenario test regime for an integrated in-vehicle Human Machine Interface (HMI) based

on test scenarios suggested in previous studies. TRACE (Traffic Accident Causation in Europe) [61] adopted a case study method with scenarios based on National crash statistics and in-depth crash data. APROSYS (Advanced Protection Systems) [62]–[64] proposed various test scenarios for cars, heavy trucks, motorcyclists, pedestrians and pedal cyclists, based on various sources including SAVE-U [65], COMPOSE (subproject of PReVENT [66]) and GIDAS (German In-depth Accident Study) databases [67]. The interactIVe (accident avoidance by active intervention for Intelligent Vehicles) project [68] applied Hardware-in-the-loop testing, driving simulator and test track experiments to assess crash avoidance intervention systems. ASSESS [69] (Assessment of Integrated Vehicle Safety Systems) developed multiple test mechanisms for collision avoidance. ‘Accident data study in support of development of Autonomous Emergency Braking (AEB) test procedures’ project [70] developed types of evaluation scenarios: 1) stopped lead vehicle, 2) slow lead vehicle with constant speed, and 3) braking lead vehicle with constant deceleration determined based on GIDAS, STATS 19 (2008) and OTS (2000-2009) databases. The results of this project were used in the EURO NCAP AEB test procedure [71].

Test Matrix scenarios can be implemented in field tests, Hardware-in-the-Loop (HIL) test, driving simulator test and computer simulation. Field tests were used by all certification authorities. Driving simulator and computer simulation have also been used to reduce the cost and time. One example of evaluation using simulator is shown in Figure 1.5.



Figure 1.5 Urban simulator environment in HASTE [58]

The choices of test scenarios in Test Matrix based evaluations are primarily based on crash databases. A series of research on pre-crash scenarios was conducted [72]–[76]. As shown in Figure 1.6, the “44-crashes typology” was developed by General Motors. The “pre-crash scenarios” typology was devised by United States Department of Transportation based the NASS crash databases GES (General Estimates System) [77] and CDS (Crashworthiness Data System) [78]. Volpe combined crash information from both typologies and developed the 37 pre-crash scenarios that depict vehicle movements and dynamics as well as the critical events occurring immediately prior to crashes involving at least one other light vehicle [76]. Volpe further used the GES, NMVCCS (National Motor Vehicle Crash Causation Survey) [79], and EDR (Event Data Recorder) [80] databases to generate the top five scenario groups as shown in Figure 1.7. The major crash databases in the U.S. and EU are summarized in APPENDIX B. More comprehensive reviews of crash analysis can be found in [81].

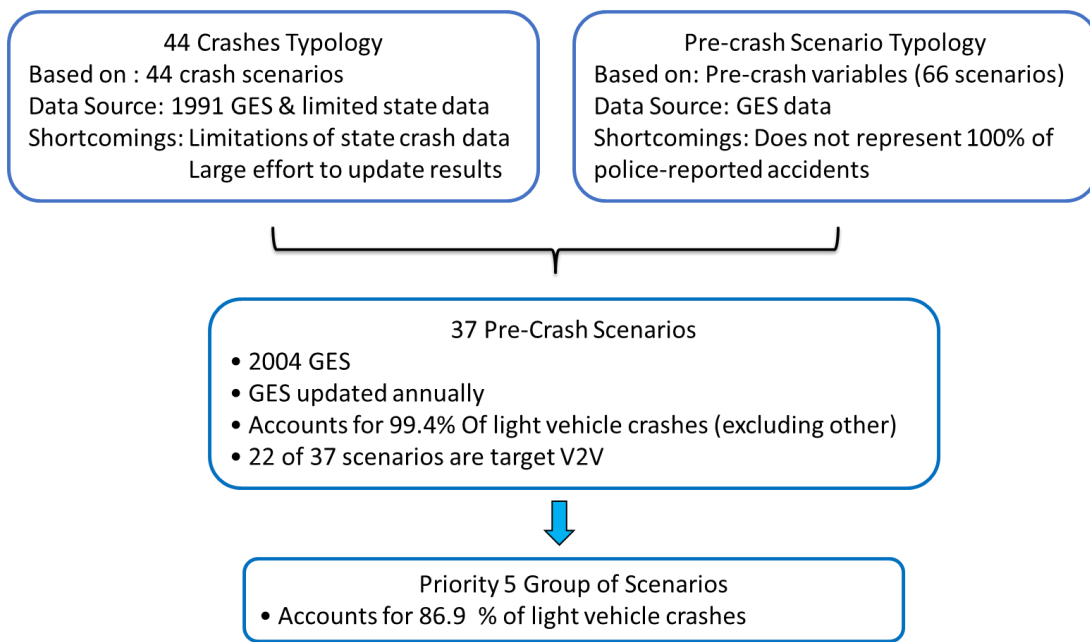


Figure 1.6 Pre-crash scenarios defined by NHTSA [75]

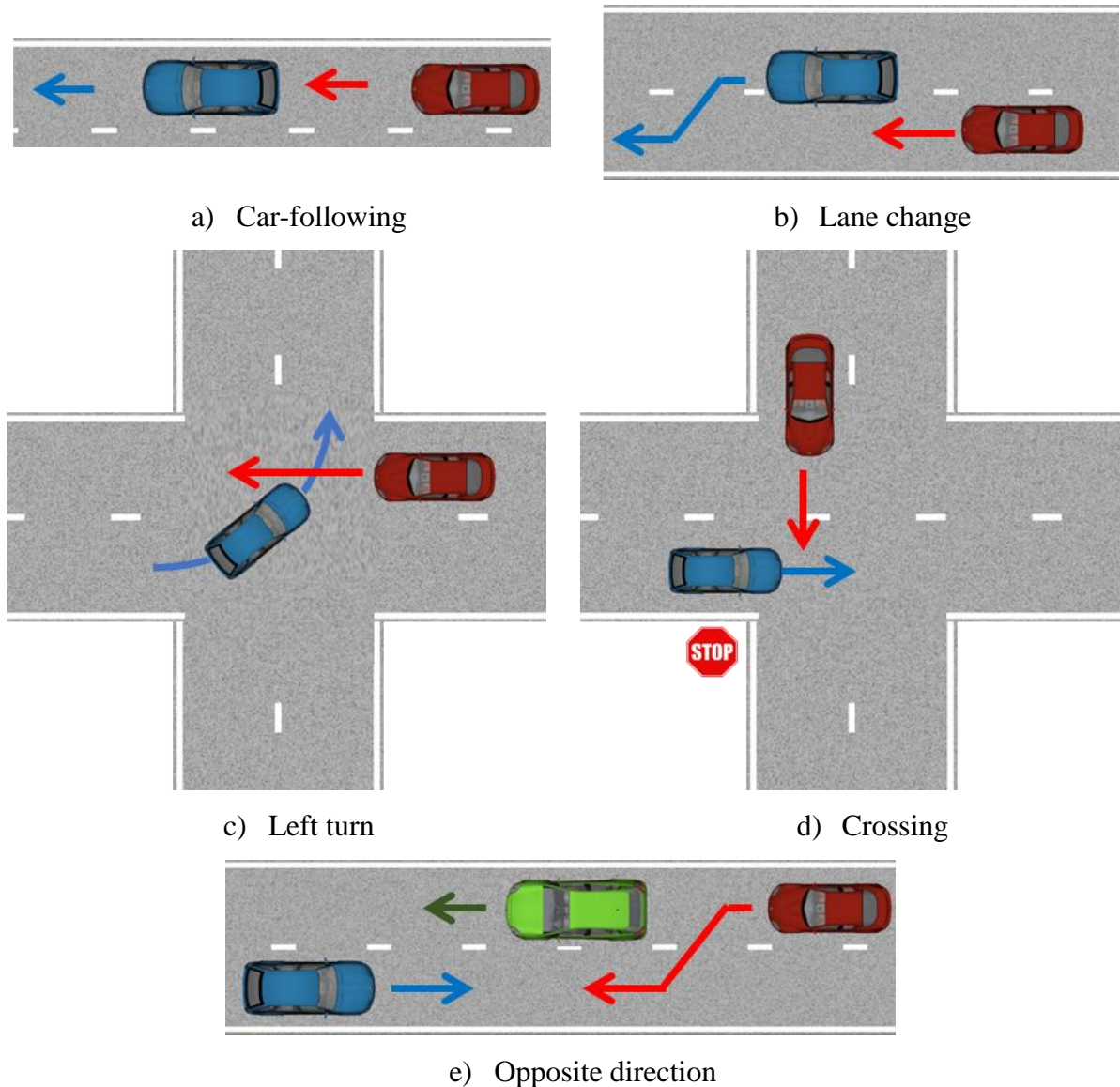


Figure 1.7 Five priority scenario groups in vehicle to vehicle crashes [75]

The main benefits of the Test Matrix method are that the defined test procedure is repeatable, reliable and can be finished relatively quickly [82]. However, there are many difficulties to overcome. First, all the test scenarios are fixed and predefined. Therefore, control systems can achieve good scores in these tests, but the performance under broader conditions may not be adequately assessed. In an analogy, “*Having a standard test is akin to holding an SAT exam for students with all problems pre-announced. Students do well in the test, but the score may tell very little about how much they really learn*” [82]. Moreover, the Test Matrix scenarios are usually selected based on crash databases in which most of

the crashes were caused by Human-controlled Vehicles (HVs). The test scenarios of HV safety and their weights in the evaluation may not accurately reflect the safety-critical scenarios for AVs. Past projects that studied Test Matrix methods are summarized in Table 1.4.

Table 1.4 Projects studying the Test Matrix method

Project	Institute	Year	Test scenario	Evaluation approach	Basis
CAMP	Ford/GM/ NHTSA	1999	26 tests to evaluate FCW system performance	Test track	GM "44 Crashes"
HASTE	HASTE consortium	2005	Three levels of road complexities	Simulator Test track	Real world scenarios
AIDE	AIDE consortium	2005	15 scenarios for a fully integrated in-vehicle HMI	Simulator	HMI conflict scenarios in previous research
TRACE	LMS, LAB, INRETS, VW, TNO, ALLIANZ	2006	Scenarios from crash database	Simulator Test track Computer simulation	National statistics combined with in-depth crash data
Pre-Crash Scenario Typology for Crash Avoidance Research	Volpe	2007	37 pre-crash scenarios for light vehicles	Crash data analysis	GES (General Estimates System)
APROSYS	APROSYS consortium	2007	Scenarios for car, heavy trucks, motorcyclists, pedestrians and pedal cyclists	Simulator Test track	SAVE-U COMPOSE PReVENT INVENT project GIDAS data
CICAS	U of Minnesota PATH VTech	2008	Scenarios for intersection conflict	Test track	
ASSESS	ASSESS consortium	2010	Stopped lead vehicle Slow lead vehicle with constant speed Braking lead vehicle with constant deceleration	Test track	GIDAS
interactIVe	interactIVe consortium	2011	Multiple scenarios for active	Hardware-in-the-loop testing	Previous studies based on

Project	Institute	Year	Test scenario	Evaluation approach	Basis
			intervention systems	Simulator Test track	real traffic crashes
Accident data study in support of development of Autonomous Emergency Braking (AEB) test procedures	Loughborough University	2012	EURO NCAP AEB test procedure	Test track	STATS 19 (2008) OTS (2000-2009)
Depiction of priority light-vehicle pre-crash scenarios for safety applications based on vehicle-to-vehicle communications	Volpe	2013	37 pre-crash scenarios for light vehicle impact	Crash data analysis	GES NMVCCS EDR
Development of Performance Evaluation Procedures for Active Safety Systems	UMTRI	2013	11 scenarios to assess DBS and CIB	Test track	Real traffic accidents

1.3.2 Worst-case scenario evaluation

The Worst-Case Scenario Evaluation (WCSE) methodology was proposed to identify the truly challenging scenarios for any vehicles with or without active control systems. Ma [83], [84] first applied WCSE on rollover and jackknifing of articulated vehicles based on a dynamic game theory, in which control inputs and disturbance inputs compete in a two-player game situation. Ungoren [85] solved the problem as a one-player game by considering the vehicle and its control system as a combined dynamic system, and the iterative dynamic programming method was conducted to solve the WCSE problem numerically. Kou [86] applied the WCSE method to evaluate the Integrated Chassis Control (ICC) system. Initial conditions suitable for searching optimal disturbance were investigated through theoretical and practical means. In general the vehicle (with or without control systems) is modeled mathematically and WCSE is treated as a horizon optimization problem to solve for a trajectory (e.g. a sequence of steering inputs) that minimizes or maximizes the cost function (e.g. rollover index) [86]. When the system is linear, the worst bounded inputs are derived from the convolution of impulse responses [87]. For nonlinear systems, the solution of the Hamilton-Jacobi-Bellman equations is derived by variational calculus to solve the optimal trajectory problem [88].

While the WCSE method can identify the weakness of a vehicle and vehicle control systems, it did not consider the probability of the occurrence of such Worst-Case scenarios [89], [90]. Therefore, the WCSE results do not provide sufficient information about the risk in real driving scenarios, and may not be the fairest way to compare between or evaluate different designs. Moreover, when the control algorithms are not available in analytical or numerical form (e.g., only as a black box) or complex (e.g. evolving systems [91] with millions of lines of code), the WCSE methods may have difficulties finding the worst scenarios, or will take a very long time to do so.

1.3.3 Monte Carlo simulations

Some researchers built stochastic models based on data obtained from N-FOTs and ran Monte Carlo simulations to evaluate AVs. Yang et al. [92] evaluated collision avoidance systems by building an “errorable” driver model to simulate human inattention based on Road-Departure Crash-Warning (RDCW) FOT and Intelligent Cruise Control (ICC) FOT naturalistic driving databases. Woodrooffe et al. [93] generated 1.5 million forward collision scenarios based on naturalistic driving conflicts and used them to evaluate collision warning and collision mitigation braking technologies on heavy trucks.

A key benefit of this approach is that all the scenarios/models are extracted from naturalistic driving records and thus represent real-world driving scenarios. Using simulations instead of field tests may reduce the evaluation cost. However, if Monte Carlo simulations are used directly, the non-safety-critical parts of naturalistic driving will dominate and thus the simulations are not done efficiently. When hardware or human is in the loop, this approach may not be able to accelerate the procedure.

1.3.4 Summary

Four types of existing AV evaluation approaches were reviewed in Sections 1.2 and 1.3. Their main pros/cons are summarized in Table 1.5. The N-FOT approach is time-consuming and is the non-accelerated approach to be improved. The Test Matrix methods identify critical scenarios based on analysis of crash data. The Worst-Case Scenario

evaluation identifies critical scenarios by studying the AV dynamics and control algorithms. The Monte Carlo Simulations build stochastic test models based on naturalistic driving databases. The Test Matrix and Worst-Case Scenario approach successfully reduce the time required significantly compared with the N-FOT approach. However, the test scores may not be directly related to the real world crash rate. The Monte Carlo simulations can be used to estimate safety benefit of AVs. However, it cannot reduce the non-safety critical events to reduce the test efforts. A new approach is needed to achieve both goals: reflect real-world safety benefits, and accelerated.

Table 1.5 Summary of AV evaluation approaches

Method	Basis	Advantages	Limitations
N-FOT	Public road testing	Real-world field test	Inefficient; expensive and time-consuming
Test Matrix	Crash data	Efficient, repeatable	Test scenarios are fixed and predefined. The failure modes of AVs might not be reflected in the existing crash scenarios.
Worst-Case Scenario evaluation	AV model	Worst-Case scenarios	The probabilities for the Worst-Case scenarios are not considered.
Monte Carlo Simulation	N-FOT driving data	Stochastic tests	It does not reduce the test of non-safety critical events

1.4 Objective, Approaches, and Scope of the Study

The objective of this research is to develop an approach that can significantly accelerate the evaluation procedure of AVs and accurately represents their real-world safety benefits. Such an approach can be used by car companies to make AVs safer and can be used to develop government certification process.

We propose the Accelerated Evaluation concept to achieve this goal. The core idea is that by skewing the statistics of the ‘principle other vehicles’, we can reduce the noncritical or “boring” parts of daily driving so that the test duration is reduced i.e. the evaluation procedure is accelerated. More specifically, the Accelerated Evaluation consists six steps:

- 1) Collect a large quantity of naturalistic driving data.
- 2) Extract events that have potential conflicts between an AV and surrounding HVs.
- 3) Model the behaviors of “other vehicles” as the major disturbance to AVs. The randomness is modeled as random variables vector \mathbf{x} with probabilistic distribution $f(\mathbf{x})$.
- 4) Skew the disturbance statistics to reduce the non-safety-critical portion of daily driving by replacing $f(\mathbf{x})$ with the accelerated distribution $f^*(\mathbf{x})$.
- 5) Conduct Monte Carlo tests with the skewed (accelerated) probability density function $f^*(\mathbf{x})$, resulting in more intense interactions/crash between the AV and HVs.
- 6) “Skew back” the results of the accelerated tests to understand the performance of AVs under naturalistic driving conditions using the statistics analysis.

The procedure of the Accelerated Evaluation is shown in Figure 1.8.

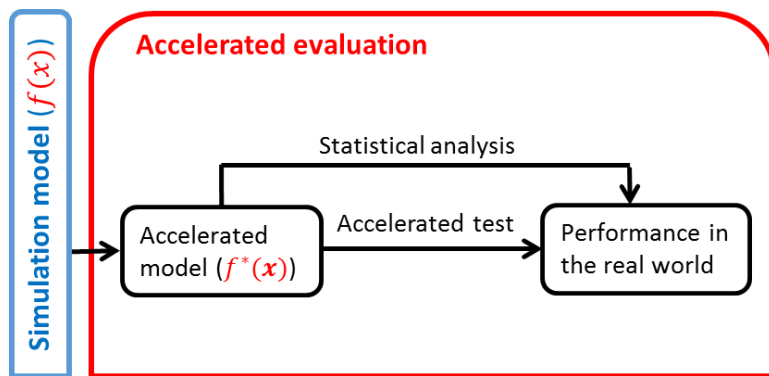


Figure 1.8 Concept of the Accelerated Evaluation method

The scope of this study includes:

1. We focus on the interaction between AV and other Human Controlled Vehicles (HVs). In the early phase of AV deployment, AVs mostly encounter HVs. It is critical for AVs to deal with HVs including their imperfectness. The AV to AV and HV to HV interactions are beyond the scope of this study (except when used as a benchmark).
2. The sensors and controls of the AV are assumed to work perfectly. The HVs making unsafe maneuvers are modeled as the primary disturbance to AVs. The

measurement and perception errors and control inaccuracy are also beyond the scope of this study.

3. Human drivers are assumed to react to AVs in the same way as they do to other HVs. Some automakers, like GM, work hard to hide sensors and make their prototype AVs look "normal" [94]. In this research, we assumed AVs look similar to HVs, so other vehicles do not treat AVs differently.
4. Only the first impact in a crash event will be considered. Secondary impacts may occur but are outside of the scope of this study.

1.5 Contributions

We propose a new AV evaluation approach – The “Accelerated Evaluation” approach. The main contributions are in the following three aspects:

- **The “Accelerated Evaluation” concept is new in the field of AV testing and evaluation.**

In this approach, driver behaviors reflected in the N-FOT are modeled statistically. The test duration is dramatically reduced because the non-safety-critical events are compressed. For crash analysis, the test mileage can be reduced by a factor of 10,000 to 100,000. This technique thus can reduce the development and validation time for AVs significantly.

- **We developed four Accelerated Evaluation methods.**

- i. *Accelerated Evaluation based on the analysis of likelihood of the naturalistic driving*

This method accelerates the evaluation procedure by reducing the relatively safe events with a high likelihood of occurring. An import observation of the safety-critical events is that they all have a low probability of occurring [22], [26]. By modeling the surrounding HVs with stochastic models and modifying their statistics, the most common but “boring” parts are removed. Thus, the cost and duration of the evaluation process can be reduced.

ii. Accelerated Evaluation based on Importance Sampling

By changing the statistics of the HVs, more intense interactions happen between the AV and its surrounding vehicles. By taking the amplified results and the modified statistic information in the Importance Sampling framework, the evaluation metrics (e.g. the crash rate) can be calculated with the statistical equivalence between the accelerated tests and naturalistic driving rigorously proved.

iii. Adaptive Accelerated Evaluation approach

The “Adaptive Accelerated Evaluation”, provides a procedure to find the best way to skew the probabilistic density functions of HVs to maximally reduce the evaluation duration. If the statistics changed too little or improperly, the acceleration rate is not sufficient. To accelerate 10,000 times, the change must be significant. We propose an iterative way to find the optimal parameters in the accelerated tests based on the Cross Entropy method. In each iteration, the modified statistical distributions of the HVs are updated based on the results from a small set of tests using the previous distributions. With this approach, we can significantly reduce the time needed to find an effective way to modify the HV distributions to significantly accelerate the evaluation.

iv. Accelerated Evaluation of the dynamic interactions between AVs and HVs

It is more challenging to evaluate AVs in a dynamic interaction. In a static sampling scenario, the randomness of the driver behavior is modeled as a set of distributions but sample only once at a particular moment. For instance, in the lane change scenario, safety is primarily determined by the vehicle making the lane change. The decision is made at the moment when the driver believe that it is safe to change the lane after multiple checking of the rear mirrors. We call this type of stochastic interactions static sampling scenarios. In a dynamic sampling scenario, such as in the car-following situation, drivers adjust their speed constantly affected by the lead vehicle movement, host vehicle speed, road/weather conditions and other factors. The statistics of the HV behaviors are state-dependent and change over time. Safety is determined by the states over a period of time, generated stochastically in a dynamic procedure. A new approach is proposed to evaluate the dynamic

interactions. The driving scenario is modeled as a Discrete Markov Chain. The statistics of the HVs in each time step during the whole car-following is folded into one joint distribution. By studying of the joint distribution using, the dynamic interactions were examined in the Accelerated Evaluation. Stochastic optimization approach is used to find a set of AE distributions in each step to significantly accelerate the evaluation procedure. The Importance Sampling techniques are used as the framework again to ensure the accuracy of the results in the accelerated tests.

- **We applied the Accelerated Evaluation method on two common driving scenarios.**

Two common driving scenarios - the car-following and lane change scenarios were analyzed using the Accelerated Evaluation approaches. The surrounding HVs were modeled based on two large naturalistic driving databases created and maintained by the University of Michigan Transportation Research Institute: the Safety Pilot Model Deployment database [33]–[36], and the Integrated Vehicle-Based Safety Systems [31], [32] project. The probabilities of conflict, crash and injury events for prototype AV models were calculated based on the Accelerated Evaluation method. Non-accelerated (i.e. naturalistic driving) tests were conducted to validate the proposed approaches and calculate its acceleration efficiency.

1.6 Outline of the Dissertation

The remainder of this dissertation is organized as follows. In CHAPTER 2, an Accelerated Evaluation approach is developed based on likelihood analysis of the naturalistic driving. In CHAPTER 3 the Importance Sampling techniques are applied to improve the reliability and accuracy of the Accelerated Evaluation method. In CHAPTER 4, the Adaptive Accelerated Evaluation is developed to achieve maximum accelerated rates. In CHAPTER 5, an Accelerated Evaluation approach is developed to study the dynamic interaction between HV and AV. Finally, conclusions and future research directions are outlined in CHAPTER 6.

CHAPTER 2

ACCELERATED EVALUATION BASED ON LIKELIHOOD ANALYSIS

2.1 Introduction

The core idea of the Accelerated Evaluation method is to reduce the non-safety-critical driving events. In this chapter, we introduce an approach that accelerates the evaluation by reducing the events with a high likelihood of occurring but do not contribute to the final risk calculation. The approach is demonstrated in the car-following scenario. First, we built a three-car car-following model based on a naturalistic driving database. Then the Accelerated Evaluation approach is applied to accelerate the evaluation. Finally, the results are compared to the naturalistic driving safety records.

2.2 The Three-car Car-following Model

A microscopic simulation environment was built to evaluate the AV performance interacting with HVs in car-following scenarios. As shown in Figure 2.1, three vehicles are included in the scenario: the lead HV, the AV in the middle to be evaluated, and the trailing HV.

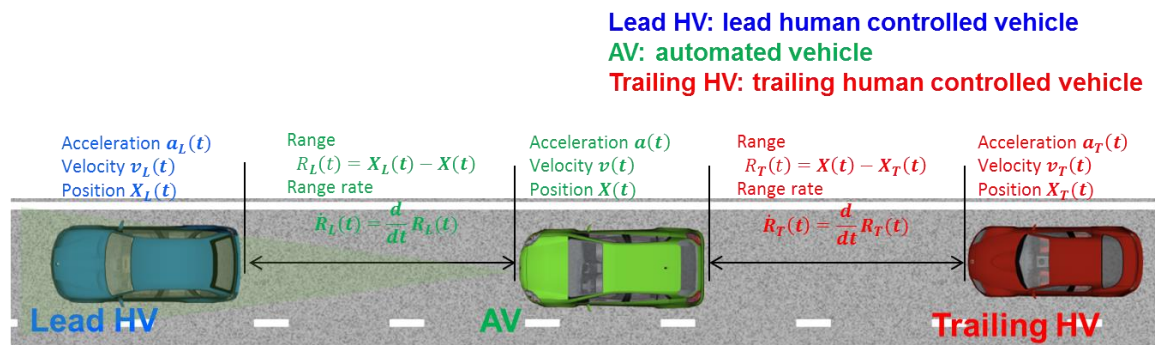


Figure 2.1 The three car-following simulation scenario

2.2.1 Stochastic lead vehicle model

In the car-following scenarios, it is critical to model the lead vehicle motion. In the Test Matrix method, the lead vehicle motion is predefined. For example, in the EURO-NCAP Autonomous Emergency Braking (AEB) test protocol [95], three scenarios are defined as shown in Figure 2.2: 1) stopped lead vehicle, 2) slow lead vehicle with constant speed, and 3) lead vehicle braking at constant deceleration. In another research, Lee [96] selected 100 challenging lead vehicle motions from the SAVEME naturalistic database as shown in Figure 2.3. As all the scenarios were extracted from naturalistic driving, they represent real-world driving scenarios. However, the querying approach (Time To Collision < 11 s) is somewhat ad hoc. It was also not clear how to assign a final performance score based on the simulation results of these 100-case scenarios. Yang [97] searched the whole Road Departure Crash Warning (RDCW) database [29] and used all available lead vehicle trajectories to evaluate AVs. This approach avoids the issue of choosing scenarios. However, the exhaustive simulation study takes a long time to finish.

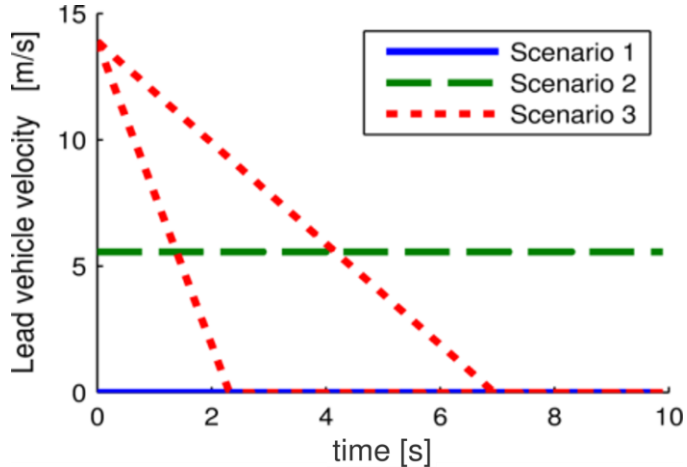


Figure 2.2 Lead vehicle speed profiles used in the EURO-NCAP AEB test

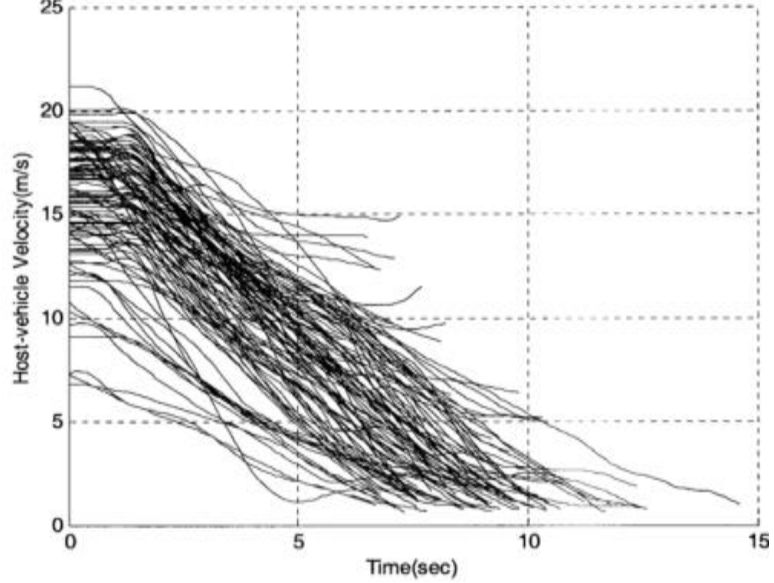


Figure 2.3 Speed queried from the SAVEME database with Time To Collision < 11 s [96]

In this research, the lead vehicle is modeled as a discrete time Markov Chain. The lead vehicle velocity and acceleration are used as the two state variables. The acceleration in the next time step $a_L(k + 1)$ is modeled as a random variable with distribution dependent on the current acceleration $a_L(k)$ and velocity $v_L(k)$, that is,

$$\mathbb{P}(a_L(k + 1)|a_L(k), v_L(k)) = f_{LV}(a_L(k + 1)|a_L(k), v_L(k)). \quad (2.1)$$

The data from the Integrated Vehicle-Based Safety Systems (IVBSS) database [98] is used to fit the driver model. 108 licensed drivers were recruited to participate in the study. Participants were in one of three age groups: 20 to 30 (younger), 40 to 50 (middle-aged), and 60 to 70 years old (older), and are gender balanced. Each participant drove a vehicle equipped with the integrated safety system and data acquisition system for approximately six weeks. Figure 2.4 shows all recorded trips with 213,000 miles traveled.

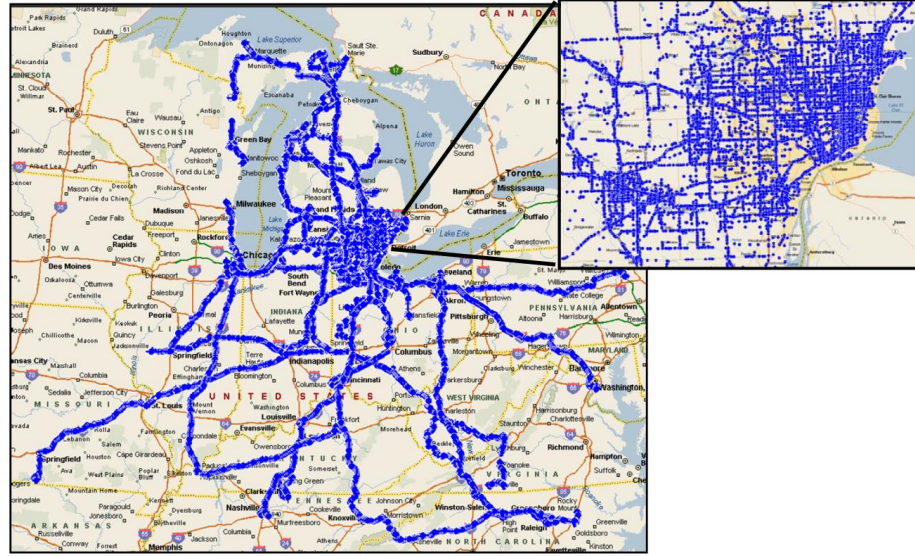


Figure 2.4 Light vehicle trips in the IVBSS database [32]

Vehicle acceleration and speed were extracted from the IVBSS database with sampling time $T_s = 0.3$ s. The data was further divided into bins defined by speed interval of 1 mph. As shown in Figure 2.5, for each driver and speed interval, the data set $[a_L(k+1), a_L(k), v_L(k)]$ were collected with the acceleration quantized by 0.03 m/s^2 and speed quantized by 1 mph. 1.5 million data points were extracted from IVBSS database.

The data sets were further aggregated for all 108 drivers to represent the diversity of behaviors among drivers. For each speed interval, a two-dimensional (2-D) histogram is calculated to represent the statistics of the stochastic behaviors. Figure 2.6 shows the histogram for $v_L \in (40, 41] \text{ mph}$. The color represents the normalized frequency of the $[a_L(k+1), a_L(k), v_L(k)]$ set such that

$$\sum_{a_L(k+1)} \sum_{a_L(k)} f_{hist}^{LV}(a_L(k+1), a_L(k) | v_L(k)) = 1 \quad (2.2)$$

where $f_{hist}^{LV}(\cdot)$ is the normalized frequency. It can be seen that the center of the histogram where $a_L(k+1) = a_L(k) = 0$ has the maximum frequency, which represents constant speed cruising.

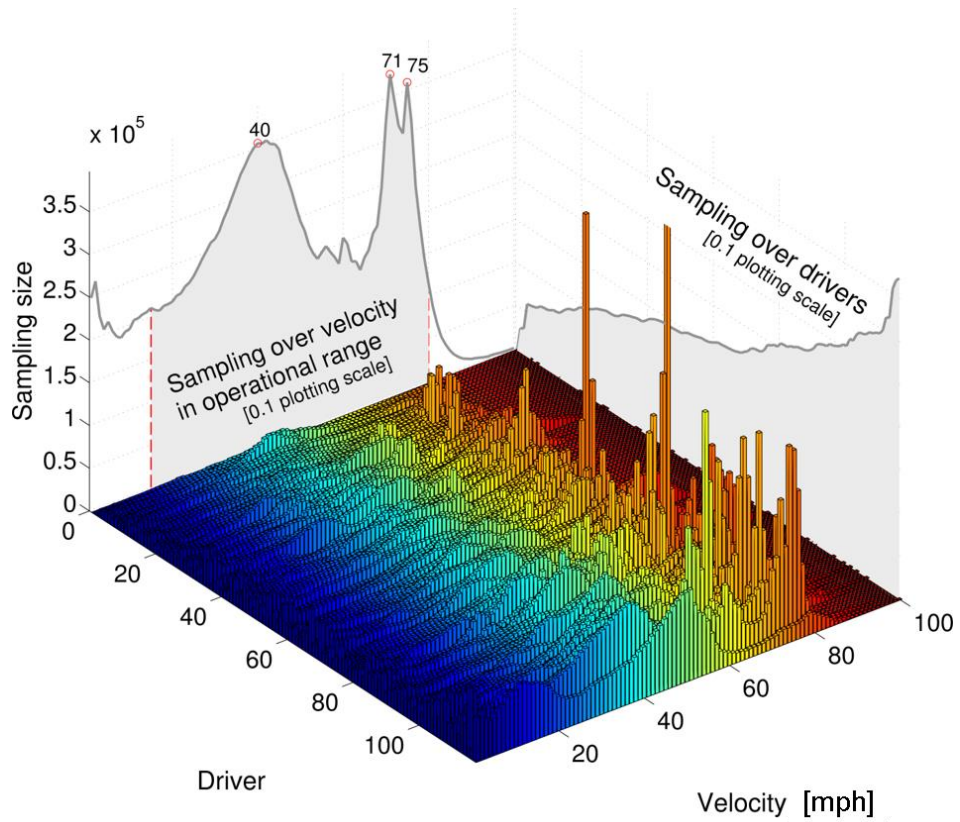


Figure 2.5 Data extracted from the IVBSS database

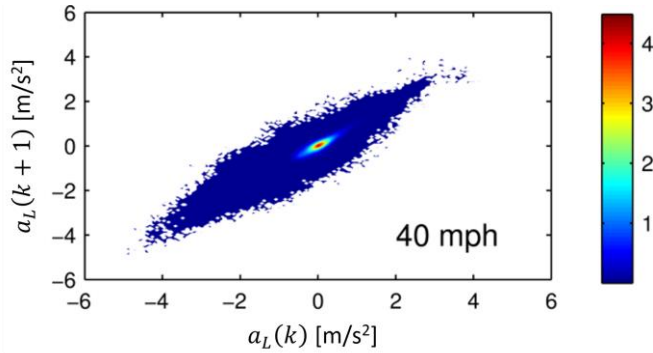


Figure 2.6 Histogram of the lead HV with speed between 40 mph and 41 mph

The 2-D histogram can be modeled by the Gaussian Mixture Model (GMM) [99].
The acceleration in the next step is calculated from

$$\begin{aligned}
& f_{LV}(a_L(k+1)|a_L(k), v_L(k)) \\
&= \sum_{i=1}^M w_i(v_L(k)) f_G \left(\begin{bmatrix} a_L(k+1) \\ a_L(k) \end{bmatrix} \middle| \boldsymbol{\mu}_i(v_L(k)), \boldsymbol{\Sigma}_i(v_L(k)) \right)
\end{aligned} \tag{2.3}$$

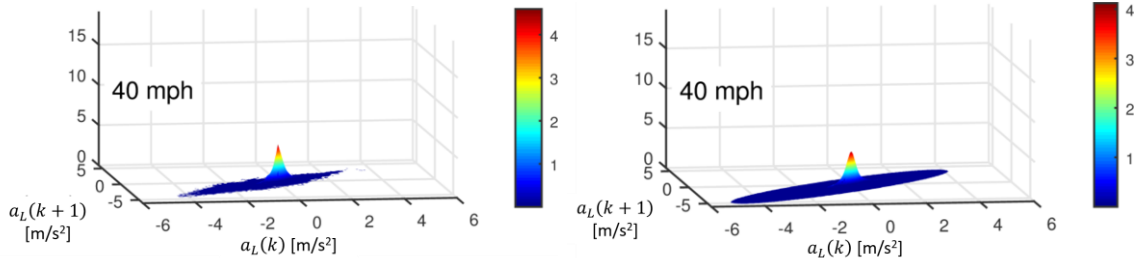
where w_i are the mixture weights satisfying $\sum_{i=1}^M w_i = 1$, and $f_G(\cdot)$ is the component density, in the form of a 2-variate Gaussian model

$$\begin{aligned}
& f_G \left(\begin{bmatrix} a_L(k+1) \\ a_L(k) \end{bmatrix} \middle| \boldsymbol{\mu}_i(v_L(k)), \boldsymbol{\Sigma}_i(v_L(k)) \right) \\
&= \frac{1}{2\pi |\boldsymbol{\Sigma}_i(v_L(k))|^{1/2}} \exp \left\{ -\frac{1}{2} \left(\begin{bmatrix} a_L(k+1) \\ a_L(k) \end{bmatrix} \right. \right. \\
&\quad \left. \left. - \boldsymbol{\mu}_i(v_L(k)) \right)^T \boldsymbol{\Sigma}_i(v_L(k))^{-1} \left(\begin{bmatrix} a_L(k+1) \\ a_L(k) \end{bmatrix} - \boldsymbol{\mu}_i(v_L(k)) \right) \right\}
\end{aligned} \tag{2.4}$$

where $\boldsymbol{\mu}_i$ is the mean vector and $\boldsymbol{\Sigma}_i$ is the covariance matrix. The velocity in the next time step is calculated from

$$v_L(k+1) = v_L(k) + T_s \cdot a_L(k). \tag{2.5}$$

The model parameters are estimated using Expectation-Maximization algorithm [100]. The number of components for the GMM is set to four to provide an adequate degree of freedom but not too large to run into problems in over-fitting. Figure 2.7 shows fitting results in a three-dimensional plot. The histogram of the naturalistic driving data is displayed in Figure 2.7 a). The fitted GMM model with the same speed intervals is plotted on the right-hand side of Figure 2.7 b).



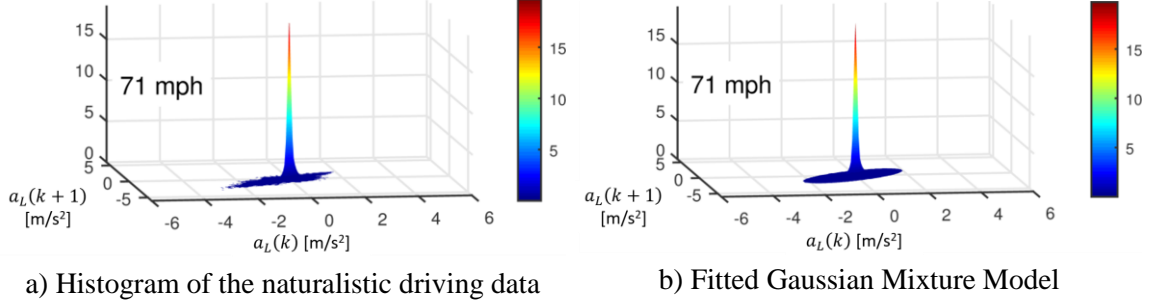


Figure 2.7 Lead HV statistics modeled by the Gaussian Mixture Model

2.2.2 Trailing vehicle model

Trailing vehicle refers to the vehicle in the same lane and is directly behind the subject vehicle. For AVs with a forward collision avoidance system, the likelihood to collide with a lead vehicle can be significantly reduced. Struck by the car from behind may become the major type of crashes. To include crash from behind for a more complete analysis, the trailing vehicle behavior is modeled.

Car-following behaviors have been intensively studied and modeled for computer simulations. In [101]–[107], car-following behaviors were modeled based on the assumption that drivers react to the range $R_T(t)$ (the distance between the front end of the host vehicle and the rear end of the lead vehicle) and/or its derivative – the range rate $\dot{R}_T(t)$ as shown in Figure 2.1. Table 2.1 summarizes many of the well-known car-following models. A linear model was first suggested by Pipe [101] in 1953, in which the acceleration of the host vehicle $a_T(t)$ was controlled by the delayed range rate $\dot{R}_T(t - \tau)$ with a constant feedback gain, where τ is the reaction time. Gazis, Herman, and Rothery [102] then modified the model with a nonlinear control gain as a function of $R_T(t)$ and the speed of the host vehicle $v_T(t)$, often referred as the GHR model. Over the years, many efforts have been devoted to finding the best parameters of the GHR model but without conclusive results [105]–[107]. Tyler [103] derived the car-following model based on the optimal control approach in 1964. The range and range-rate errors were optimized over a quadratic cost function. Gipps developed a car-following model [108] based on a kinematic analysis that always guarantee crash-free even the lead vehicle brake at its maximum deceleration.

Table 2.1 Deterministic car-following model

Researcher	Model	Parameters	Equation
Pipe (1953)	Linear	C, τ_T	$a_T(t + \tau_T) = C \cdot \dot{R}_T(t)$
Gazis et al. (1961)	Nonlinear	C, τ_T, m, l	$a_T(t + \tau_T) = \frac{C \cdot v_T(t)^m}{R_T(t)^l} \dot{R}_T(t)$
Newell (1961)	Exponential convergence	$v_T^{desire}, \lambda_T, R_{Tmin}$	$v_T(t + \tau_T) = v_T^{desire}(1 - \exp\{-\lambda_T(R_T(t) - R_{Tmin})/v_T^{desire}\})$
Tyler (1964)	Linear optimal control	$C_1, C_2, \tau_T, T_{hw}^{desire}$	$a_T(t + \tau_T) = C_1 \dot{R}_T(t) + C_2 [R(t) - T_{hw}^{desire} v_T(t)]$
Gipps (1981)	Crash free	a_n, b_n	$v_T(t + \tau_T) = \min \left\{ \begin{array}{l} v_T(t) + 2.5 a_n \tau \left(1 - \frac{v_T(t)}{v_{T0}} \right) \sqrt{0.025 + \frac{v_T(t)}{v_{T0}}} \\ b_n \tau_T + \sqrt{b_n^2 \tau_T^2 - b_n \left[2(R_T(t) - R_{min}) - v_T(t) \tau_T - \frac{v_L(t)^2}{\hat{b}} \right]} \end{array} \right\}$

Most of the driver models focus on normal driving behaviors. Good fitting results and crash-free simulations are generally considered as model performance metrics [97, p. 13]. However, the majority of crashes occur due to human errors [109], [110]. Therefore, it is important to understand driver errors that lead to unsafe situations. Error-free models are useful to study the average traffic flow or human behaviors but are not very helpful to evaluate safety systems. An ‘errorable’ driver model that can simulate the mistakes of human drivers was developed by Yang and Peng (the “Michigan” model) [111], which was used to evaluate longitudinal collision warning systems [92]. Tang et al. [112], Przybyla et al. [113] and Bi et al. [114] built other longitudinal or lateral errorable models based on this concept.

In general, errorable driver models consist of three components as shown in Figure 2.8: deterministic driving principles, stochastic driving behaviors, and error mechanisms. The deterministic driving principles establish the basic relationship between the control stimulus variables (range and range rate) and the response of the driver (acceleration). A stochastic driver behavior block is added to describe driver imperfection and variations.

Finally, errorable mechanisms based on statistical and psychophysical knowledge of human behavior are included as the third component of the model.

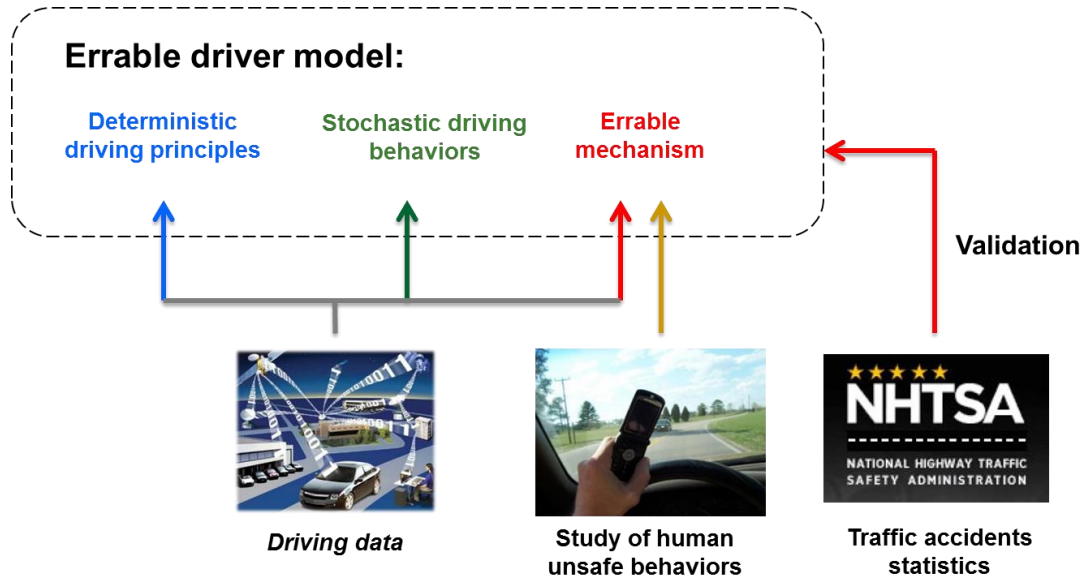


Figure 2.8 Concept of the errorable driver model

In this research, we use the Michigan errorable driver model (referred as the *Michigan model* below) to simulate the trailing vehicle in the car-following scenarios. In the *Michigan model*, a modified Tyler's model was used as the deterministic driving principle. The desired time headway and the variance longitudinal acceleration were modeled as stochastic variables to simulate the randomness in human driving behaviors. The variation of the desired time headway is used to model the different driving styles among drivers, and the change in one driver over a long time. Given the desired range, the imperfection of human control is captured by the variation of the acceleration. Three error-inducing mechanisms were modeled: perceptual limitation, distraction, and time delay. The perceptual limitation of human drivers is modeled by quantizing the range-rate measurement. Two types of distractions were considered in the *Michigan model*: “mind-off-the-road” and “eyes-off-the-road” that are likely caused by secondary tasks, such as answering a cell phone or talking to passengers. During “mind-off-the-road” distraction, drivers are assumed to keep eyes on the road while doing the secondary tasks. The secondary tasks increase the mental load and degrades the driving performance. If a human

driver fully devotes him/herself to a secondary task, very often he/she will move the eyes to this task and stop updating the driving information. This situation is defined as “eyes-off-the-road”. The mind-off-the-road, the eyes-off-the-road, and time delay were modeled as stochastic behaviors.

The *Michigan model* was compared to Pipes model, Gazis model and Tyler model and showed better accuracy and robustness in [111]. As shown in Figure 2.9, the *Michigan model* shows a smaller error compared with other three models. It also shows good consistency between the training set and the evaluation set.

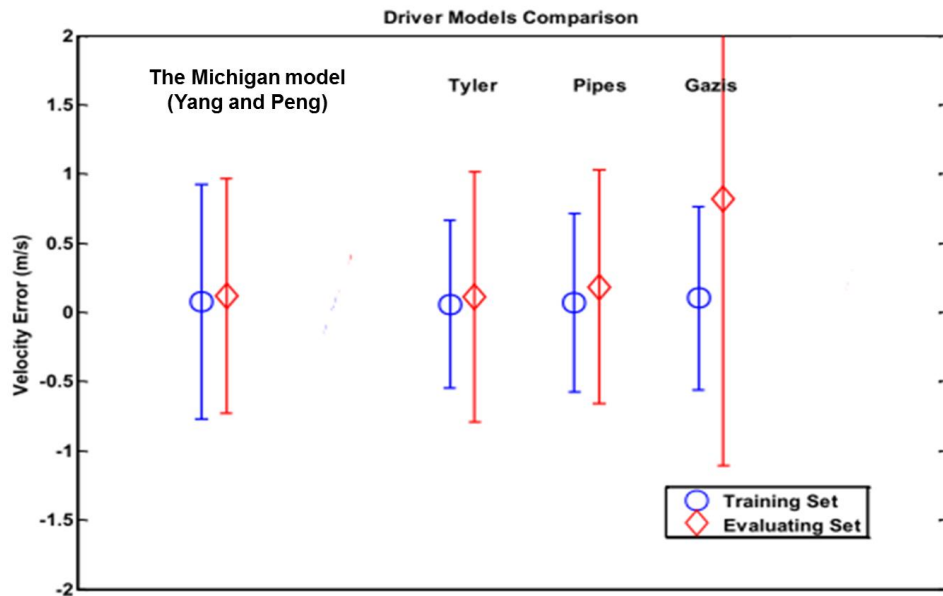


Figure 2.9 Comparison results of the trailing HV model [111]

The overall structure of the *Michigan model* is shown in Figure 2.10. The model parameters were fitted to data extracted from the RDCW naturalistic driving database [29]. Figure 2.11 shows an example result from the *Michigan model*. The trailing HV followed the lead HV well both at high and low speed while the driver stayed focus. However, the trailing driver got distracted at about 45 s while the lead vehicle started to decelerate abruptly. The trailing HV failed to respond to the deceleration and collide into the lead vehicle.

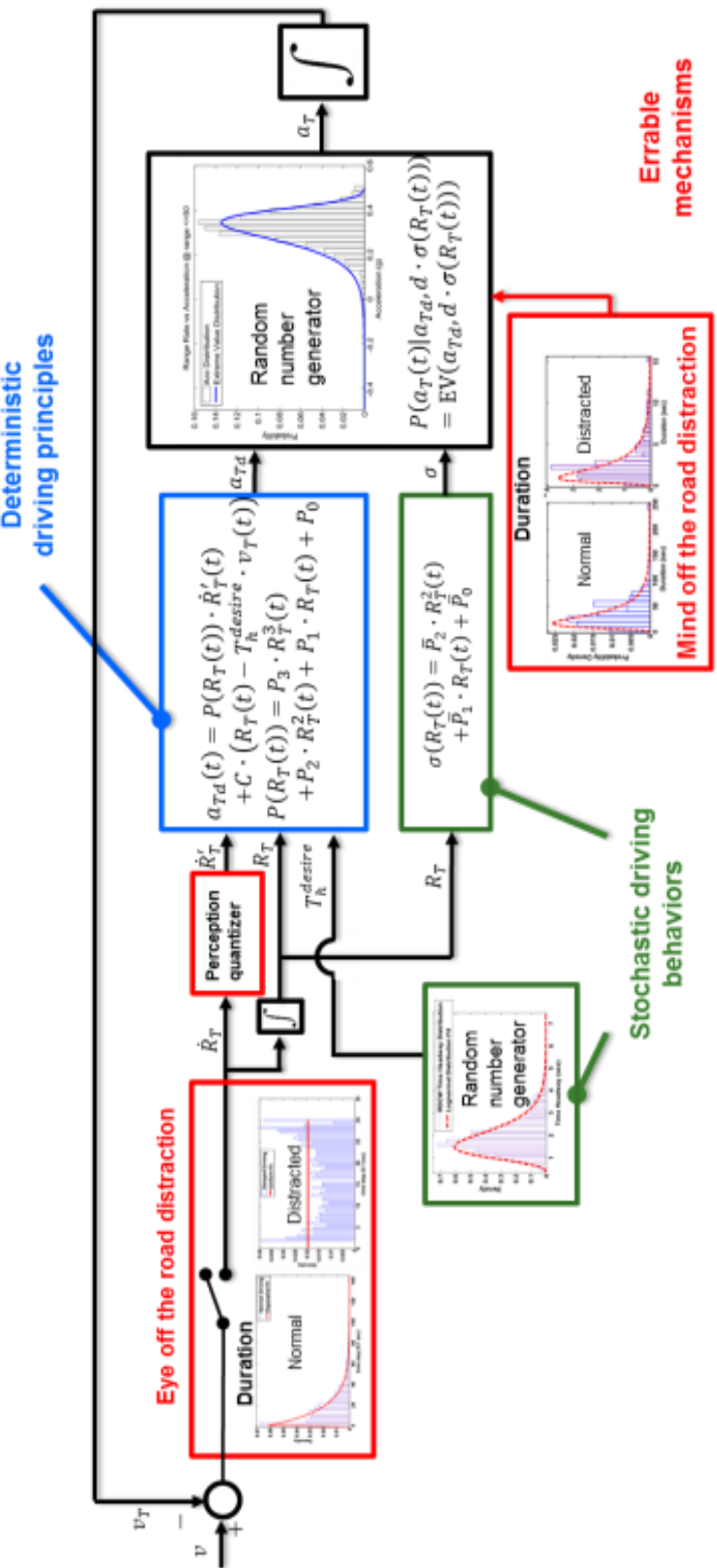


Figure 2.10 Structure of the Michigan errorable car-following model (based on [111])

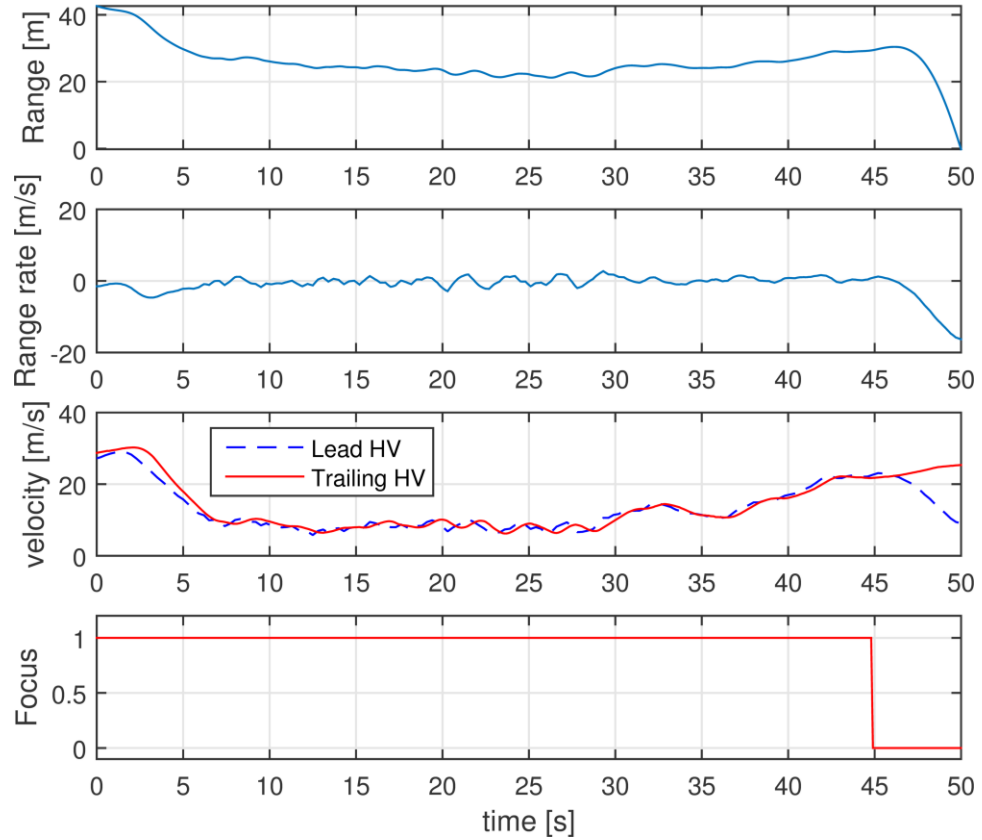


Figure 2.11 One crash example of the *Michigan model*

2.3 Accelerated Evaluation based on Likelihood Analysis

The driver models developed in the previous section emulates driving behaviors in the naturalistic driving. An accelerated model is needed to accelerate the evaluation procedure. An important observation of the safety-critical events is that they have a low probability of occurring [22], [26].

We propose the Accelerate Evaluation approach based on likelihood analysis. The core idea of this method is that by reducing the safe events that have a high likelihood of occurring, the overall exposure rate for critical scenarios is increased and the evaluation of AV is accelerated. In the following, this idea is demonstrated in the three-car car-following scenarios.

There is randomness in both lead HV and trailing HV models. We can change the statistics in both models to amplify the interactions between the HVs and the AV. As maintaining a proper range with the lead HV is the responsibility of the AV, only the statistics of lead HV is modified for simplicity. It can be seen from Figure 2.6 and Figure 2.7 that the center area of the histogram has a much high probability. To emphasize the tail part of the distribution, the histogram is plotted in logarithmic scale in Figure 2.12.

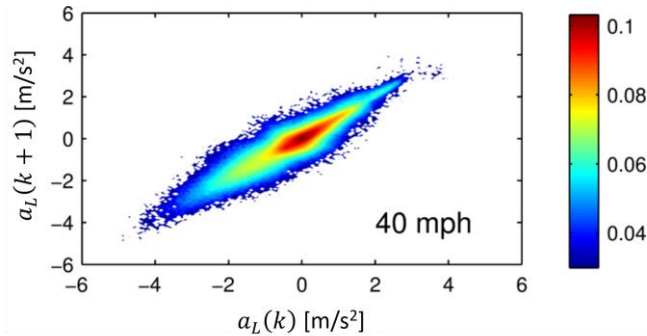


Figure 2.12 Empirical distribution of the naturalistic driving in logarithmic scale for data at vehicle speed between 40 mph and 41 mph

The corresponding GMM model is plotted on a logarithmic scale in Figure 2.13. The center of the histogram represents cruising with little speed variation. The exterior of the distribution embodies rarer events with low probability of occurring.

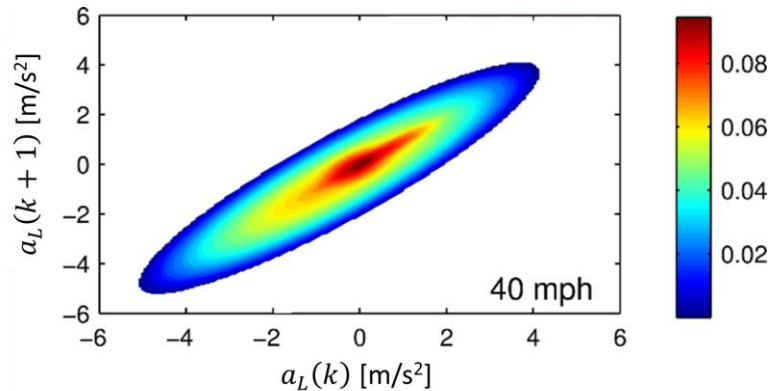


Figure 2.13 GMM fitted lead vehicle model in the logarithmic scale for data with vehicle speed between 40 mph and 41 mph

To reduce the most frequent driving scenarios, we remove 99.5 % of the high probability density data. Figure 2.14 shows the procedure to generate the accelerated distribution. The percentage of eliminated events can be adjusted based on time/budget constraints.

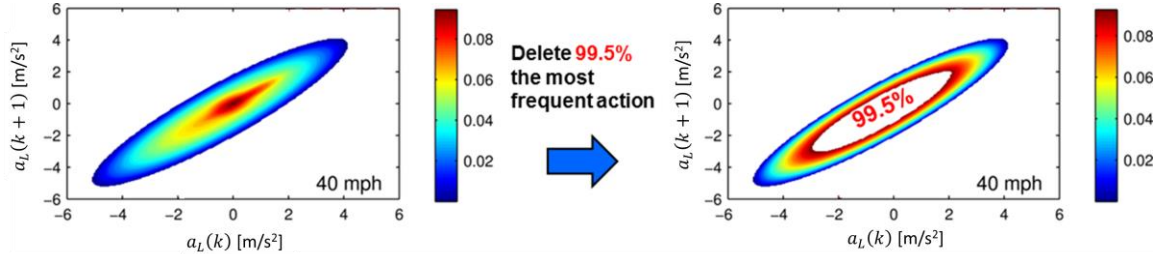


Figure 2.14 Procedure to generate accelerated transition matrix

Figure 2.15 shows the accelerated and normal lead vehicle velocity profiles generated by the Accelerated Evaluation method. It can be seen that the lead vehicle velocity has more frequent and harsher actions than in the normal (non-accelerated) conditions.

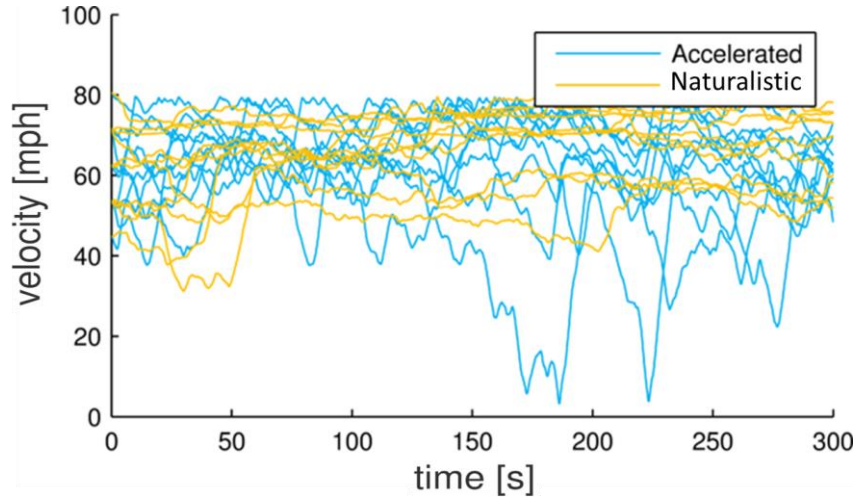


Figure 2.15 A comparison of the velocity profiles of the lead human controlled vehicle in accelerated and non-accelerated (naturalistic) tests

2.4 Simulation Analysis

In this section, simulations are conducted to demonstrate the Accelerated Evaluation approach. The accelerated lead HV model in Figure 2.14 and the *Michigan model* in Figure 2.10 are applied to construct the three-car car-following scenario in Figure 2.1. Two AVs are designed based on production vehicles, which are evaluated by the results in the accelerated tests with two metrics: the crash rate and relative speed, in both frontal crashes and rear crashes. Finally, the accelerated rate is approximated by comparing the crash rate for HV in the accelerated tests and in real world, followed by the discussion of the benefits and limitations of the proposed method.

2.4.1 Automated vehicle models

Two AVs were designed to demonstrate the proposed Accelerated Evaluation method. Both AVs are equipped with ACC (Adaptive Cruise Control) [115] and AEB (Autonomous Emergency Braking). As shown in Figure 2.16, the AVs are controlled by the ACC algorithm when the situation is perceived to be safe. The AEB algorithms become active when a threat is detected. If the AEB fails to prevent the crash, the simulation terminates. Otherwise, the control is returned back to the ACC. Both the AVs use the same ACC algorithms but different AEB designs. The AEB models used in this dissertation are based on the work in [116] which extracted the control algorithms from two production vehicles: Volvo V60 and Infiniti M37S. We name the two AV designs as Design A and Design B.

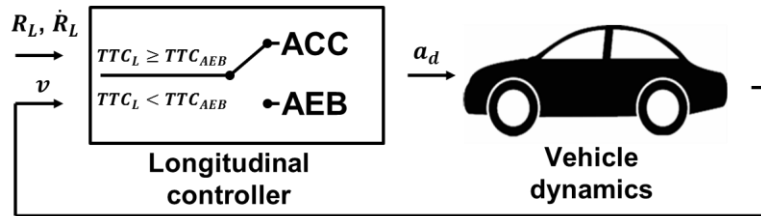


Figure 2.16 Layout of the AV control model

The ACC is approximated by a discrete Proportional-Integral (PI) controller [115] to achieve a desired time headway t_{HW}^{desire} . Define the time headway error as

$$t_{HW}^{Err} = t_{HW} - t_{HW}^{desire} \quad (2.6)$$

where t_{HW} is the current time headway, defined as

$$t_{HW} = R_L/v. \quad (2.7)$$

Use t_{HW}^{Err} as the controller input, the PI controller can be designed as

$$a_d(t) = K_p t_{HW}^{Err}(t) + K_i \int_0^t t_{HW}^{Err}(\tau) d\tau \quad (2.8)$$

where a_d is the desired acceleration commanded by ACC controller; gains K_p and K_i are the proportional and integration gains calculated using Matlab Control Toolbox® with the following two requirements: 1) Loop bandwidth = 10 rad/s; 2) Phase margin = 60 degree. The ACC control is saturated at ± 5 m/s².

The AEB model was extracted from a 2011 Volvo V60, based on a test conducted by ADAC (Allgemeiner Deutscher Automobil-Club e.V.) [116]. The test results were analyzed to reconstruct the AEB algorithms by Gorman [117] using together the test track data, owner's manuals, information from European New Car Assessment Program (Euro NCAP), and videos during vehicle operation.

The AEB algorithm becomes active when a risk is detected, and in Gorman's reconstruction [117] it was assumed that the risk is only based on a threshold value of "Time-To-Collision", defined as

$$TTC_L = -\frac{R_L}{\dot{R}_L} < TTC_{AEB} \quad (2.9)$$

where TTC_{AEB} is the threshold to activate AEB system as a function of vehicle speed. Figure 2.17 shows the relationship between TTC_{AEB} and vehicle speed. The Lower Speed Thresholds of Operation (LSTO) were estimated in [117] obtained from the owner's manuals and validated by data and statements in the ADAC test report [116], representing by the left vertical lines in Figure 2.17. The AEB will not activate if the speed of the AV is below the LSTO. In this research, we evaluate the AV within the operational range of the AEB. The lower threshold of the speed for the lead HV, AV and trailing HV are set to be 5 m/s.

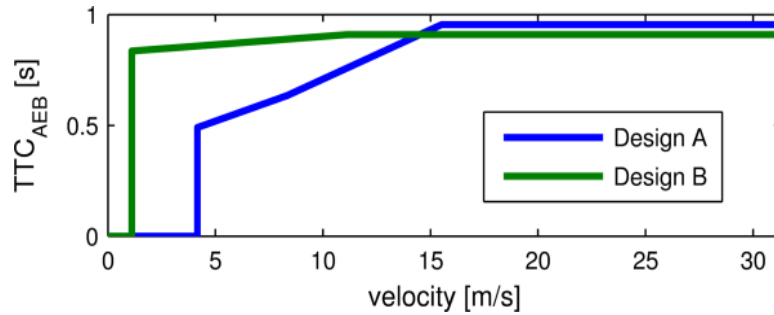


Figure 2.17 AEB triggering threshold dependent on the vehicle speed

Once triggered, AEB aims to achieve a target deceleration a_{AEB} . The build-up of deceleration is subject to a rate limit r_{AEB} as shown in Figure 2.18. The desired a_{AEB} of Design B is -10 m/s^2 . However, in reality, the maximum deceleration may not reach this level due to tire/road conditions. The existence of Anti-lock Braking Systems (ABS) also prevents the longitudinal tire force from reaching its peak value to avoid tires locked-up and losing control of the vehicle. In this research, we set the maximum deceleration to be -8 m/s^2 .

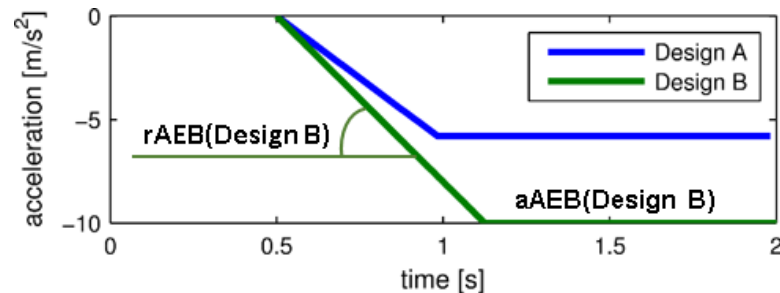


Figure 2.18 Acceleration profiles of the AEB designs

A first order lag with a time constant τ_{AV} is used to model the transfer function from the commanded acceleration to the actual acceleration for simplicity. The roads are assumed to be flat and straight with good adhesion. The effects of tire dynamics, chassis, and braking systems are not considered in this research.

The vehicle and control models presented in the section may not be good representations of the actual systems in the production vehicles. The simulation results thus should not be interpreted as rigorous evaluation results for the two production vehicles. If more accurate simulations are desired, the proposed accelerated evaluation process can be used in junction with more accurate simulation models such as CarSim® [118] and more detailed control algorithms.

2.4.2 Evaluation metrics

Two evaluation metrics were used: crash rate and relative velocity Δv at crash.

A crash happens when $R_L(t) < 0$. The crash rate of N simulations is defined as

$$r_c(N) = \frac{1}{N} \sum_{n=1}^N d_n \quad (2.10)$$

where n is the index of simulation tests, N is the total number of crashes. d_n is the distance travelled in test n , defined as

$$d_n = \int_{t=0}^{t_{crash}} v^{(n)}(t) dt \quad (2.11)$$

where $v^{(n)}(t)$ represents the velocity of AV at time t in the n^{th} test and t_{crash} is the time when the crash happens.

As each test runs under the same stochastic condition, based on the Law of Large Numbers, the sampling average will converge to the expected value when the sample size approaches infinity, i.e.,

$$r_c(n) \rightarrow \mu_c := \mathbb{E}(r_c) \quad \text{for } n \rightarrow \infty. \quad (2.12)$$

Moreover, the Central limit theorem implies that, when n is large, $r_c(n)$ follows the normal distribution $\mathcal{N}(\mu_c, \sigma_c^2)$ approximately.

The simulations continue until the relative error $r_{rel}(n) < b_{rr}$ with a confidence level larger than $(1 - \alpha) * 100\%$ (both b_{rr} and α are small positive number to be selected), i.e.

$$P(r_{rel}(n) < b_{rr}) \geq 1 - \alpha. \quad (2.13)$$

The relative error is defined as

$$r_{rel}(n) = \left| \frac{r_c(n) - \mu_c}{\mu_c} \right| \quad (2.14)$$

which can be approximated by

$$r_{rel}(n) \approx \frac{\hat{\sigma}_{c_n} z_\alpha}{\sqrt{n} r_c(n)} \quad (2.15)$$

where $\hat{\sigma}_{c_n}^2$ is the variance of $\{r_c(1), r_c(2), \dots, r_c(n)\}$. z_α is defined as

$$z_\alpha = \Phi^{-1}(1 - \alpha/2) \quad (2.16)$$

where Φ^{-1} is the quantile function of the standard normal distribution $\Phi(0,1)$.

2.4.1 Simulation results

Each simulation test will start with the same initial values and end when a crash occurs. The average crash rate is calculated after each test. Keep running the car-following tests until the relative error $r_{rel} < 10\%$ with 97 % confident level ($\alpha = 0.03$). The simulation parameters are listed in Table 2.2.

Table 2.2 Parameters the car-following simulation

Var.	Unit	Value	Var.	Unit	Value
a_{L_0}	m/s^2	0	T_{HW}^{desire}	s	2
a_0	m/s^2	0	T_s	s	0.3
a_{T_0}	m/s^2	0	v_0	m/s	20
a^{Max}	m/s^2	8	v_{L_0}	m/s	20
a^{Min}	m/s^2	-8	v_{T_0}	m/s	20
a_L^{Max}	m/s^2	8	v^{Max}	m/s	40
a_L^{Min}	m/s^2	-8	v^{Min}	m/s	5
a_T^{Max}	m/s^2	8	v_L^{Max}	m/s	40
a_T^{Min}	m/s^2	-8	v_L^{Min}	m/s	5
g	m/s^2	9.81	v_T^{Max}	m/s	40
R_{L_0}	m	$T_{HW_d}^{desire} * v_{L_0}$	v_T^{Min}	m/s	5
R_{T_0}	m	$T_{HW_d}^{desire} * v_{T_0}$			

The estimated crash rates are shown in Figure 2.19. The frontal crash and the rear crash are defined as the collisions of the AV with the lead HV and trailing HV respectively. Design B, equipped with a more aggressive algorithm, traveled a longer distance to encounter a frontal crash than Design A. Both designs showed similar rear crash rates.

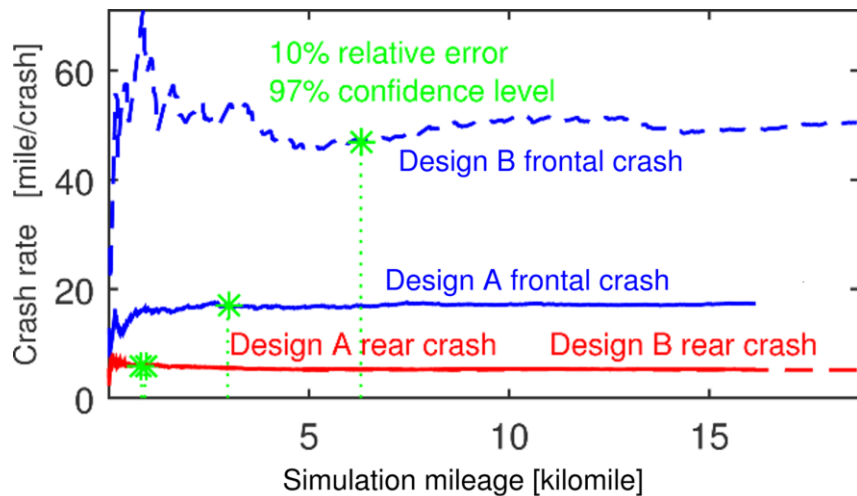


Figure 2.19 Estimated crash rate

The rear crash happens because the trailing HV fails to maintain a safe distance or gets distracted when the AV decelerates. Theoretically, Design B should have a higher rear crash rate since it is equipped with an AEB generating higher decelerations. The reason that the rear crash rates are similar is that the majority of crashes are caused by inattention of the trailing HVs when AV is controlled by ACC. As shown in Figure 2.20, among all the rear crashes, only 2.5 % happens with AEB being activated for Design A and 4.0 % for Design B. Although Design B brakes harder and has $(4 \% - 2.5 \%) / 2.5\% \times 100\% = 60\%$ more rear crashes with AEB on than Design A, because non-AEB-related crashes dominate, the overall rear crash rates of the two designs are similar.

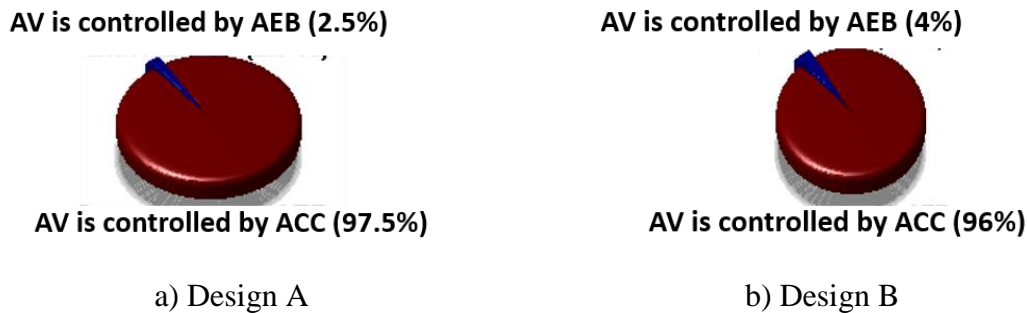


Figure 2.20 Status of AV controller when rear crashes happen

The relative velocity Δv is defined as

$$\Delta v = |\dot{R}_L(t_{crash})|. \quad (2.17)$$

The histograms of relative velocities are shown in Figure 2.21 with means and $\pm\sigma$ error bars. It is shown that Design B has lower Δv than Design A on average in frontal crashes. Both AVs have similar Δv in rear crashes.

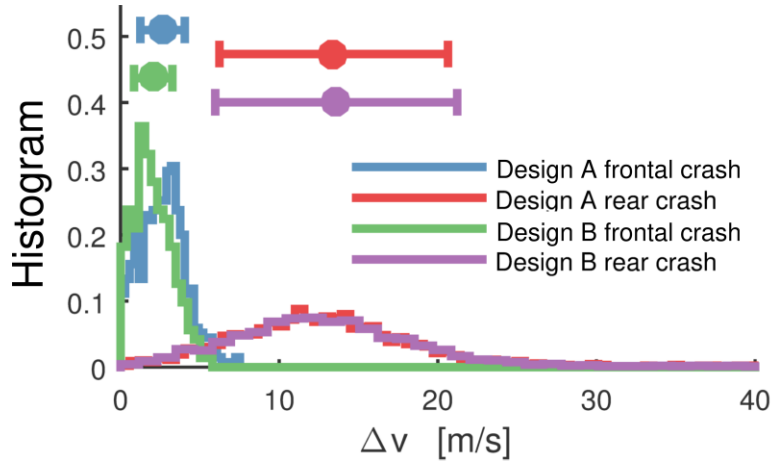


Figure 2.21 Estimation of relative velocity during crash

2.4.2 Benefits and limitations of the proposed method

The benefit of the proposed approach is that it provides a method to generate accelerated test scenarios that have a much higher crash rate based on the analysis of real-world driving statistics. To illustrate the effect of the acceleration, an HV-HV car-following scenario was simulated and compared with the real world crash rate. As shown in Figure 2.22, the two-car model was built by using the lead HV and trailing HV models in the previous sections. With the same accelerated setting, the crash rate between the two was found to be 6.98 miles/crash. In 2013, the average crash rate for the police-reported rear end crash is 0.817 million miles/crash in the U.S. [42, p. 70]. Considering approximately half of the accidents are not reported to the police [42, p. 5], the crash rate was estimated to have increased by roughly $0.817e6/2/6.98=5.85e4$ times in the accelerated test.

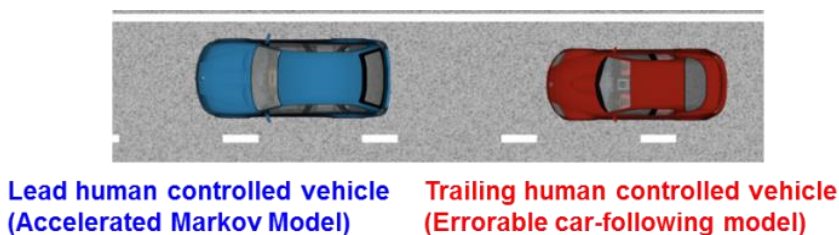


Figure 2.22 Simulation layout for human controlled vehicles

Although this method significantly accelerated the evaluation procedure, it does not provide a direct relationship between crash rate in the accelerated tests and crash rate in the real world. Therefore, this method provides a relative ‘score’ between AVs but may not accurately estimate the absolute value of the crash rate. In the next chapters, we will generalize the method by establishing a rigorous connection between the accelerated test results and real world performance.

2.5 Summary

A procedure to accelerate the evaluation of AVs using naturalistic driving data was developed in this Chapter. The general idea is to reduce the frequent events that are not safety critical in the daily driving so that a higher level of exposure to critical scenarios is achieved. This method can accelerate the evaluation procedure and the acceleration rate can be controlled by changing the probability density function that is eliminated. Two AVs equipped with ACC and AEB were designed based on production vehicles to demonstrate the accelerated evaluation approach. The simulation results showed that the overall evaluation time was reduced by a factor of 5.85e4.

CHAPTER 3

ACCELERATED EVALUATION BASED ON IMPORTANCE SAMPLING TECHNIQUES

3.1 Introduction

In this chapter, we introduce a new accelerated evaluation method to calculate the real-world benefits from the accelerated test results with a rigorous mathematical basis. The fundamental efficiency limitations of Monte Carlo simulations are first analyzed. A statistical framework of the Accelerated Evaluation is then established based on the Importance Sampling techniques. Frontal collision due to unsafe cut-ins is used as the target crash scenario to demonstrate the proposed approach.

3.2 Importance Sampling Techniques

3.2.1 Limitations of the Monte Carlo approach

Monte Carlo simulations [119] aim to generate unbiased statistical samples for a stochastic process. To analyze the Monte Carlo method, let us start by introducing some mathematical notations. Let Ω be the sample space for all possible events, and $\mathcal{E} \subset \Omega$ be the rare events of interest, i.e., the occurrence of a crash. Let \mathbf{x} be a random vector describing the motions of surrounding HVs. The indicator function of the event \mathcal{E} is defined as

$$I_{\mathcal{E}}(\mathbf{x}) = \begin{cases} 1, & \text{if } \mathbf{x} \in \mathcal{E} \\ 0, & \text{otherwise} \end{cases}. \quad (3.1)$$

Our task is to estimate the probability of \mathcal{E} happening, i.e.

$$\gamma = \mathbb{P}(\mathcal{E}) = \mathbb{E}(I_{\mathcal{E}}(\mathbf{x})). \quad (3.2)$$

The Monte Carlo approach generates independent and identically distributed samples $\mathbf{x}_1, \mathbf{x}_2, \dots, \mathbf{x}_n$ of \mathbf{x} , and then calculate the sample average

$$\hat{\gamma}_n = \frac{1}{n} \sum_{i=0}^n I_{\mathcal{E}}(\mathbf{x}_i). \quad (3.3)$$

We state some statistical properties of Monte Carlo method. First, under mild conditions, the Strong Law of Large Numbers [119] holds, i.e.

$$\mathbb{P} \left(\lim_{n \rightarrow \infty} \hat{\gamma}_n = \gamma \right) = 1. \quad (3.4)$$

Moreover, the Central Limit Theorem [119] states that, when n is large, $\hat{\gamma}_n$ follows approximately the normal distribution $\mathcal{N}(\mathbb{E}(\hat{\gamma}_n), \sigma^2(\hat{\gamma}_n))$ with mean

$$\mathbb{E}(\hat{\gamma}_n) = \mathbb{E} \left(\frac{1}{n} \sum_{i=0}^n I_{\mathcal{E}}(\mathbf{x}_i) \right) = \gamma \quad (3.5)$$

and variance

$$\sigma^2(\hat{\gamma}_n) = \text{Var}(\hat{\gamma}_n) = \text{Var} \left(\frac{1}{n} \sum_{i=0}^n I_{\mathcal{E}}(\mathbf{x}_i) \right) = \frac{1}{n^2} \sum_{i=0}^n \text{Var}(I_{\mathcal{E}}(\mathbf{x}_i)) = \frac{\gamma(1-\gamma)}{n}. \quad (3.6)$$

The accuracy of the estimation is represented by the relative half-width. With the Confidence Level at $100(1 - \alpha)\%$, the relative half-width of $\hat{\gamma}_n$ is defined as

$$l_r = \frac{l_\alpha}{\gamma} \quad (3.7)$$

where l_α is the half-width given by

$$l_\alpha = z_\alpha \sigma(\hat{\gamma}_n) \quad (3.8)$$

and z_α is the quartile of standard normal distribution with significance level α defined as

$$z_\alpha = \Phi^{-1}(1 - \alpha/2) \quad (3.9)$$

where Φ^{-1} is the quantile function of the standard normal distribution $\Phi(0,1)$. The target of estimation accuracy is to ensure l_r is smaller than a constant β , it can be shown that

$$\frac{l_\alpha}{\gamma} = \frac{z_\alpha \sigma(\hat{\gamma}_n)}{\gamma} = \frac{z_\alpha}{\gamma} \sqrt{\frac{\gamma(1-\gamma)}{n}} = z_\alpha \sqrt{\frac{1-\gamma}{\gamma n}} \leq \beta \quad (3.10)$$

which implies

$$n \geq \frac{z_\alpha^2}{\beta^2} \cdot \frac{1-\gamma}{\gamma}. \quad (3.11)$$

The reason that the Monte Carlo approach is slow is because it takes many samples to build a confidence interval that has a satisfactory half-width. As shown in Eq. (3.11), when \mathcal{E} is rare, *i.e.* $\gamma \rightarrow 0$, the required test number n goes to infinity.

3.2.2 Importance Sampling techniques

The Importance Sampling (IS) theory provides techniques aiming to reduce the required test numbers in Eq. (3.11) that are effective in handling rare events with general overviews in [120]–[123]. IS has been successfully applied to evaluate critical events in reliability [124], finance [125], insurance [126], earthquake [127], and telecommunication networks [128]. The mathematical foundation and the implementation of this technique have been mostly studied from the viewpoint of these domains. The research in this dissertation first applies this technique to AV evaluation.

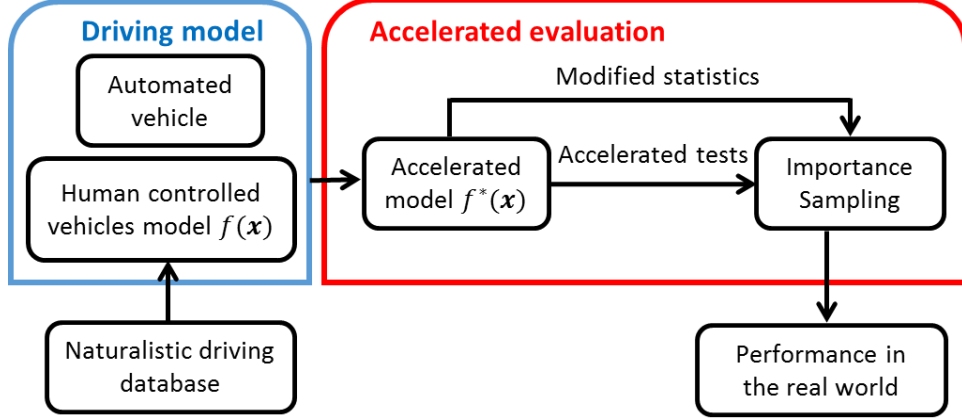


Figure 3.1 Procedure of the Accelerated Evaluation method based on Importance Sampling techniques

We describe the IS techniques as follows. Let $f(\mathbf{x})$ be the original joint density function of the random vector \mathbf{x} . The core idea of IS is to replace $f(\mathbf{x})$ with a new density $f^*(\mathbf{x})$ (named as the AE distribution) that has a higher likelihood for the rare events to happen. Using a different distribution leads to biased samples, and the advantage of IS is to provide a mechanism to compensate for this bias. The IS techniques are very suitable for Accelerated Evaluation, in which probabilistic distributions of HVs are modified to enhance the interactions between AV and HVs. IS provides a mathematical basis to guarantee the statistical equivalence of the accelerated tests and naturalistic driving. The Accelerated Evaluation procedure is described in Figure 3.1.

We define the likelihood ratio L (mathematically named as the Radon-Nikodym derivative [129]) as

$$L(\mathbf{x}) = \frac{f(\mathbf{x})}{f^*(\mathbf{x})}. \quad (3.12)$$

The probability of \mathcal{E} satisfies

$$\begin{aligned}
\mathbb{P}(\mathcal{E}) &= \mathbb{E}_f(I_{\mathcal{E}}(\mathbf{x})) \\
&= \int I_{\mathcal{E}}(\mathbf{x})f(\mathbf{x})d\mathbf{x} \\
&= \int [I_{\mathcal{E}}(\mathbf{x})L(\mathbf{x})]f^*(\mathbf{x})d\mathbf{x} \\
&= \mathbb{E}_{f^*}(I_{\mathcal{E}}(\mathbf{x})L(\mathbf{x})).
\end{aligned} \quad (3.13)$$

One required condition for Eq. (3.13) to hold is that $f^*(\mathbf{x})$ must be absolutely continuous with respect to $f(\mathbf{x})$ within \mathcal{E} , i.e.

$$\forall \mathbf{x} \in \mathcal{E}: f^*(\mathbf{x}) = 0 \Rightarrow f(\mathbf{x}) = 0 \quad (3.14)$$

which guarantees the existence of L in Eq. (3.13). The IS sample is $I_{\mathcal{E}}(\mathbf{x}_i)L(\mathbf{x}_i)$ where \mathbf{x}_i is generated under $f^*(\mathbf{x})$, which is an unbiased estimator for γ . The overall IS estimator for n tests is then

$$\hat{\gamma}_n = \frac{1}{n} \sum_{i=0}^n I_{\mathcal{E}}(\mathbf{x}_i)L(\mathbf{x}_i). \quad (3.15)$$

Note that although a continuous distribution function is used in this paper, similar approaches can be applied to discrete distributions as well.

Now consider the relative half-width constructed by the IS

$$\begin{aligned} l_r &= \frac{l_\alpha}{\gamma} = \frac{z_\alpha \sigma(\hat{\gamma}_n)}{\gamma} = \frac{z_\alpha \sqrt{\mathbb{E}_{f^*}(\hat{\gamma}_n^2) - \mathbb{E}_{f^*}^2(\hat{\gamma}_n)}}{\gamma \sqrt{n}} \\ &= \frac{z_\alpha \sqrt{\mathbb{E}_{f^*}(I_{\mathcal{E}}^2(\mathbf{x}) L^2(\mathbf{x})) - \gamma^2}}{\gamma \sqrt{n}} \\ &= \frac{z_\alpha}{\sqrt{n}} \sqrt{\frac{\mathbb{E}_{f^*}(I_{\mathcal{E}}^2(\mathbf{x}) L^2(\mathbf{x}))}{\gamma^2} - 1} \leq \beta. \end{aligned} \quad (3.16)$$

The required minimum test number is then

$$n \geq \frac{z_\alpha^2}{\beta^2} \left(\frac{\mathbb{E}_{f^*}(I_{\mathcal{E}}^2(\mathbf{x}) L^2(\mathbf{x}))}{\gamma^2} - 1 \right). \quad (3.17)$$

When $f^*(x)$ is properly chosen, $\mathbb{E}_{f^*} \left(I_{\xi}^2(x) L^2(x) \right)$ can be close to γ^2 , resulting in a smaller number of tests (i.e., the evaluation is accelerated).

3.3 Evaluation of AV in Lane Change Scenario using Importance Sampling

The lane change (cut-in) scenario is used as an example to show the benefits of the proposed Accelerated Evaluation method. Lane change, defined as a vehicle moving from one lane to another in the same direction of travel [27], can cause a frontal collision crash for the following vehicle when the time gap is too short. Successful completion of a lane change requires attention to the vehicles in both the original lane and the adjacent lane [130]. In the US, there are between 240,000 and 610,000 reported lane-change crashes, resulting in 60,000 injuries annually [27]. However, few protocols have been published regarding the evaluation of AV functions (e.g., AEB systems) under lane change scenarios. Therefore, we aim to develop such an evaluation procedure based on the Accelerated Evaluation approach in this research.

3.3.1 Extraction of lane changes events from the naturalistic driving database

Human drivers' lane change behaviors have been analyzed and modeled for more than half a century. Early studies based on controlled experiments usually have short test horizons and limited control settings [131]. More recently, researchers started to use large scale N-FOT databases to model the lane change behaviors. Lee et al. [131] examined steering, turn signal and brake pedal usage, eye glance patterns, and safety envelope of 500 lane changes. The 100-Car Naturalistic Driving Study analyzed lane change events leading to rear-end crashes and near-crashes [27]. Zhao et al. [132] analyzed the safety critical variables in mandatory and discretionary lane changes for heavy trucks [31]. Most of these studies are based on hundreds of lane changes. To build a more accurate model, we use the data collected in the Safety Pilot Model Deployment (SPMD) project [34], which contains more than 400,000 lane changes.

In this research, we developed a lane change statistical model and demonstrated its usage for accelerated evaluation of a frontal collision avoidance algorithm. The data used

is from the SPMD database. The SPMD program aims to demonstrate connected vehicle technologies in a real-world environment. It recorded naturalistic driving of 2,842 equipped vehicles in Ann Arbor, Michigan for more than two years. As of April 2015, 34.9 million miles were logged, making SPMD one of the largest public N-FOT databases ever.

As shown in Figure 3.2, a lane change was detected and recorded by an SPMD vehicle when the Lane Change Vehicle (LCV) crosses the lane markers. In the SPMD program, 98 sedans are equipped with a data acquisition system and MobilEye® [133], which provides: a) relative position to the lane change vehicle (range), and b) lane tracking measures pertaining to the lane delineation both from the painted boundary lines and road edge characteristics. The error of range measurement is around 10 % at 90 m and 5 % at 45 m [134].

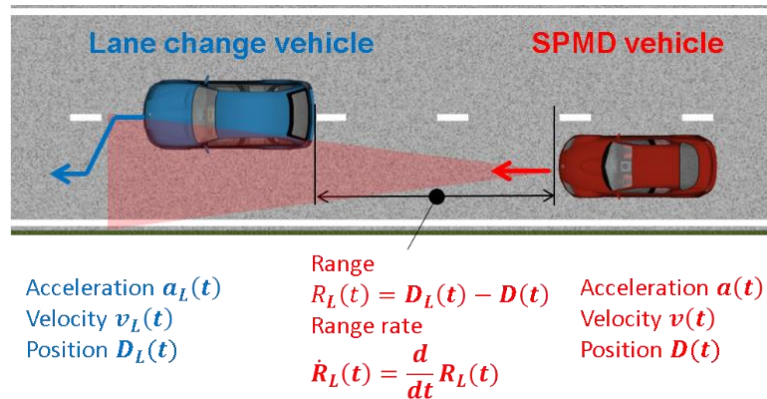


Figure 3.2 Lane change scenarios that may cause frontal crashes

The following criteria were applied to ensure consistency of the used dataset:

- $v(t_{LC}) \in (2 \text{ m/s}, 40 \text{ m/s})$
- $v_L(t_{LC}) \in (2 \text{ m/s}, 40 \text{ m/s})$
- $R_L(t_{LC}) \in (0.1 \text{ m}, 75 \text{ m})$

where t_{LC} is the time when the center line of the LCV crosses the lane markers; v_L and v are the velocities of the LCV and the SPMD vehicle; R_L is the range defined as the distance between the rear edge of the LCV and the front edge of the SPMD vehicle. 403,581 lane changes were detected in total. Figure 3.3 shows the locations of the identified lane changes.

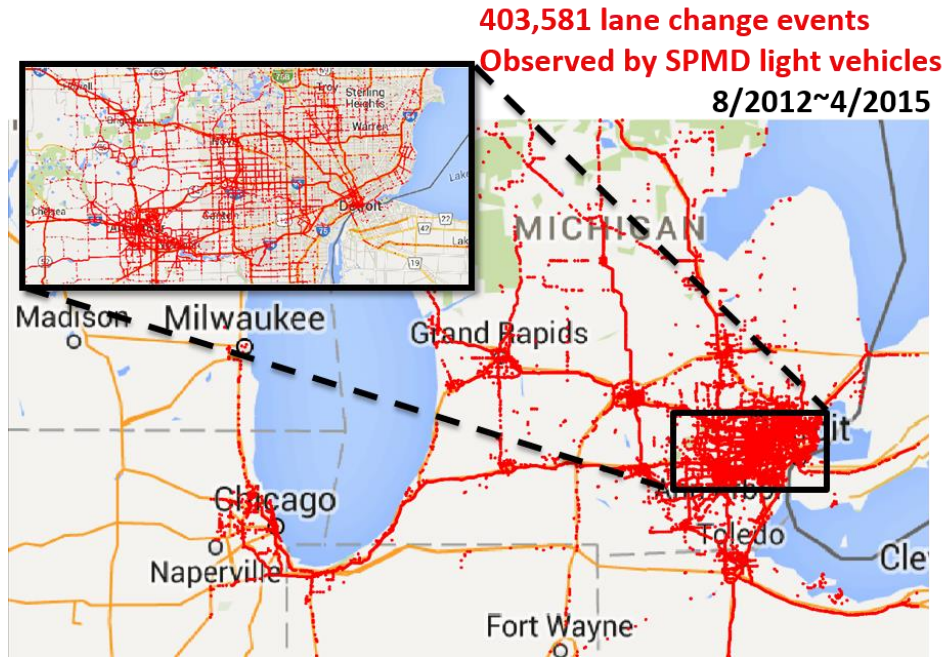


Figure 3.3 Recorded lane change events in the SPMD database

3.3.2 Lane changes model

A lane change can be divided into three phases: the decision to initiate a lane change, gap (range) acceptance, and lane change execution [131]. In this research, we focus on the effects of gap acceptance which is used in safety assessments to indicate safe lane change distance or time headway [135]. The gap acceptance is mainly captured by three variables: $v_L(t_{LC})$, $R_L(t_{LC})$ and Time To Collision (TTC) of AVs, defined as

$$TTC_L = -\frac{R_L}{\dot{R}_L} \quad (3.18)$$

where \dot{R}_L is the derivative of R_L . In the following, unless mentioned specifically, v_L , R_L and TTC_L are the variables at t_{LC} .

The distribution of v_L denoted as $f_{v_L}(x)$ is shown in Figure 3.4. The division of highways and local roads is embodied in the bimodal shape of the histogram. v_L is assumed to remain constant during the lane change. Only the events with a negative range rate are used to build the lane change model. Out of 403,581 lane change events, 173,692 are with negative range rates.

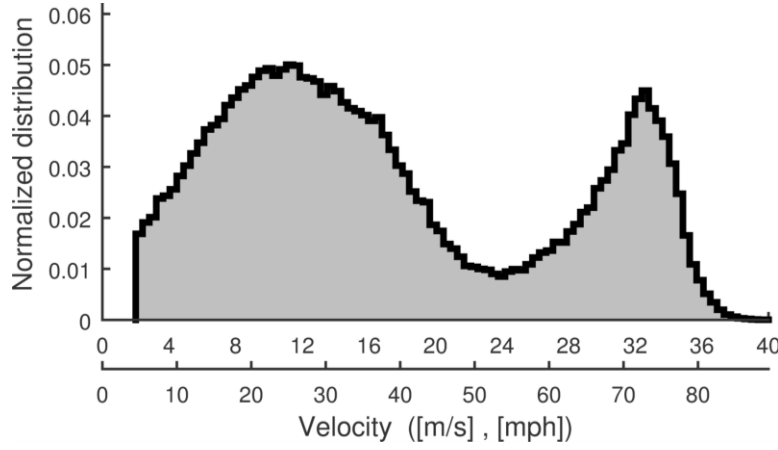


Figure 3.4 Distribution of vehicle speed of the cut-in vehicle in the lane change scenario

To capture the influence of vehicle speed v_L and range and TTC, we divided lane change events into low, medium and high speed conditions. Figure 3.5 shows the empirical distributions of the range reciprocal (denoted as R_L^{-1}) in different speed intervals. It is shown that v_L has little influence on the distribution of R_L^{-1} .

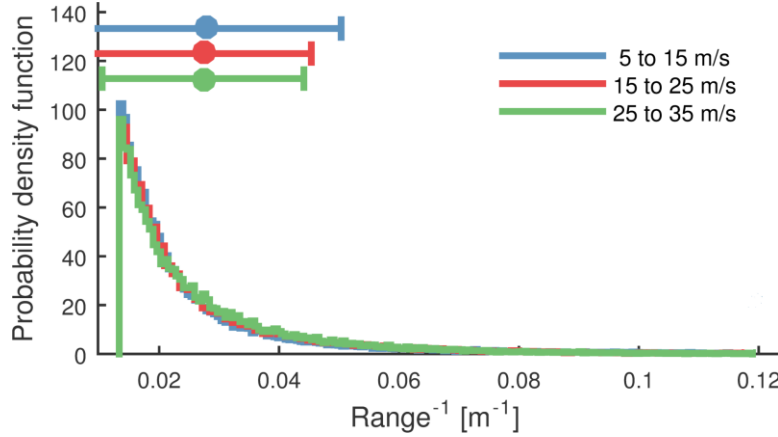


Figure 3.5 Distributions of the reciprocal of the range at the lane change moment

Figure 3.6 illustrates the fitting of R_L^{-1} using a Pareto distribution defined as

$$f_{R_L^{-1}}(x | k_{R_L^{-1}}, \sigma_{R_L^{-1}}, \mu_{R_L^{-1}}) = \frac{1}{\sigma_{R_L^{-1}}} \left(1 + k_{R_L^{-1}} \frac{x - \mu_{R_L^{-1}}}{\sigma_{R_L^{-1}}} \right)^{-1-1/k_{R_L^{-1}}} \quad (3.19)$$

where the shape parameter $k_{R_L^{-1}}$, the scale parameter $\sigma_{R_L^{-1}}$, and the threshold parameter $\mu_{R_L^{-1}}$ are all positive. The Matlab® function “*gpdfit*” is used in the fitting based on Expectation-Maximization approach [100].

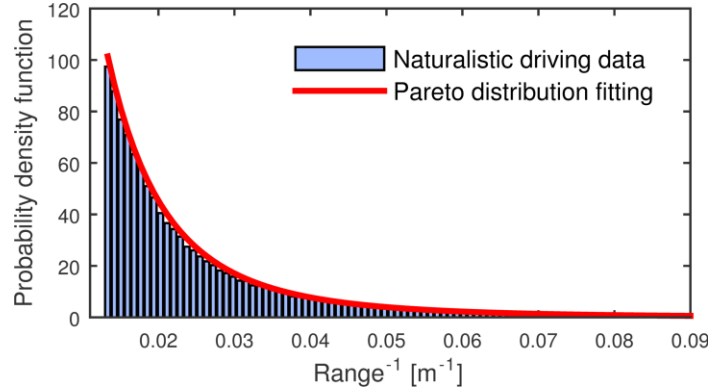


Figure 3.6 Distribution of the reciprocal of range fitted with the Pareto distribution

The empirical distributions of TTC_L^{-1} in different speed intervals are shown in Figure 3.7. As the vehicle speed increases, the mean of TTC_L^{-1} decreases. TTC_L^{-1} can be approximated by an exponential distribution

$$f_{TTC_L^{-1}}(x | \lambda_{TTC_L^{-1}}) = \frac{1}{\lambda_{TTC_L^{-1}}} e^{-x/\lambda_{TTC_L^{-1}}} \quad (3.20)$$

where the scaling factor $\lambda_{TTC_L^{-1}}$ varies with the speed of the LCV.

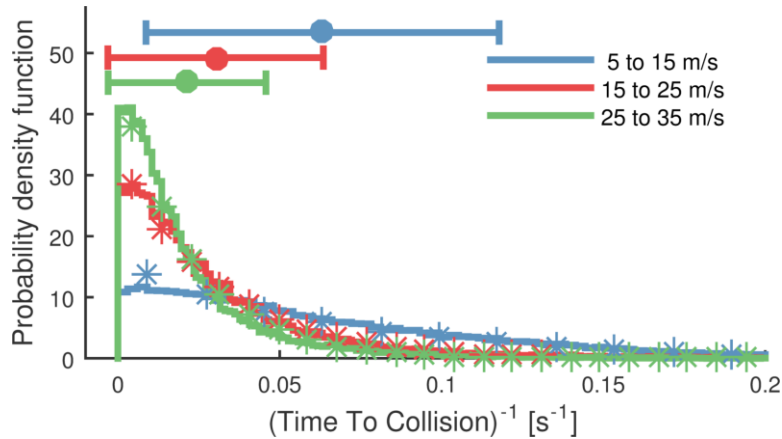


Figure 3.7 Distributions of the reciprocal of the Time To Collision at the lane change moment

The dependence of $\lambda_{TTC_L^{-1}}$ on vehicle speed is shown in Figure 3.8. As the vehicle speed increases, $\lambda_{TTC_L^{-1}}$ decreases. The blue circles represent $\lambda_{TTC_L^{-1}}$ at the center point of each v_L interval. We use linear interpolation and extrapolation to create smooth $\lambda_{TTC_L^{-1}}$ for all vehicle speeds.

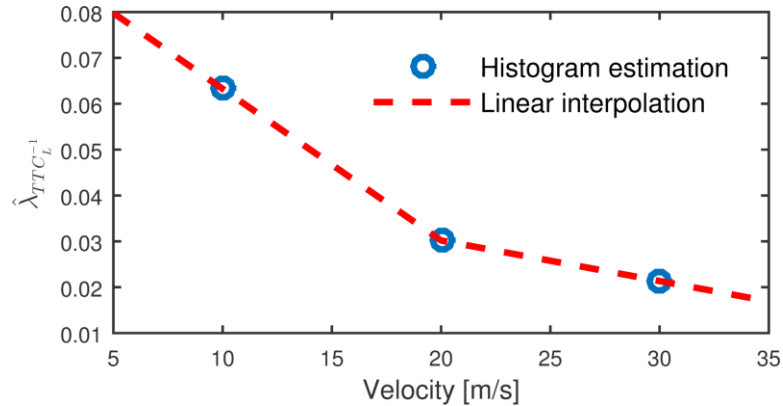


Figure 3.8 Interpolation/extrapolation of the parameters of Time To Collision at different velocities

The effect of range on TTC is limited, as can be seen in Figure 3.9. This indicates that R_L and TTC_L can be modeled independently given the same v_L .

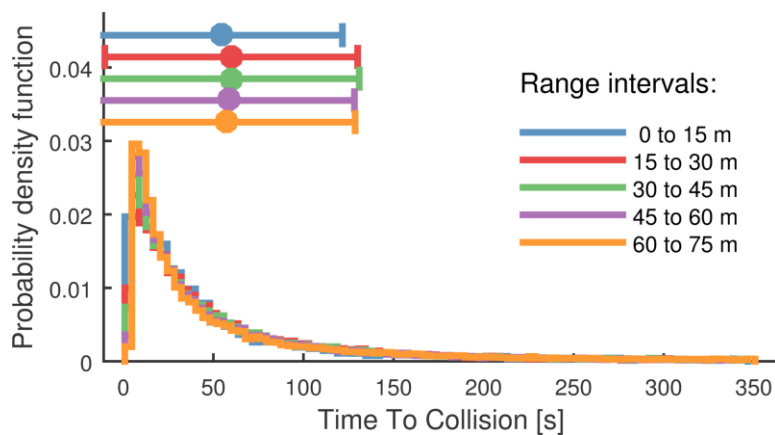


Figure 3.9 Distribution of Time To Collision in different range intervals

\dot{R}_L can then be calculated from Eq. (3.21).

$$\dot{R}_L = -\frac{TTC_L^{-1}}{R_L^{-1}} \quad (3.21)$$

Finally, the velocity of the host vehicle v can be calculated from

$$v = v_L - \dot{R}_L. \quad (3.22)$$

In summary, the lane change events are generated in the following order: a) generate v_L based on the empirical distributions $f_{v_L}(x)$ shown in Figure 3.4; b) generate R_L^{-1} using $f_{R_L^{-1}}(x|k_{R_L^{-1}}, \sigma_{R_L^{-1}}, \mu_{R_L^{-1}})$ shown in Figure 3.6; c) generate TTC_L^{-1} using $f_{TTC_L^{-1}}(x|v_L)$ shown in Figure 3.8; and finally d) calculate v using Eqs. (3.21) and (3.22).

3.3.3 Accelerated Evaluation of AV in the lane change scenario

The lane change scenario is modeled as a slower lane changing vehicle cut-in in front of an AV as shown in Figure 3.2. The events of interest are defined as

$$\mathcal{E} = \{\min(R_L(t)) < R_\epsilon | t_{LC} < t \leq t_{LC} + T_{LC}\} \quad (3.23)$$

where T_{LC} represents duration of the lane change test; R_ϵ is the critical range. Eq. (3.23) means that if the minimum range is smaller than R_ϵ anytime during the lane change event, this lane change belongs to the \mathcal{E} set.

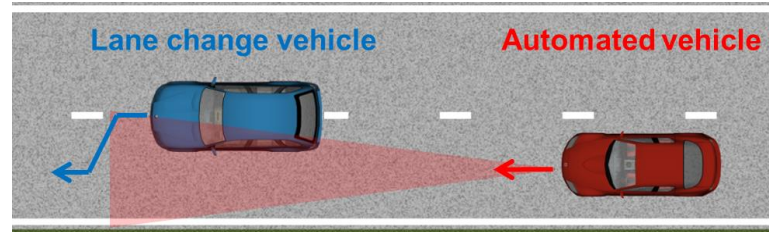


Figure 3.10 Lane change scenario for AV evaluation

The random vector \mathbf{x} consists of three random variables $[v_L, TTC_L^{-1}, R_L^{-1}]$. v_L is generated using the empirical distributions $f_{v_L}(x)$ shown in Figure 3.4. The IS approach considers the modified probability density functions of TTC_L^{-1} and R_L^{-1} denoted by $f_{TTC_L^{-1}}^*(\mathbf{x})$ and $f_{R_L^{-1}}^*(\mathbf{x})$. Because the independence of R_L and TTC_L shown in Figure 3.9,

$$\begin{aligned} f(\mathbf{x}) &= \mathbb{P}(R_L^{-1} = m, TTC_L^{-1} = n, v_L = l) \\ &= \mathbb{P}(R_L^{-1} = m)\mathbb{P}(TTC_L^{-1} = n|v_L = l)\mathbb{P}(v_L = l) \\ &= f_{R_L^{-1}}(m)f_{TTC_L^{-1}}(n|v_L = l)f_{v_L}(l). \end{aligned} \quad (3.24)$$

Similarly, the AE distribution

$$f^*(\mathbf{x} = [m, n]) = f_{R_L^{-1}}^*(m)f_{TTC_L^{-1}}^*(n|v_L = l)f_{v_L}(l) \quad (3.25)$$

The likelihood ratio is then calculated from

$$L(R_L^{-1} = m, TTC_L^{-1} = n, v_L = l) = \frac{f(\mathbf{x})}{f^*(\mathbf{x})} = \frac{f_{R_L^{-1}}(m)f_{TTC_L^{-1}}(n|v_L = l)}{f_{R_L^{-1}}^*(m)f_{TTC_L^{-1}}^*(n|v_L = l)}. \quad (3.26)$$

From Eq. (3.13), the probability of \mathcal{E} can be estimated as

$$\mathbb{P}(\mathcal{E}) = \mathbb{E}_f(I_{\mathcal{E}}(\mathbf{x})) = \mathbb{E}_{f^*}(I_{\mathcal{E}}(\mathbf{x})L(\mathbf{x})) \approx \widehat{\mathbb{E}}_{f^*}(I_{\mathcal{E}}(\mathbf{x})L(\mathbf{x})) \quad (3.27)$$

where $\widehat{\mathbb{E}}_{f^*}(\cdot)$ denotes the empirical average.

3.4 Simulation Analysis

The estimation of the benefits of AV in crash and injury events are used to demonstrate the effectiveness of the proposed Accelerated Evaluation approach.

3.4.1 Analysis of crash events

A crash event occurs when the range becomes negative within T_{LC} after the lane change such that

$$\mathcal{E}_c = \{\min(R_L(t)) < 0 \mid t_{LC} < t \leq t_{LC} + T_{LC}\}. \quad (3.28)$$

To accelerate the evaluation procedure, $f_{TTC_L^{-1}}$ is modified to be

$$f_{TTC_L^{-1}}^*(x) = \frac{1}{\lambda_{TTC_L^{-1}} - \theta_{TTC_L^{-1}}} e^{-\frac{x}{\lambda_{TTC_L^{-1}} - \theta_{TTC_L^{-1}}}} \quad (3.29)$$

and $f_{R_L^{-1}}$ is modified as

$$f_{R_L^{-1}}^*(x) = \frac{1}{\sigma_{R_L^{-1}}} \left(1 + (k_{R_L^{-1}} - \theta_{R_L^{-1}}) \frac{x - \mu_{R_L^{-1}}}{\sigma_{R_L^{-1}}} \right)^{-1 - \frac{1}{k_{R_L^{-1}} - \theta_{R_L^{-1}}}} \quad (3.30)$$

where $\theta_{TTC_L^{-1}} = 0.8$ and $\theta_{R_L^{-1}} = 0.3$. Here the parameters are tuned manually. In the next chapter, we will introduce an adaptive method to calculate the optimal parameters of the AE distribution.

The Design B developed in Section 2.4.1 is used as the AV model. Both accelerated and the non-accelerated simulations (crude Monte Carlo approach) were conducted to demonstrate the performance and validity of the proposed approach. Figure 3.11 shows that estimated crash rate in accelerated and naturalistic driving conditions. The statistical features from the Accelerated Evaluation simulations converge to the results under naturalistic driving conditions, which demonstrates that the Accelerated Evaluation approach is statistically unbiased.

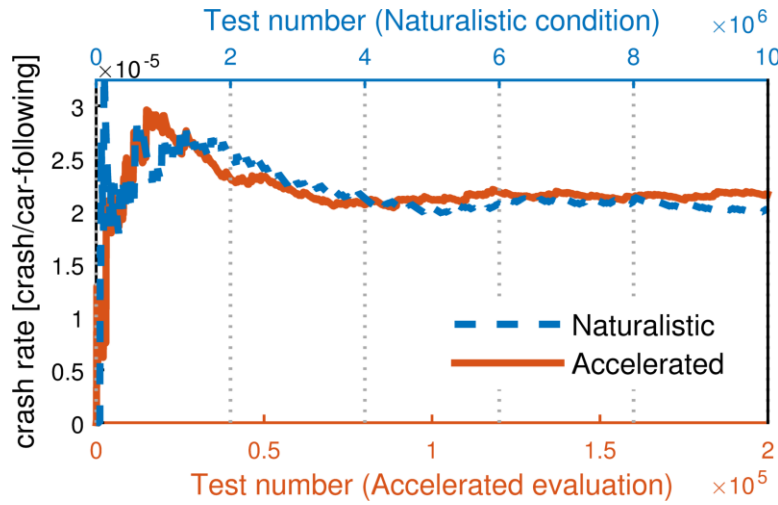


Figure 3.11 Estimation of crash rate in the lane change scenario

The convergence is reached when the relative half-width l_r (defined in Section 3.2.1) is below $\beta = 0.2$ with 80% confidence. Figure 3.12 shows that the accelerated tests achieve this confidence level after $N_{acc} = 1.14e5$ simulations, while the naturalistic simulations take $N_{nature} = 6.13e6$ simulations to converge.

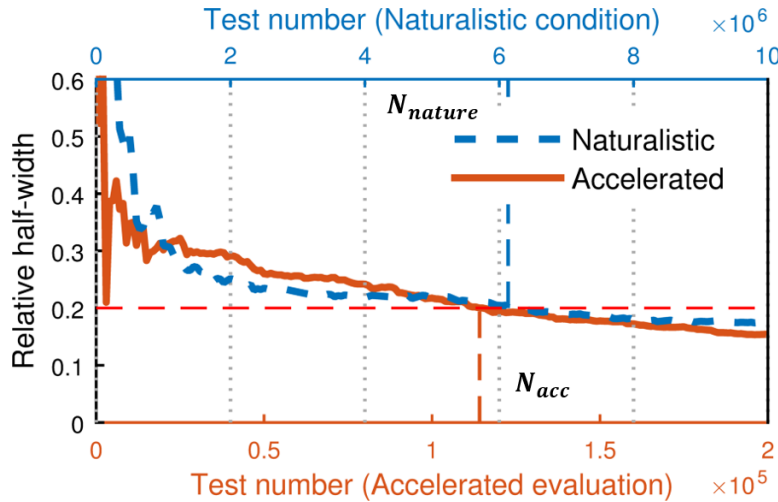


Figure 3.12 Convergence of crash rate estimation in the lane change scenario

In the SPMD database, during 1,325,964 miles naturalistic driving, 173,592 lane changes with negative range rates were found. The frequency of negative range rate lane change is estimated to be

$$r_{lc} = \frac{1,325,964}{173,592} = 7.64 \text{ [mile/lane change].} \quad (3.31)$$

The driving distance needed in naturalistic test is thus

$$D_{nature} = r_{lc} \cdot N_{nature} = 4.71e7 \text{ miles.} \quad (3.32)$$

The test distance in the Accelerated Evaluation is

$$D_{acc} = \sum_{n=1}^{N_{acc}} \int_{t=t_{LC}}^{t_{LC}+\mathcal{T}_{LC}} v^{(n)}(t) dt = 7.48e3 \text{ miles} \quad (3.33)$$

where $v^{(n)}(t)$ represents the velocity of AV at time t in the n_{th} test and the termination time

$$\mathcal{T}_{LC} = \min\{\min(t | R_L(t) < 0), T_{LC}\}. \quad (3.34)$$

The accelerated rate is defined as

$$r_{acc} = \frac{D_{nature}}{D_{acc}} = 6.30e3 \quad (3.35)$$

which is achieved by the application of IS as well as using the modeling of lane change scenarios.

It is noted that the N_{acc} vary with different choices of confidence level $(1 - \alpha)$ and the threshold of the relative half-width β . Substituting Eq. (3.9) to Eq. (3.17), we have

$$N_{acc} \propto \frac{\Phi^{-1} \left(1 - \frac{\alpha}{2}\right)^2}{\beta^2}. \quad (3.36)$$

N_{acc} is proportional to the square of the function $\Phi^{-1}(1 - \alpha/2)$ and the inverse of the square of β . Figure 3.13 shows a numerical example of the influence of the confidence level on N_{acc} and relative error r_{rel} (defined in Eq. (2.14), where the expectation of the

crash rate μ_c is approximated by the crash rate calculating from all 2e5th accelerated test) with $\beta = 0.2$. It can be seen that as the confidence level increases N_{acc} increases almost linearly yet r_{rel} decreases slowly after $1 - \alpha > 80\%$. In a real world evaluation, α and β can be chosen based on time/budget constraints. In this dissertation, we choose $1 - \alpha = 80\%$ and $\beta = 0.2$.

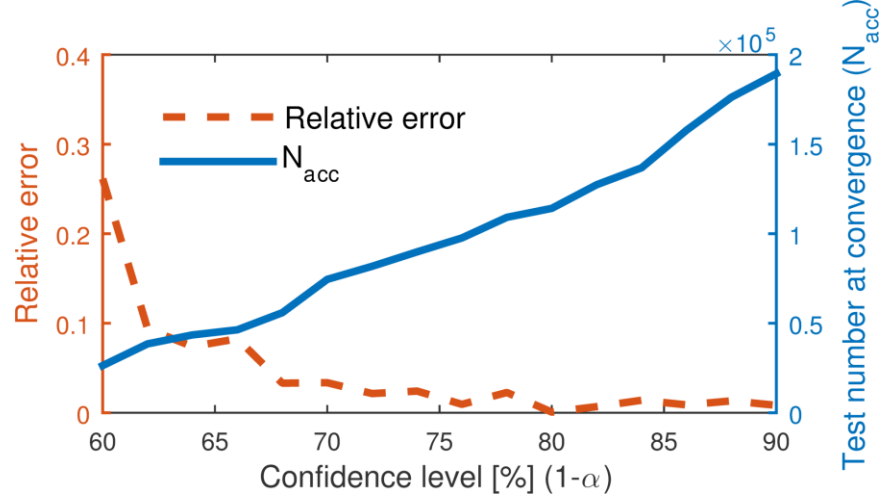


Figure 3.13 Influence of the confidence level on the relative error and test number at convergence

3.4.2 Analysis of injury events

Injury rate is another important indicator of the performance of AVs. Here we focus on injuries with the Maximum Abbreviated Injury Score [136] equal or larger than 2 (MAIS2+), representing moderate-to-fatal injuries. The probability of injury is related to the relative velocity at the crash time t_{crash}

$$\Delta v = -\dot{R}_L(t_{crash}) > 0. \quad (3.37)$$

The probability of moderate-to-fatal injuries for the AV passengers is estimated by a nonlinear model

$$P_{inj}(\Delta v) = \begin{cases} \frac{1}{1 + e^{-(\beta_0 + \beta_1 \Delta v + \beta_2)}} & \text{crash} \\ 0 & \text{no crash} \end{cases} \quad (3.38)$$

which was proposed by Kusano and Gabler [137], and is shown in Figure 3.14 with parameters $\beta_0 = -6.068$, $\beta_1 = 0.1$, and $\beta_2 = -0.6234$. Δv is in the unit of [km/h]. The injury rate $E(P_{inj}(\Delta v))$ is estimated as

$$\mathbb{E}(P_{inj}(\Delta v)) = \widehat{\mathbb{E}}_{f^*}(P_{inj}(\Delta v)) \approx \frac{1}{n} \sum_{i=0}^{N_{acc}} P_{inj}(\Delta v(\mathbf{x}_n)) L(\mathbf{x}_n) \quad (3.39)$$

where \mathbf{x}_n represents the random variables $([v_L, TTC_L^{-1}, R_L^{-1}])$ in the n^{th} simulation.

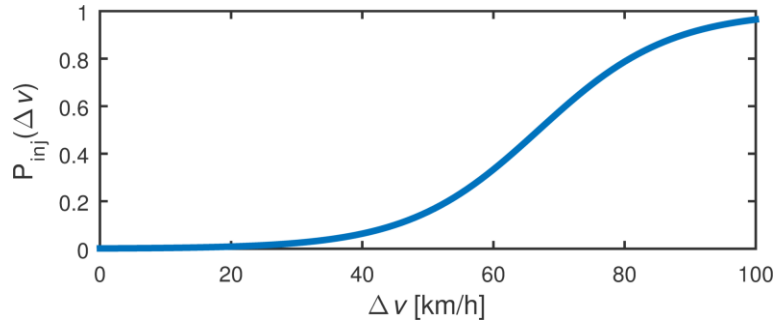


Figure 3.14 Moderate-to-fatal injury model for forward collisions

Figure 3.15 shows that estimated injury rate in the accelerated test converges to the result under naturalistic driving conditions, demonstrating that the Accelerated Evaluation approach is unbiased in the injury index evaluation.

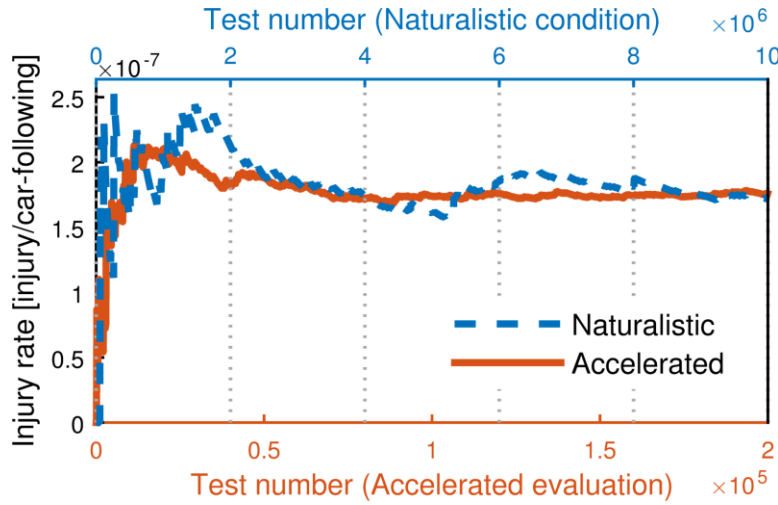


Figure 3.15 Estimation of injury rate in the lane change scenario

The convergence is reached when the relative half-width l_r (defined in Eq. (3.7)) is below $\beta = 0.2$ with 80% confidence. Figure 3.16 shows that the accelerated tests achieve this confidence level after $N_{acc} = 7.41\text{e}4$ simulations, while the naturalistic simulations take $N_{nature} = 6.12\text{e}6$ simulations to converge.

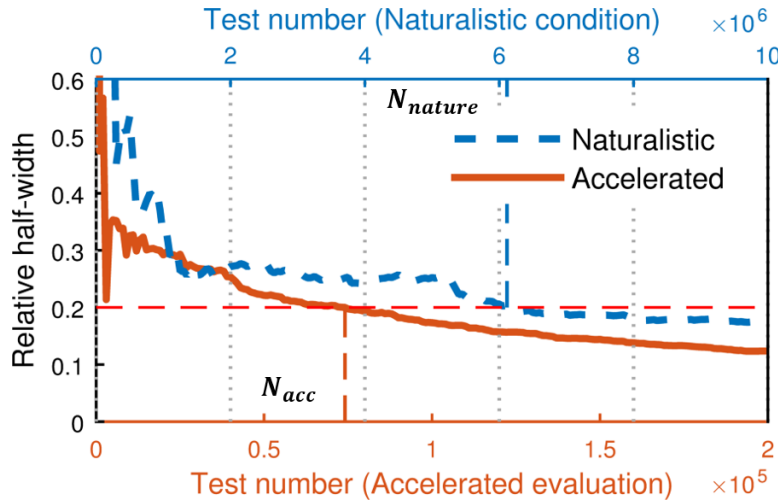


Figure 3.16 Convergence of injury rate estimation in the lane change scenario

The accelerated rates of crash and injury events are summarized in Table 3.1. The accelerated rates of injuries are higher than that of crashes. This is because injuries occur with lower probabilities than crashes. In general, the IS techniques provide larger accelerated rate when target events are rarer.

Table 3.1 Accelerated rates of crash and injury events

	D_{nature}	D_{acc}	r_{acc}
	mile	mile	-
Crash	4.71e7	7.48e3	6.30e3
Injury	4.70e7	4.85e3	9.70e3

3.5 Summary

In this chapter, we propose an approach to accelerating the evaluation of AVs based on Importance Sampling technologies. Lane change scenarios with the human-controlled vehicles making unsafe cut-ins were used to demonstrate the approach. Lane changes models are modeled based on over 400,000 lane changes events collected by the University of Michigan Safety Pilot Model Deployment Program. The acceleration is achieved by using skewed statistics of collected human driver behaviors, which generate risky test scenarios. By using Importance Sampling, the statistical information is preserved so that the safety benefits of AVs in non-accelerated cases can be accurately calculated. The occurrence of crashes and injuries of a modeled automated vehicle are calculated to demonstrate the approach.

CHAPTER 4

ADAPTIVE ACCELERATED EVALUATION

4.1 Introduction

In the previous chapter, statistics of the cut-in HV $f(\mathbf{x})$ is replaced by a somewhat arbitrarily selected AE distribution $f^*(\mathbf{x})$ to accelerate the evaluation. When the AV design changes or the evaluation metrics are modified, $f^*(\cdot)$ may need to be reselected to maintain a high rate of acceleration. In this chapter, instead of tuning $f^*(\mathbf{x})$ manually, we develop an Adaptive Accelerated Evaluation (AAE) approach to searching for the optimal $f^*(\mathbf{x})$. As shown in Figure 4.1, a family of $\boldsymbol{\vartheta}$ -parameterized distributions $\tilde{f}_{\boldsymbol{\vartheta}}(\mathbf{x})$ is first defined. Through a recursive optimization procedure, the optimal parameter of $\boldsymbol{\vartheta}$ is numerically obtained in a recursive way. As a result, the Accelerated Evaluation tests adjusts themselves to be “adaptive” to the new test requirement.

This chapter begins with an introduction to the theoretical optimal AE distribution. The AAE algorithm is then developed based on the Cross Entropy method. Finally, conflict, crash, and injury events in the lane change scenario are analyzed to demonstrate the AAE method.

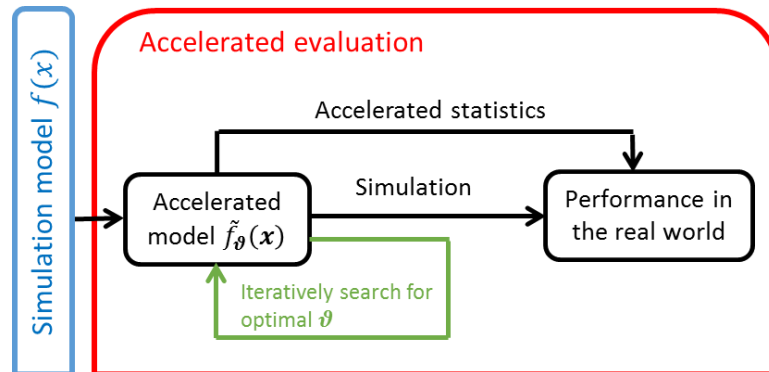


Figure 4.1 Procedure of the Adaptive Accelerated Evaluation

4.2 The Adaptive Accelerated Evaluation

4.2.1 The zero-variance distribution

We first point out an important observation: for any distribution, there is a theoretically optimal distribution

$$f_{zv}^*(\mathbf{x}) = \begin{cases} \frac{f(\mathbf{x})}{\gamma}, & I_{\mathcal{E}}(\mathbf{x}) = 1 \\ 0, & I_{\mathcal{E}}(\mathbf{x}) = 0 \end{cases}. \quad (4.1)$$

With $f_{zv}^*(\mathbf{x})$, any sampled \mathbf{x} leads to a rare event so that the indicator function $I_{\mathcal{E}}(\mathbf{x})$ constantly equals to one. This distribution is optimal in the sense that any sample generated from it has zero variance, and hence the required test number to construct confidence level to any precision is 1; thus it is also known as the zero-variance AE distribution [122].

The likelihood ratio for $f_{zv}^*(\mathbf{x})$ is calculated as

$$L_{zv}(\mathbf{x}) = \frac{f(\mathbf{x})}{f_{zv}^*(\mathbf{x})} = \gamma. \quad (4.2)$$

The probability of the rare events is calculated by

$$\hat{\gamma}_n = \frac{1}{n} \sum_{i=0}^N I_{\mathcal{E}}(\mathbf{x}_n) L(\mathbf{x}_n) = \frac{1}{n} \sum_{i=0}^n \gamma = \gamma. \quad (4.3)$$

Thus $\hat{\gamma}_n$ equals to γ for all n . Unfortunately, this distribution cannot be implemented because it requires the knowledge of γ , which is exactly what we want to estimate. However, it provides a benchmark of good AE distributions. In other word, a good AE distribution should be close to the zero-variance distribution as much as possible.

4.2.2 The Cross Entropy method

The goal of the AAE is to find an AE distribution that is close to the theoretically optimal AE distribution $f_{zv}^*(\mathbf{x})$. The Cross Entropy Method [138]–[140] is used to recursively approach the optimal parameter $\boldsymbol{\vartheta}^*$.

Let $\tilde{f}_{\boldsymbol{\vartheta}}(\mathbf{x})$ be a family of distributions that are modified from the original HV distributions $f(\mathbf{x})$ by some mapping functions and a control parameter vector $\boldsymbol{\vartheta}$. The difference between $\tilde{f}_{\boldsymbol{\vartheta}}(\mathbf{x})$ and $f_{zv}^*(\mathbf{x})$ is represented by the Kullback–Leibler (KL) divergence

$$f_{KL}(\tilde{f}_{\boldsymbol{\vartheta}}(\mathbf{x}), f_{zv}^*(\mathbf{x})) = \int \log \left[\frac{f_{zv}^*(\mathbf{x})}{\tilde{f}_{\boldsymbol{\vartheta}}(\mathbf{x})} \right] f_{zv}^*(\mathbf{x}) d\mathbf{x}. \quad (4.4)$$

When $\tilde{f}_{\boldsymbol{\vartheta}}(\mathbf{x}) = f_{zv}^*(\mathbf{x})$, $f_{KL}(\tilde{f}_{\boldsymbol{\vartheta}}(\mathbf{x}), f_{zv}^*(\mathbf{x})) = 0$. The idea of Cross Entropy is to find an AE distribution that has the minimum KL divergence with $f_{zv}^*(\mathbf{x})$, i.e.

$$\boldsymbol{\vartheta}^* = \arg \min_{\boldsymbol{\vartheta}} f_{KL}(\tilde{f}_{\boldsymbol{\vartheta}}(\mathbf{x}), f_{zv}^*(\mathbf{x})). \quad (4.5)$$

Substituting Eq. (4.4) into Eq. (4.5), we have

$$\begin{aligned} \boldsymbol{\vartheta}^* &= \arg \min_{\boldsymbol{\vartheta}} \int \log \left[\frac{f_{zv}^*(\mathbf{x})}{\tilde{f}_{\boldsymbol{\vartheta}}(\mathbf{x})} \right] f_{zv}^*(\mathbf{x}) d\mathbf{x} \\ &= \arg \min_{\boldsymbol{\vartheta}} \int \{ \log[f_{zv}^*(\mathbf{x})] f_{zv}^*(\mathbf{x}) - \log[\tilde{f}_{\boldsymbol{\vartheta}}(\mathbf{x})] f_{zv}^*(\mathbf{x}) \} d\mathbf{x}. \end{aligned} \quad (4.6)$$

Note the first term inside the integration is independent of $\boldsymbol{\vartheta}$, Eq. (4.6) can be simplified to

$$\boldsymbol{\vartheta}^* = \arg \max_{\boldsymbol{\vartheta}} \int \log[\tilde{f}_{\boldsymbol{\vartheta}}(\mathbf{x})] f_{zv}^*(\mathbf{x}) d\mathbf{x}. \quad (4.7)$$

Substituting Eq. (4.1) into Eq. (4.7), we have

$$\boldsymbol{\vartheta}^* = \arg \max_{\boldsymbol{\vartheta}} \int \log[\tilde{f}_{\boldsymbol{\vartheta}}(\mathbf{x})] \frac{f(\mathbf{x})}{P(\mathcal{E})} I_{\mathcal{E}}(\mathbf{x}) d\mathbf{x}. \quad (4.8)$$

Since $P(\mathcal{E})$ is a constant, it can be taken out of the optimal equation.

$$\boldsymbol{\vartheta}^* = \arg \max_{\boldsymbol{\vartheta}} \int \log[\tilde{f}_{\boldsymbol{\vartheta}}(\mathbf{x})] f(\mathbf{x}) I_{\mathcal{E}}(\mathbf{x}) d\mathbf{x} \quad (4.9)$$

Here we apply the IS techniques to increase the sampling efficiency by using the distribution $\tilde{f}_{\boldsymbol{\vartheta}_i}(\mathbf{x})$ in the previous iteration. Let

$$\tilde{L}_{\boldsymbol{\vartheta}_i}(\mathbf{x}) = \frac{f(\mathbf{x})}{\tilde{f}_{\boldsymbol{\vartheta}_i}(\mathbf{x})}. \quad (4.10)$$

From Eq. (4.8), $\boldsymbol{\vartheta}_{i+1}$ can be derived as

$$\begin{aligned} \boldsymbol{\vartheta}_{i+1} &= \arg \max_{\boldsymbol{\vartheta}} \int \log[\tilde{f}_{\boldsymbol{\vartheta}}(\mathbf{x})] \tilde{L}_{\boldsymbol{\vartheta}_i} I_{\mathcal{E}}(\mathbf{x}) \tilde{f}_{\boldsymbol{\vartheta}_i}(\mathbf{x}) d\mathbf{x} \\ &\approx \arg \max_{\boldsymbol{\vartheta}} \widehat{\mathbb{E}}_{\tilde{f}_{\boldsymbol{\vartheta}_i}} [\log(\tilde{f}_{\boldsymbol{\vartheta}}(\mathbf{x})) \tilde{L}_{\boldsymbol{\vartheta}_i}(\mathbf{x}) I_{\mathcal{E}}(\mathbf{x})] \end{aligned} \quad (4.11)$$

where $I_{\mathcal{E}}(\mathbf{x})$ are test results in the i^{th} iteration using $\tilde{f}_{\boldsymbol{\vartheta}_i}(\mathbf{x})$, and $\widehat{\mathbb{E}}_{\tilde{f}_{\boldsymbol{\vartheta}_i}}[\cdot]$ denotes the empirical average.

4.3 Adaptive Accelerated Evaluation in the Lane Change Scenario

There are many possible choices for the family of AE distribution $\tilde{f}_{\boldsymbol{\vartheta}}(\mathbf{x})$. Here we develop $\tilde{f}_{\boldsymbol{\vartheta}}(\mathbf{x})$ based on a popular class named the Exponential Change of Measure (ECM). We use the lane change model developed in the previous chapter to demonstrate the AAE approach in which $\mathbf{x} = [v_L, TTC_L^{-1}, R_L^{-1}]$ following distributions $f_{v_L}(x)$, $f_{TTC_L^{-1}}(x)$ and $f_{R_L^{-1}}(x)$. Same as the process described in CHAPTER 3, we will modify $f_{TTC_L^{-1}}(x)$ and $f_{R_L^{-1}}(x)$ in the accelerated model and use Importance Sampling to estimate the safety performance in real world driving.

Recall that $TTC_L^{-1} \sim \exp(\lambda_{TTC_L^{-1}}(v_L))$, i.e.

$$f_{TTC_L^{-1}}(x) = \frac{1}{\lambda_{TTC_L^{-1}}} \exp\left(-\frac{x}{\lambda_{TTC_L^{-1}}}\right). \quad (4.12)$$

The ECM considers the family

$$\tilde{f}_{TTC_L^{-1}}(x) = \exp\left(\vartheta_{TTC_L^{-1}} x - \Psi\left(\vartheta_{TTC_L^{-1}}^{ECM}\right)\right) f_{TTC_L^{-1}}(x) \quad (4.13)$$

parametrized by $\vartheta_{TTC_L^{-1}}^{ECM} < 1/\lambda_{TTC_L^{-1}}$, where $\Psi\left(\vartheta_{TTC_L^{-1}}^{ECM}\right)$ is the logarithmic moment generation function of TTC_L^{-1} , i.e.,

$$\begin{aligned} \Psi\left(\vartheta_{TTC_L^{-1}}^{ECM}\right) &= \log \mathbb{E}\left(\exp\left(\vartheta_{TTC_L^{-1}}^{ECM} TTC_L^{-1}\right)\right) \\ &= \log \int_0^{+\infty} \exp\left(\vartheta_{TTC_L^{-1}}^{ECM} x\right) f_{TTC_L^{-1}}(x) dx \\ &= \log \int_0^{+\infty} \exp\left(\vartheta_{TTC_L^{-1}}^{ECM} x\right) \frac{1}{\lambda_{TTC_L^{-1}}} \exp\left(-\frac{x}{\lambda_{TTC_L^{-1}}}\right) dx \end{aligned} \quad (4.14)$$

Calculate the integration, we have

$$\begin{aligned} \Psi\left(\vartheta_{TTC_L^{-1}}^{ECM}\right) &= \log \frac{-1}{1 - \lambda_{TTC_L^{-1}} \vartheta_{TTC_L^{-1}}^{ECM}} \left[\exp\left(-\left(\frac{1}{\lambda_{TTC_L^{-1}}} - \vartheta_{TTC_L^{-1}}^{ECM}\right)x\right) \right]_0^{+\infty} \\ &= \log \frac{-1}{1 - \lambda_{TTC_L^{-1}} \vartheta_{TTC_L^{-1}}^{ECM}} (0 - 1) \\ &= \log \frac{1}{1 - \lambda_{TTC_L^{-1}} \vartheta_{TTC_L^{-1}}^{ECM}}. \end{aligned} \quad (4.15)$$

Substituting Eq. (4.15) into Eq. (4.13), we have the ECM function of $f_{TTC_L^{-1}}(x)$

$$\begin{aligned}
& \tilde{f}_{TTC_L^{-1}}(x) \\
&= \exp\left(\vartheta_{TTC_L^{-1}}^{ECM} x - \log \frac{1}{1 - \lambda_{TTC_L^{-1}} \vartheta_{TTC_L^{-1}}^{ECM}}\right) \frac{1}{\lambda_{TTC_L^{-1}}} \exp\left(-\frac{1}{\lambda_{TTC_L^{-1}}} x\right) \\
&= \frac{\exp\left(\vartheta_{TTC_L^{-1}}^{ECM} x\right)}{\frac{1}{1 - \lambda_{TTC_L^{-1}} \vartheta_{TTC_L^{-1}}^{ECM}} \lambda_{TTC_L^{-1}}} \exp\left(-\frac{1}{\lambda_{TTC_L^{-1}}} x\right) \\
&= \left(\frac{1}{\lambda_{TTC_L^{-1}}} - \vartheta_{TTC_L^{-1}}^{ECM}\right) \exp\left(-\left(\frac{1}{\lambda_{TTC_L^{-1}}} - \vartheta_{TTC_L^{-1}}^{ECM}\right) x\right)
\end{aligned} \tag{4.16}$$

where $\vartheta_{TTC_L^{-1}}^{ECM} < 1/\lambda_{TTC_L^{-1}}$ and $\lambda_{TTC_L^{-1}} > 0$. To make $\vartheta_{TTC_L^{-1}}^{ECM}$ have the same scale as $\lambda_{TTC_L^{-1}}$, we apply a nonlinear mapping by letting

$$\vartheta_{TTC_L^{-1}}^{ECM} = \frac{\vartheta_{TTC_L^{-1}}}{\vartheta_{TTC_L^{-1}} \lambda_{TTC_L^{-1}} - \lambda_{TTC_L^{-1}}^2} \tag{4.17}$$

with $\vartheta_{TTC_L^{-1}} < \lambda_{TTC_L^{-1}}$. Substitute Eq. (4.17) into (4.16), we have

$$\tilde{f}_{TTC_L^{-1}}(x|\vartheta_{TTC_L^{-1}}) = \left(\frac{1}{\lambda_{TTC_L^{-1}} - \vartheta_{TTC_L^{-1}}}\right) \exp\left(-\frac{x}{\lambda_{TTC_L^{-1}} - \vartheta_{TTC_L^{-1}}}\right). \tag{4.18}$$

Nominally R_L^{-1} follows a Pareto distribution, i.e.

$$f_{R_L^{-1}}(x) = \text{Pareto}\left(x|k_{R_L^{-1}}, \sigma_{R_L^{-1}}, \mu_{R_L^{-1}}\right). \tag{4.19}$$

The ECM cannot be applied to a Pareto distribution directly. Therefore, we first construct an exponential distribution

$$\tilde{f}_{R_L^{-1}}(x) = \frac{1}{\lambda_{R_L^{-1}}} \exp\left(-\frac{1}{\lambda_{R_L^{-1}}} x\right) \tag{4.20}$$

with $\lambda_{R_L^{-1}}$, which makes Eq. (4.20) to have the smallest least square error to Eq. (4.19).

Then we apply ECM to Eq. (4.20) with parameter $\vartheta_{R_L^{-1}}^{ECM}$ and nonlinear mapping

$$\vartheta_{R_L^{-1}}^{ECM} = \frac{\vartheta_{R_L^{-1}}}{\vartheta_{R_L^{-1}}\lambda_{R_L^{-1}} - \lambda_{R_L^{-1}}^2} \quad (4.21)$$

to Eq. (4.20). We have

$$\tilde{f}_{R_L^{-1}}(x|\vartheta_{R_L^{-1}}) = \left(\frac{1}{\lambda_{R_L^{-1}} - \vartheta_{R_L^{-1}}} \right) \exp \left(-\frac{x}{\lambda_{R_L^{-1}} - \vartheta_{R_L^{-1}}} \right) \quad (4.22)$$

with $\vartheta_{R_L^{-1}} < \lambda_{R_L^{-1}}$.

Now we have the two family of distributions $\tilde{f}_{TTC_L^{-1}}$ and $\tilde{f}_{R_L^{-1}}$ ready. We will apply the Cross Entropy method to calculate the optimal parameter $\vartheta_{TTC_L^{-1}}$ and $\vartheta_{R_L^{-1}}$ iteratively.

Let $\boldsymbol{\vartheta}_i = [\vartheta_{R_L^{-1}}^{(i)}, \vartheta_{TTC_L^{-1}}^{(i)}]$ be the parameters to be optimized used in the i^{th} iteration.

The joint distribution of the lane change event is

$$\tilde{f}_{\boldsymbol{\vartheta}}(x) = \tilde{f}_{R_L^{-1}}(R_L^{-1}|\vartheta_{R_L^{-1}}) \tilde{f}_{TTC_L^{-1}}(TTC_L^{-1}|\vartheta_{TTC_L^{-1}}) f_{v_L}(v_L). \quad (4.23)$$

Substituting Eq. (4.23) into Eq. (4.11), we have

$$\begin{aligned} \boldsymbol{\vartheta}_{i+1} = \arg \max_{\boldsymbol{\vartheta}} \widehat{E}_{\tilde{f}_{\boldsymbol{\vartheta}_i}} & \left[\log \left(\tilde{f}_{R_L^{-1}}(R_L^{-1}|\boldsymbol{\vartheta}) \right) \tilde{L}_{\boldsymbol{\vartheta}_i}(x) I_{\mathcal{E}}(x) + \right. \\ & \left. \log \left(\tilde{f}_{TTC_L^{-1}}(TTC_L^{-1}|\boldsymbol{\vartheta}) \right) \tilde{L}_{\boldsymbol{\vartheta}_i}(x) I_{\mathcal{E}}(x) + f_{v_L}(v_L) \tilde{L}_{\boldsymbol{\vartheta}_i}(x) I_{\mathcal{E}}(x) \right]. \end{aligned} \quad (4.24)$$

Because $f_{v_L}(l) \tilde{L}_{\boldsymbol{\vartheta}_i}(x) I_{\mathcal{E}_{\boldsymbol{\vartheta}_i}}(x)$ is not a function of $\boldsymbol{\vartheta}$, it can be eliminated from the optimization.

$$\begin{aligned} \boldsymbol{\vartheta}_{i+1} = \arg \max_{\boldsymbol{\vartheta}} \widehat{\mathbb{E}}_{\tilde{f}_{\boldsymbol{\vartheta}_i}} & \left[\log \left(\tilde{f}_{R_L^{-1}} \left(R_L^{-1} | \boldsymbol{\vartheta}_{R_L^{-1}} \right) \right) \tilde{L}_{\boldsymbol{\vartheta}_i}(\mathbf{x}) I_{\mathcal{E}}(\mathbf{x}) + \right. \\ & \left. \log \left(\tilde{f}_{TT C_L^{-1}} \left(TT C_L^{-1} | \boldsymbol{\vartheta}_{TT C_L^{-1}} \right) \right) \tilde{L}_{\boldsymbol{\vartheta}_i}(\mathbf{x}) I_{\mathcal{E}}(\mathbf{x}) \right]. \end{aligned} \quad (4.25)$$

It is shown from (4.25) that $\boldsymbol{\vartheta}_{R_L^{-1}}$ and $\boldsymbol{\vartheta}_{TT C_L^{-1}}$ can be solved separately. The parameters used in the $(i+1)^{th}$ can be calculated from

$$\boldsymbol{\vartheta}_{R_L^{-1}}^{(i+1)} = \arg \max_{\boldsymbol{\vartheta}_{R_L^{-1}}} \widehat{\mathbb{E}}_{\tilde{f}_{\boldsymbol{\vartheta}_i}} \left[\log \left(\tilde{f}_{R_L^{-1}} \left(R_L^{-1} | \boldsymbol{\vartheta}_{R_L^{-1}} \right) \right) \tilde{L}_{\boldsymbol{\vartheta}_i}(\mathbf{x}) I_{\mathcal{E}}(\mathbf{x}) \right] \quad (4.26)$$

and

$$\boldsymbol{\vartheta}_{TT C_L^{-1}}^{(i+1)} = \arg \max_{\boldsymbol{\vartheta}_{TT C_L^{-1}}} \widehat{\mathbb{E}}_{\tilde{f}_{\boldsymbol{\vartheta}_i}} \left[\log \left(\tilde{f}_{TT C_L^{-1}} \left(TT C_L^{-1} | \boldsymbol{\vartheta}_{TT C_L^{-1}} \right) \right) \tilde{L}_{\boldsymbol{\vartheta}_i}(\mathbf{x}) I_{\mathcal{E}}(\mathbf{x}) \right]. \quad (4.27)$$

The empirical average can be estimated by N samples of \mathbf{x} . Thus Eq. (4.26) can be further derived as

$$\boldsymbol{\vartheta}_{R_L^{-1}}^{(i+1)} = \arg \max_{\boldsymbol{\vartheta}_{R_L^{-1}}} \frac{1}{N} \sum_{n=1}^N \log \left(\tilde{f}_{R_L^{-1}} \left(R_{L_n}^{-1} | \boldsymbol{\vartheta}_{TT C_L^{-1}} \right) \right) \tilde{L}_{\boldsymbol{\vartheta}_i}(\mathbf{x}_n) I_{\mathcal{E}}(\mathbf{x}_n) \quad (4.28)$$

where i denotes the i^{th} iteration. \mathbf{x}_n denotes the n^{th} sample of $[v_L, TT C_L^{-1}, R_L^{-1}]$. The constant $1/N$ can be taken out of the arg max function. By substituting Eq. (4.22) into (4.28), we have

$$\begin{aligned} & \boldsymbol{\vartheta}_{R_L^{-1}}^{(i+1)} \\ &= \arg \max_{\boldsymbol{\vartheta}_{R_L^{-1}}} \sum_{n=1}^N \log \left[\frac{1}{\lambda_{R_L^{-1}} - \boldsymbol{\vartheta}_{R_L^{-1}}} \exp \left(-\frac{R_{L_n}^{-1}}{\lambda_{R_L^{-1}} - \boldsymbol{\vartheta}_{R_L^{-1}}} \right) \right] \tilde{L}_{\boldsymbol{\vartheta}_i}(\mathbf{x}_n) I_{\mathcal{E}}(\mathbf{x}_n) \\ &= \arg \max_{\boldsymbol{\vartheta}_{R_L^{-1}}} \sum_{n=1}^N \left[-\log \left(\lambda_{R_L^{-1}} - \boldsymbol{\vartheta}_{R_L^{-1}} \right) - \frac{R_{L_n}^{-1}}{\lambda_{R_L^{-1}} - \boldsymbol{\vartheta}_{R_L^{-1}}} \right] \tilde{L}_{\boldsymbol{\vartheta}_i}(\mathbf{x}_n) I_{\mathcal{E}}(\mathbf{x}_n). \end{aligned} \quad (4.29)$$

Let

$$g_{\boldsymbol{\vartheta}_{R_L^{-1}}} = \sum_{n=1}^N \left(-\log \left(\lambda_{R_L^{-1}} - \boldsymbol{\vartheta}_{R_L^{-1}} \right) - \frac{R_{L_n}^{-1}}{\lambda_{R_L^{-1}} - \boldsymbol{\vartheta}_{R_L^{-1}}} \right) \tilde{L}_{\boldsymbol{\vartheta}_i}(\mathbf{x}_n) I_{\mathcal{E}}(\mathbf{x}_n). \quad (4.30)$$

To find the $\vartheta_{R_L^{-1}}$ that maximizes function $g_{\vartheta_{R_L^{-1}}}$ in Eq. (4.29), we set the first order derivative of $g_{\vartheta_{R_L^{-1}}}$ to be zero.

$$\begin{aligned} \frac{dg_{\vartheta_{R_L^{-1}}}}{d\vartheta_{R_L^{-1}}} &= \sum_{n=1}^N \left(\frac{1}{\lambda_{R_L^{-1}} - \vartheta_{R_L^{-1}}} - \frac{R_L^{-1}}{\left(\lambda_{R_L^{-1}} - \vartheta_{R_L^{-1}}\right)^2} \right) \tilde{L}_{\vartheta_i}(\mathbf{x}_n) I_{\mathcal{E}}(\mathbf{x}_n) \\ &= \frac{1}{\left(\lambda_{R_L^{-1}} - \vartheta_{R_L^{-1}}\right)^2} \sum_{n=1}^N \left(\lambda_{R_L^{-1}} - \vartheta_{R_L^{-1}} - R_L^{-1} \right) \tilde{L}_{\vartheta_i}(\mathbf{x}_n) I_{\mathcal{E}}(\mathbf{x}_n) = 0 \end{aligned} \quad (4.31)$$

Because $\vartheta_{R_L^{-1}} < \lambda_{R_L^{-1}}$, we have

$$\sum_{n=1}^N \left(\lambda_{R_L^{-1}} - \vartheta_{R_L^{-1}} - R_L^{-1} \right) \tilde{L}_{\vartheta_i}(\mathbf{x}_n) I_{\mathcal{E}}(\mathbf{x}_n) = 0. \quad (4.32)$$

In each iteration N should be picked large enough to have $\sum_{n=1}^N I_{\mathcal{E}}(\mathbf{x}_n) > 0$, which means at least one event of interest (e.g. crash) happens in one iteration. Because $\tilde{L}_{\vartheta_i}(\mathbf{x}_n) > 0$. We have

$$\sum_{n=1}^N \tilde{L}_{\vartheta_i}(\mathbf{x}_n) I_{\mathcal{E}}(\mathbf{x}_n) > 0. \quad (4.33)$$

$\vartheta_{R_L^{-1}}$ can be solved from Eq. (4.32).

$$\vartheta_{R_L^{-1}} = \frac{\sum_{n=1}^N \left(\lambda_{R_L^{-1}} - R_L^{-1} \right) \tilde{L}_{\vartheta_i}(\mathbf{x}_n) I_{\mathcal{E}}(\mathbf{x}_n)}{\sum_{n=1}^N \tilde{L}_{\vartheta_i}(\mathbf{x}_n) I_{\mathcal{E}}(\mathbf{x}_n)} \quad (4.34)$$

Taking $\vartheta_{R_L^{-1}}$ in Eq. (4.31), we have

$$\frac{dg_{\vartheta_{R_L^{-1}}}}{d\vartheta_{R_L^{-1}}} \begin{cases} > 0 & \text{when } \vartheta_{R_L^{-1}} < \frac{\sum_{n=1}^N \left(\lambda_{R_L^{-1}} - R_L^{-1} \right) \tilde{L}_{\vartheta_i}(\mathbf{x}_n) I_{\mathcal{E}}(\mathbf{x}_n)}{\sum_{n=1}^N \tilde{L}_{\vartheta_i}(\mathbf{x}_n) I_{\mathcal{E}}(\mathbf{x}_n)} \\ < 0 & \text{when } \vartheta_{R_L^{-1}} > \frac{\sum_{n=1}^N \left(\lambda_{R_L^{-1}} - R_L^{-1} \right) \tilde{L}_{\vartheta_i}(\mathbf{x}_n) I_{\mathcal{E}}(\mathbf{x}_n)}{\sum_{n=1}^N \tilde{L}_{\vartheta_i}(\mathbf{x}_n) I_{\mathcal{E}}(\mathbf{x}_n)} \end{cases}. \quad (4.35)$$

So $\vartheta_{R_L^{-1}}$ in Eq. (4.34) is the global maxima. The optimal parameter in the next iteration $\vartheta_{R_L^{-1}}$ can be derived analytically

$$\vartheta_{R_L^{-1}}^{(i+1)} = \frac{\sum_{n=1}^N (\lambda_{R_L^{-1}} - R_L^{-1}) \tilde{L}_{\vartheta_i}(\mathbf{x}_n) I_{\mathcal{E}}(\mathbf{x}_n)}{\sum_{n=1}^N \tilde{L}_{\vartheta_i}(\mathbf{x}_n) I_{\mathcal{E}}(\mathbf{x}_n)} \quad (4.36)$$

where n is the index for each simulation. Similarly, apply Eq. (4.16) to Eq. (4.11). The optimal parameter $\vartheta_{R_L^{-1}}$ can be obtained from

$$\vartheta_{TTC_L^{-1}}^{(i+1)} = \frac{\sum_{j=1}^N (\lambda_{TTC_L^{-1}} - TTC_L^{-1}) \tilde{L}_{\vartheta_i}(\mathbf{x}_n) I_{\mathcal{E}}(\mathbf{x}_n)}{\sum_1^N \tilde{L}_{\vartheta_i}(\mathbf{x}_n) I_{\mathcal{E}}(\mathbf{x}_n)}. \quad (4.37)$$

$\vartheta_{R_L^{-1}}^{(i+1)}$ and $\vartheta_{TTC_L^{-1}}^{(i+1)}$ can then be used in the $(i + 1)^{th}$ iteration.

4.4 Simulation Analysis

In the previous chapter, the crash and injury rates are calculated using a manually tuned AE distribution, which successfully accelerates the evaluation by four orders of magnitude. In this section, we will show that the same AE distribution cannot be used as a universally good candidate to calculate other rare event metrics. We will first use this AE distribution to calculate the “conflict rate” and show that, with an improper AE distribution, the “accelerated” tests may converge slowly and become less efficient even than the Monte Carlo method. Second, we will demonstrate the ability of the AAE method to avoid the “bad” AE distribution issue. By applying the new AE distribution generated by the AAE method, it is shown that once again “close-to-optimal” distributions can be found, and the evaluation can be accelerated significantly.

4.4.1 Evaluation with the non-optimized AE distributions

A conflict event happens when an AV appears in the proximity zone of the LCV between time t_{LC} and $t_{LC} + T_{LC}$. As shown in Figure 4.2, the proximity zone is the area

from 4 feet in front of the bumper of the LCV to 30 feet behind the rear bumper of the LCV [131, p. ix]. This area generally includes the blind spot and the area beside and behind the vehicle in which another vehicle is likely to travel. In our lane change model, the LCV always cut-in in front of the AV. So only the 30 feet proximity zone behind the LCV is used. Mathematically, the conflict event can be defined as

$$\mathcal{E} = \{\min(R_L(t)) < R_{\mathcal{E}} | t_{LC} < t \leq t_{LC} + T_{LC}\} \quad (4.38)$$

where $R_{\mathcal{E}} = 30$ feet.

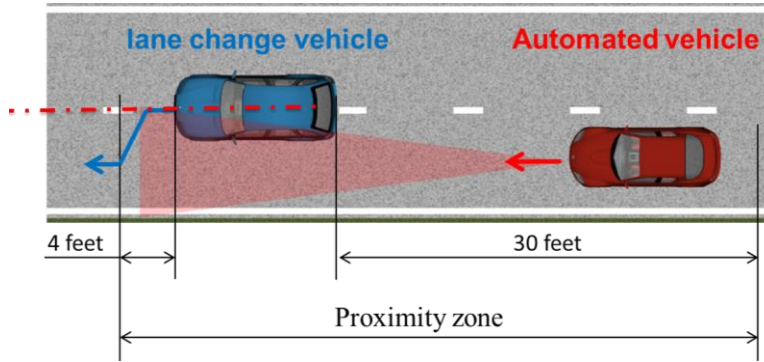


Figure 4.2 Definition of the conflict event

The AE distributions in Eqs. (3.29) and (3.30) are used. The Design B developed in Section 2.4.1 is used to as the AV model. Figure 4.3 shows that estimated conflict rate in accelerated and naturalistic driving conditions. It can be seen that although the Accelerated Evaluation is unbiased, it converges even slower than the non-accelerated test.

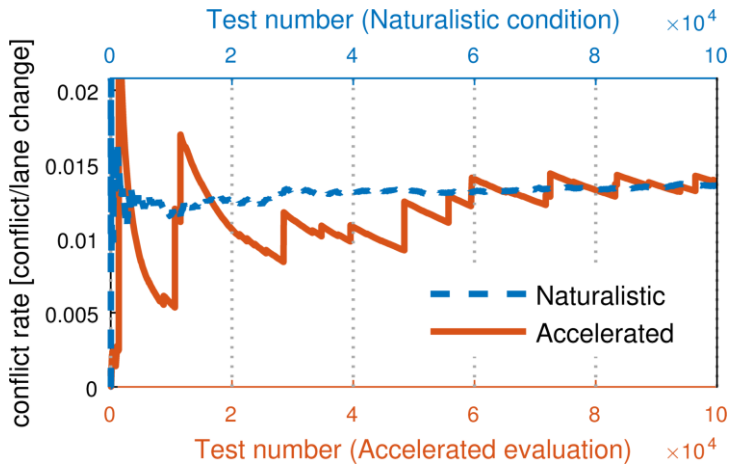


Figure 4.3 Estimation of the conflict rate in the lane change scenario (improper AE distribution)

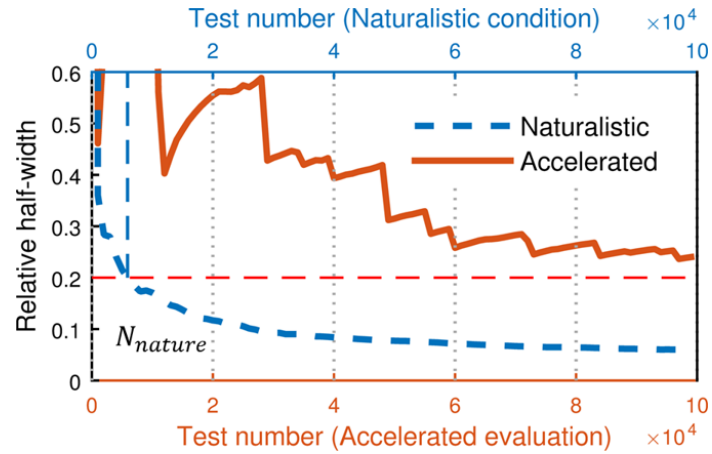


Figure 4.4 Convergence of conflict rate estimation in the lane change scenario (improper AE distribution)

Figure 4.4 shows the convergence with $\beta = 0.2$ and 80% confidence. The naturalistic simulations take $N_{nature} = 5.90e3$ simulations to converge. However, the accelerated test cannot converge even after 1e5 simulations, which shows that the “accelerated test” is even less efficient than the Monte Carlo method. When estimating the conflict rate by using $\hat{\gamma}_n = \frac{1}{n} \sum_{i=0}^n I_{\mathcal{E}}(\mathbf{x}_n) L(\mathbf{x}_n)$ from Eq. (3.15), the ideal case is that the indication function $I_{\mathcal{E}}(\mathbf{x}_n)$ is one and the likelihood ratio $L(\mathbf{x}_n)$ is closed to the expectation of the conflict rate γ . By using the AE distributions tuned for crash analysis, conflicts were generated at a higher frequency. However, because the AE distributions are tuned too much,

many times the likelihood ratio was much smaller than γ and the sampling became less consistent. Therefore, more simulations are needed to make the estimation converge. This example shows that when the evaluation metric changes, e.g. from crash rate to conflict rate, the AE distribution needs to be re-selected. Without a proper AE distribution, convergence can be slower than the Monte Carlo simulation method.

4.4.2 Evaluation with the Adaptive Accelerated Evaluation

4.4.2.1 Estimation of the conflict rate

The AAE approach is used to obtain near-optimal distribution to estimate conflict rate. 100 lane changes were simulated in each iteration to calculate the optimal parameters $\vartheta_{TTC_L^{-1}}$ and $\vartheta_{R_L^{-1}}$. The values in the tenth iteration were used to calculate the conflict rate in the lane change scenario. As shown in Figure 4.5, three sets of $\vartheta_{TTC_L^{-1}}$ and $\vartheta_{R_L^{-1}}$ are obtained with low, medium and high velocities. It is shown in Figure 4.5 that values of $\vartheta_{R_L^{-1}}$ converge to about -0.12, whereas values of $\vartheta_{TTC_L^{-1}}$ fluctuate around zero. The reason $\vartheta_{TTC_L^{-1}}$ does not change as much as $\vartheta_{R_L^{-1}}$ is because the conflict events are defined based on R_L , thus changing the parameter of R_L plays a more important role in evaluating conflict events.

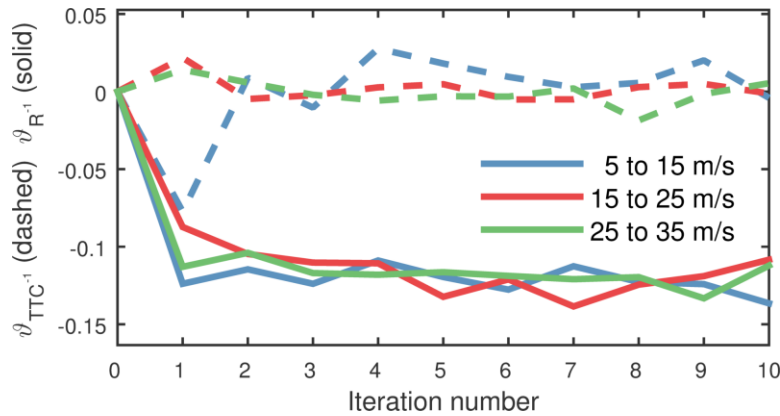


Figure 4.5 Searching for optimal parameters for conflict events with AAE

The estimation and convergence of conflict rate are shown in Figure 4.6 and Figure 4.7. It is shown that with the new distribution calculated by the AAE approach, the evaluation becomes much more efficient with $N_{acc} = 364$ while $N_{nature} = 5.90e3$. Applying Eqs. (3.32), (3.33) and (3.35), we can calculate that $D_{nature} = 4.53e4$ miles, $D_{acc} = 16.4$ miles, and $r_{acc} = 2.77e3$ respectively.

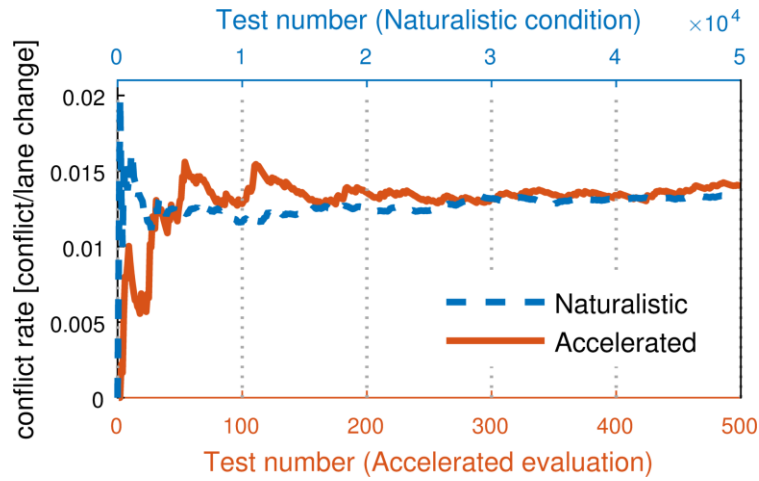


Figure 4.6 Estimation of the conflict rate in the lane change scenario (with AE distribution calculated by AAE)

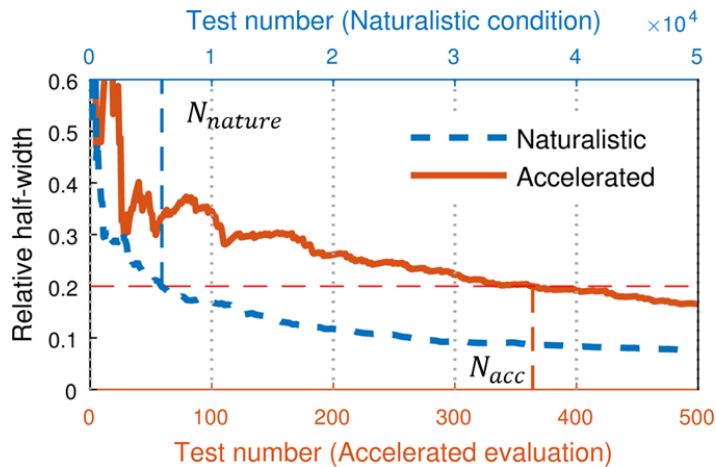


Figure 4.7 Convergence of conflict rate estimation in the lane change scenario (with AE distribution calculated by AAE)

4.4.2.2 Estimation of the crash rate and injury rate

The AAE approach was also applied to estimate the crash rate to examine its robustness. In each searching iteration, 500 lane changes were conducted. As shown in Figure 4.8 three different values of $\vartheta_{TTC_L^{-1}}$ were obtained from the iterative search for different velocity intervals, where as $\vartheta_{R_L^{-1}}$ converges to values close to zero. It can be explained that in the crash analysis, the safety critical function (AEB) on AV is mainly affected by TTC. Therefore $\vartheta_{TTC_L^{-1}}$ has a larger impact than $\vartheta_{R_L^{-1}}$ on the occurrence of the crash.

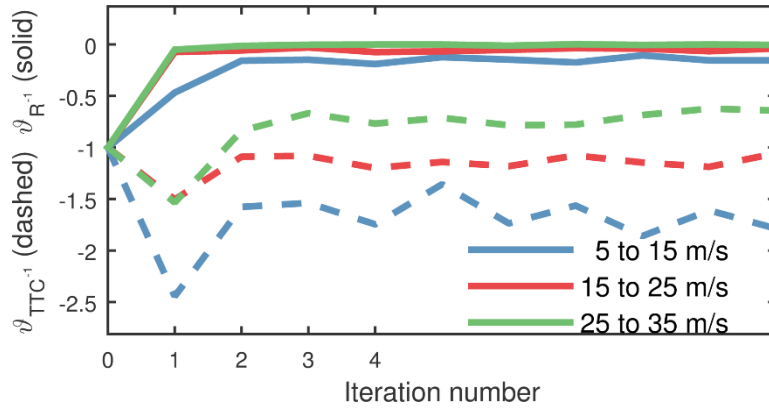


Figure 4.8 Searching for optimal parameters for crash events with AAE

Both accelerated and naturalistic tests were conducted until the crash rate converged with 80 % confidence level and $\beta = 0.2$. Figure 4.9 shows that the estimation of the crash rate calculated by the accelerated tests converges to the naturalistic driving estimation, which shows that the Accelerated Evaluation is unbiased. Figure 4.10 shows that accelerated tests achieved the confidence level β after $N_{acc} = 5.77e4$ simulations, while the naturalistic (crude Monte Carlo) method takes $N_{nature} = 6.13e6$ simulations. Applying Eqs. (3.32), (3.33) and (3.35), we can calculate that $D_{nature} = 4.71e7$ miles, $D_{acc} = 4.02e3$ miles, and $r_{acc} = 1.17e4$ respectively.

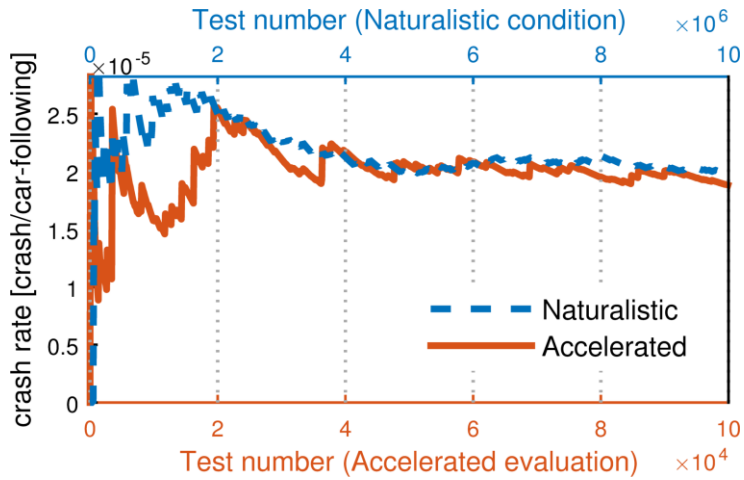


Figure 4.9 Estimation of the crash rate in the lane change scenario (with AE distribution calculated by AAE)

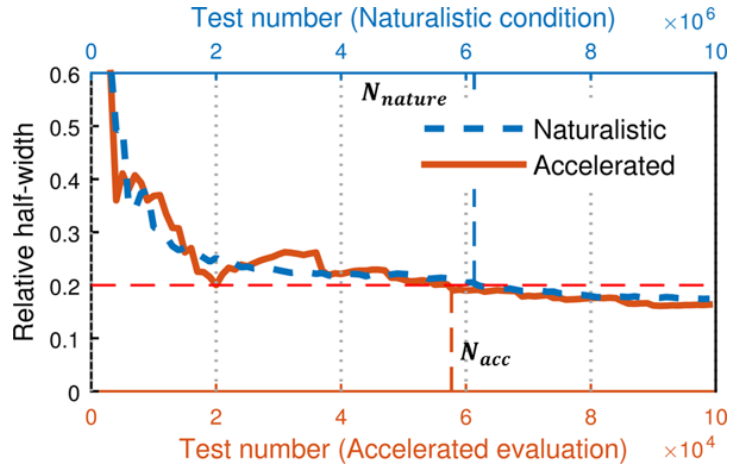


Figure 4.10 Convergence of crash rate estimation in the lane change scenario (with AE distribution calculated by AAE)

When crashes happen, passengers may get injured. We also estimate the rate moderate-to-fatal injuries of the AV passengers. The estimated injury rate can be calculated from Eq. (3.39). Both accelerated and naturalistic tests were conducted until the injury rate converged with 80 % confidence level and $\beta = 0.2$. Figure 4.11 shows that estimated injury rate in the accelerated test converges to the result under naturalistic driving conditions.

Figure 4.12 shows that accelerated tests achieved the confidence level β after $N_{acc} = 3.63e4$ simulations, while the naturalistic (crude Monte Carlo) method took

$N_{nature} = 6.12e6$ simulations. Applying Eqs. (3.32), (3.33) and (3.35), we can calculate that $D_{nature} = 4.70e7$ miles, $D_{acc} = 2.53e3$ miles, and $r_{acc} = 1.86e4$ respectively.

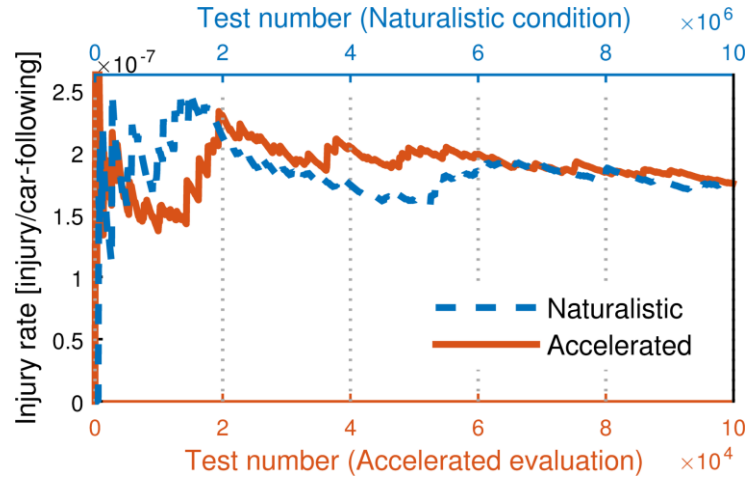


Figure 4.11 Estimation of the injury rate in the lane change scenario (with AE distribution calculated by AAE)

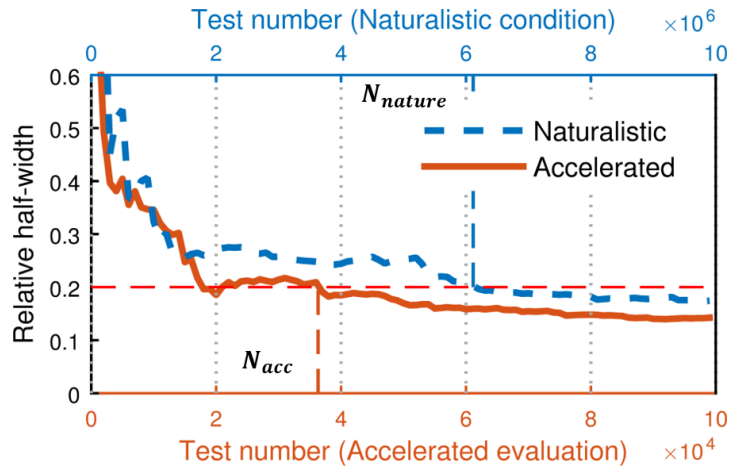


Figure 4.12 Convergence of injury rate estimation in the lane change scenario (with AE distribution calculated by AAE)

Table 5.3 summarizes the performance of Adaptive Accelerated Evaluation approach in estimating the three metrics of the AV. It is shown that in the crash and injury cases, the proposed method successfully accelerates the evaluation by four orders of magnitude, while in the conflict case, the AE method achieves over three thousand times of acceleration in test mileage.

Table 4.1 Summary of performance of the Adaptive Accelerated Evaluation approach in estimating the crash rate, injury rate, and the conflict rate in the lane change scenario

	D_{nature}	D_{acc}	r_{acc}
	mile	mile	-
Conflict	4.53e4	16.4	2.77e3
Crash	4.71e7	4.02e3	1.17e4
Injury	4.70e7	2.53e3	1.86e4

4.5 Summary

In this Chapter, the Adaptive Accelerated Evaluation approach is proposed to search for the optimal AE distributions in an iterative way. The Cross Entropy approach is used to calculate the local optimal in each iteration. A comparison of the accelerated efficiencies using distributions using non-optimized AE distributions and the distribution calculated by AAE is shown to demonstrate the effectiveness of the proposed method in the lane change conflict scenario. Three metrics of AV: conflict rate, crash rate, and injury rate, were calculated using the AAE method to demonstrate its performance. Results showed that the AAE method accelerated the evaluation mileage by roughly 3,000 to 18,000 times.

CHAPTER 5

ACCELERATED EVALUATION WITH DYNAMIC INTERACTIONS IN THE CAR-FOLLOWING SCENARIO

5.1 Introduction

In CHAPTER 3 and CHAPTER 4, the lane change HV was simulated using static sampling, in which the randomness is modeled as a set of distributions but sampled only once at the lane change moment. In some other cases, the statistics of the HV behaviors are state-dependent and sampled constantly. We call this type of stochastic process as dynamic sampling. One example is the car-following scenario, where the drivers adjust their speed stochastically according to the maneuvers of the lead vehicles. To evaluate an AV in these types of scenarios and interactions between the AV and HVs, in this chapter, we will develop a new Accelerated Evaluation approach by considering the correlations between each sample. Three types of events, the crash, injury and conflict, are analyzed to demonstrate this approach.

5.2 Model of Dynamic Interactions in Car-following Scenario

5.2.1 Extraction of naturalistic car-following events

The SPMD database introduced in Section 3.3.1 was used to model the lead HV in the car-following scenario. As shown in Table 5.1, the advantage of the SPMD database is that it has six times longer mileage than the IVBSS database [31], [32], [98], which is beneficial to model rare events.

As shown in Figure 5.1, the range and range rate were measured by Mobileye equipped on the SPMD vehicles. To ensure consistency of the used dataset, we apply the following criteria when extracting car-following events:

- $R_L(t) \in (0.1 \text{ m}, 90 \text{ m})$

- Longitude $\in (-88.2^\circ, -82.0^\circ)$
- Latitude $\in (41.0^\circ, 44.5^\circ)$
- No cut-in vehicles between HV and SPMD vehicles
- No lane changes of HV and SPMD vehicles
- Duration of car-following > 50 s

where v_L and v are the velocities of the lead HV and the SPMD vehicle; R_L is the range, defined as the distance between the rear edge of the HV and the front edge of the SPMD vehicle.

Table 5.1 Comparison of between the IVBSS database and the SPMD database

	IVBSS	SPMD
Name	Integrated Vehicle-Based Safety Systems (IVBSS)	Safety Pilot Model Deployment
Time	2010-2011	2012-2015
Mileage	213,309	1,300,000
Test vehicles	108	94
Sensor	Radar	Mobileye®
Longitudinal sensor accuracy	-	10 % error at 90 m 5 % error at 45 m

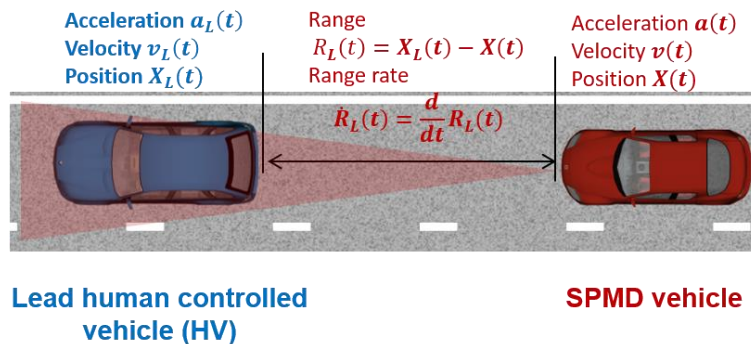


Figure 5.1 Car-following scenarios that may cause frontal crashes

163,332 car-following events were detected in the SPMD database. Figure 5.2 shows the locations of the identified car-following scenarios.

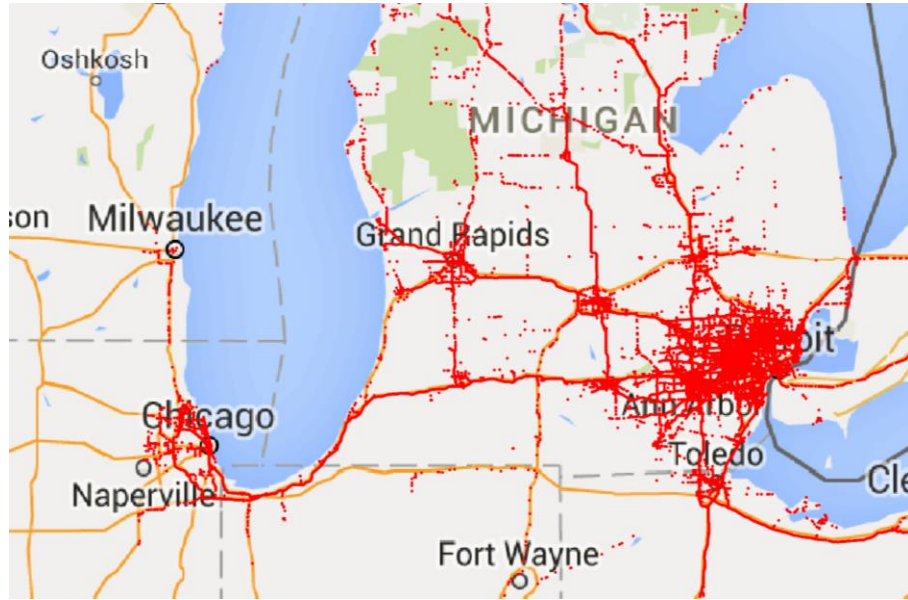


Figure 5.2 Recorded car-following events in the SPMD database

5.2.2 Lead human controlled vehicle

The randomness of human behaviors is modeled by a stochastic model. The vehicle acceleration in the next time step is calculated based on current step acceleration and velocity as shown in Eq. (5.1).

$$\begin{aligned} a_L(k+1) &= h_0 + h_1 a_L(k) + h_2 v_L(k) + u_h \\ &= [1, a_L(k), v_L(k)] \mathbf{h} + u_h \end{aligned} \quad (5.1)$$

where the driver model parameter vector $\mathbf{h} = [h_0, h_1, h_2]^T$ and $u_h \sim \mathcal{N}(0, \sigma_u^2)$.

The lead HV velocity can be calculated from

$$v_L(k) = \dot{R}_L(k) + v(k) \quad (5.2)$$

where range rate defined as

$$\dot{R}_L(k) = v_L(k) - v(k) \quad (5.3)$$

is measured by the MobilEye® sensors equipped on the SPMD vehicles.

The lead HV acceleration a_L is estimated by taking the derivative of v_L with Forward Euler Approximation [141]. A moving average filter with windows size 16 is used to smooth the estimated a_L . The velocity and acceleration in an example car-following event are shown in Figure 5.3.

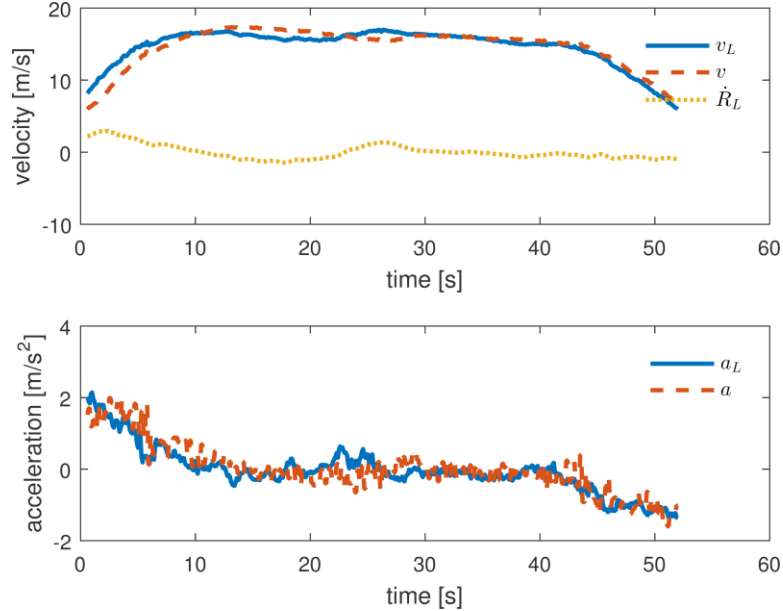


Figure 5.3 Estimation of the lead vehicle acceleration

The driver model parameter vector h is estimated based on the Least Square Method. Define the acceleration vector of the lead vehicle

$$a_L^{(n_s)}(i:j) = \left[a_L^{(n_s)}(i), a_L^{(n_s)}(i+1), \dots, a_L^{(n_s)}(j) \right] \quad (5.4)$$

with $n_s = 1, 2, \dots, N_s$ and $j \geq i$, where $a_L^{(n_s)}(i)$ represents the i th step acceleration of the HV in the n_s th car-following sequence. Define the observer vector

$$\mathbf{y}_h = \left[a_L^{(1)}(2:end), a_L^{(2)}(2:end), \dots, a_L^{(N_s)}(2:end) \right]^T \quad (5.5)$$

where end represents the index of the final element in the acceleration vector. N_s is the total number of car-following sequences in the SPMD database. Define the input vector of each car-following scenario as

$$\boldsymbol{x}_h^{(n_s)} = \begin{bmatrix} 1 & a_L^{(n_s)}(1) & v_L^{(n_s)}(1) \\ 1 & a_L^{(n_s)}(2) & v_L^{(n_s)}(2) \\ \vdots & \vdots & \vdots \\ 1 & a_L^{(n_s)}(end - 1) & v_L^{(n_s)}(end - 1) \end{bmatrix}^T. \quad (5.6)$$

Define the input vector of N_s car-following events as

$$\boldsymbol{\chi}_h = [x_h^{(1)}, x_h^{(2)}, \dots, x_h^{(N_s)}]^T. \quad (5.7)$$

The Matlab® function “robustfit” is used to fit \boldsymbol{h} with input vector $\boldsymbol{\chi}_h$ and observer vector \boldsymbol{y}_h based on “bisquare” approach [142], which is less influenced by the outlier than the normal least-squares fit [143], [144]. The standard deviation of u_h is estimated by fitting the estimation deviation ($a_L(k + 1) - [1, a_L(k), v_L(k)] \boldsymbol{h}$) with a normal distribution.

5.2.3 Automated vehicle model

In the previous chapter, the AV was designed as a combination of ACC and AEB. This is a popular design among current production AVs. The ACC module is designed as a convenience system with a low control authority (usually the acceleration is smaller than ± 0.4 g). The AEB module is designed as a safety system, which is usually tuned to activate late with a harsh braking as a safeguard for frontal collisions. In this chapter, we use an AV control model that can handle both daily driving and emergency situations proposed in [145]. In the following, we first derive the vehicle dynamic model and then design the longitudinal controller.

5.2.3.1 Vehicle dynamics

We use a longitudinal vehicle dynamic model from [115]

$$M \frac{dv(t)}{dt} = F_x(t) - Mg \sin\theta_{rg}(t) - f_{rr}mg \cos\theta_{rg}(t) \\ - 0.5\rho_{air}A_v C_d(v(t) + v_w(t))^2 \quad (5.8)$$

where M is the vehicle mass, F_x is the longitudinal force, θ_{rg} is the road grade angle, g is the gravitational constant, f_{rr} is the rolling resistance coefficient, ρ_{air} is the air density, A_v is the frontal area, C_d is the aerodynamic coefficient and v_w is the wind speed.

At equilibrium i.e. when $dv/dt = 0$, the equilibrium longitudinal force in Eq. (5.8) at v_0 can be solved from

$$F_{x0}(t) = Mg \sin\theta_{rg}(t) + f_{rr}mg \cos\theta_{rg}(t) \\ + 0.5\rho_{air}A_v C_d(v_0(t) + v_w(t))^2. \quad (5.9)$$

Eq. (5.9) can be linearized about the equilibrium point by using the Taylor series expansion

$$\frac{d\tilde{v}}{dt} + \tilde{v} = K_{AV}(\tilde{F}_x + d_{AV}) \quad (5.10)$$

where \tilde{v} is the velocity deviation, defined as

$$\tilde{v} = v - v_0 \quad (5.11)$$

and \tilde{F}_x is the longitudinal force deviation, defined as

$$\tilde{F}_x = F_x - F_{x0} \quad (5.12)$$

Parameters τ , K_{AV} , and d_{AV} were derived as $\tau = M/(\rho_{air}C_dA_v(v_0 + v_w))$, $K_{AV} = 1/\rho_{air}C_dA_v(v_0 + v_w)$, and $d_{AV} = Mg(f_{rr}\sin\theta_{rg} - \cos\theta_{rg})d\theta_{rg}/dt$. Assume $v_w = 0$ and $\theta_{rg} = 0$. Using Laplace transformation [146] on Eq. (5.10), we obtain a first order lag system representing the vehicle longitudinal dynamics.

$$\frac{\tilde{v}(s)}{\tilde{F}_x(s)} = \frac{K_{AV}}{\tau s + 1} \quad (5.13)$$

The vehicle mass was set as the summation of the curb mass of 2011 Volvo V60 [147] and the mass of two 60 kg. The frontal area, rolling resistance coefficient, frontal area, and aerodynamic coefficient were set as the same parameters of the Class E sedan model used in the commercial software CarSim® [118]. It should be noted that the vehicle models presented in the section may not be a good representation of the actual systems in a production vehicle. If more accurate simulations are desired, the proposed accelerated evaluation process can be used in junction with more accurate simulation models such as CarSim®. More details of vehicle dynamic techniques can be found in [148], [149].

5.2.3.2 Adaptive cruise control

The Adaptive cruise control is designed based on the research in [145]. The longitudinal control of AV is designed to follow the lead HV velocity and maintain a proper frontal distance. As shown in Figure 5.4, the controller is implemented in the discrete time domain.

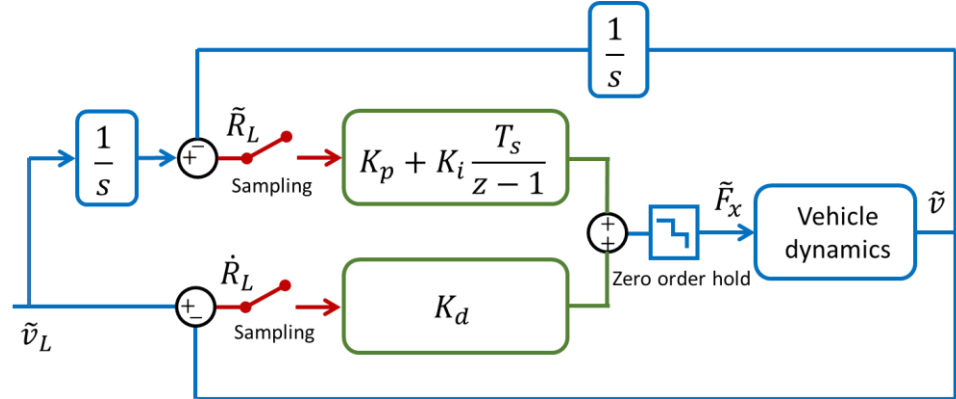


Figure 5.4 Automated vehicle model

The discrete-time control algorithm can be expressed as

$$\tilde{F}_x(z) = \left(K_p + K_i \frac{T_s}{z - 1} \right) \tilde{R}_L(z) + K_d \dot{\tilde{R}}_L(z) \quad (5.14)$$

where $F_x(z)$, $\tilde{R}_L(z)$, and $\dot{\tilde{R}}_L(z)$ are Z transformation [150] of $F_x(t)$, $\tilde{R}_L(t)$, and $\dot{\tilde{R}}_L(t)$. T_s is the time step. $\tilde{R}_L(t)$ is defined as

$$\tilde{R}_L(t) = R_L(t) - R_L^{desire} \quad (5.15)$$

where $R_L^{desire} = v_0 * t_{HW}^{desire}$ and t_{HW}^{desire} is the desired time headway. \tilde{R}_L is regulated by a discretized Proportional-Integral (PI) controller and the range rate is regulated by a Proportional (P) controller. \tilde{R}_L is calculated from

$$\tilde{R}_L(t) = \int_0^t \dot{R}_L(t) dt + R_{L0} - R_L^{desire} \quad (5.16)$$

where R_{L0} is the initial range. R_{L0} is equal to R_L^{desire} to make the test starts from an equilibrium.

5.3 The Optimal Mean Shift Approach

The statistics of the motion of the lead HV is modified to generate more intense interactions with the AV. From Eq. (5.1), the acceleration in the next step of the lead HV follows the probability density function

$$a_L(k+1) \sim \mathcal{N}(h_0 + h_1 a_L(k) + h_2 v_L(k), \sigma_u^2). \quad (5.17)$$

The general idea to accelerate the evaluation is to add a series of biases [$\delta(1), \delta(2), \dots$] to the mean of the acceleration distribution. The modified acceleration distribution becomes

$$a_L(k+1) \sim \mathcal{N}(h_0 + h_1 a_L(k) + h_2 v_L(k) + \delta(k), \sigma_u^2). \quad (5.18)$$

In this section, we first derive a car-following model into the state space form. We then calculate the optimal $\delta(k)$.

5.3.1 State space form of the car-following model

The car-following model can be linearized and rewritten in the state space form. In discrete time, the lead vehicle velocity is calculated from

$$v_L(k+1) = v_L(k) + T_s a_L(k). \quad (5.19)$$

Define velocity deviation of the lead HV as

$$\tilde{v}_L(k) = v_L(k) - v_0. \quad (5.20)$$

We have

$$\tilde{v}_L(k+1) = \tilde{v}_L(k) + T_s a_L(k). \quad (5.21)$$

Define another random variable

$$u = u_h + h_0 + h_2 v_0. \quad (5.22)$$

From Eq. (5.1) and (5.20), we have

$$a_L(k+1) = h_1 a_L(k) + h_2 \tilde{v}_L(k) + u. \quad (5.23)$$

Discretize Eq. (5.13) using the Zero Order Hold method [150],

$$\frac{\tilde{v}(z)}{\tilde{F}_x(z)} = \frac{n_v z^{-1}}{1 + d_v z^{-1}} \quad (5.24)$$

where $v'(z)$ and $F_x'(z)$ are the Z transformation of $v'(t)$ and $F_x'(t)$. Taking the inverse Z transformation of Eq. (5.24), we get

$$\tilde{v}(k+1) = d_v \tilde{v}(k) + n_v \tilde{F}(k). \quad (5.25)$$

Substituting Eqs. (5.11) and (5.22) into Eq. (5.2), we have

$$\dot{R}_L(k) = \tilde{v}_L(k) - \tilde{v}(k). \quad (5.26)$$

Discretize Eq. (5.16) and substitute Eqs. (5.15) and (5.19) in (5.16).

$$\begin{aligned} \tilde{R}_L(k+1) &= \tilde{R}_L(k) + T_s \dot{R}_L(k) \\ &= \tilde{R}_L(k) + T_s \tilde{v}_L(k) - T_s \tilde{v}(k). \end{aligned} \quad (5.27)$$

Take the inverse Z transformation [150] of Eq. (5.14).

$$\tilde{F}_x(k+1) = \tilde{F}_x(k) - K_p \tilde{R}_L(k) + (K_p + K_i T_s) \tilde{R}_L(k+1) + K_d \dot{R}_L(k+1). \quad (5.28)$$

Substitute Eqs. (5.26) and (5.27) into (5.28).

$$\begin{aligned} \tilde{F}_x(k+1) &= \tilde{F}_x(k) + T_s K_i \tilde{R}_L(k) + (K_p + T_s K_i) (T_s \tilde{v}_L(k) - T_s \tilde{v}(k)) \\ &\quad + K_d (\tilde{v}_L(k+1) - \tilde{v}(k+1)). \end{aligned} \quad (5.29)$$

Substitute Eqs. (5.25) and (5.28) into (5.29).

$$\tilde{F}_x(k+1) = q_1 a_L(k) + q_2 \tilde{v}_L(k) + q_3 \tilde{v}(k) + q_4 \tilde{F}_x(k) + q_5 \tilde{R}_L(k) \quad (5.30)$$

where $q_1 = K_d T_s$, $q_2 = K_d + K_p T_s + K_i T_s^2$, $q_3 = -K_d d_v - K_p T_s - K_i T_s^2$, $q_4 = 1 - K_d n_v$, $q_5 = T_s K_i$.

Rewriting Eqs. (5.23), (5.25), (5.21), (5.27) and (5.30) into the state space form, we have

$$\begin{aligned} \mathbf{X}(k+1) &= \mathbf{A}\mathbf{X}(k) + \mathbf{B}u(k) \\ R_L(k) &= \mathbf{C}\mathbf{X}(k) \end{aligned} \quad (5.31)$$

where $\mathbf{X}(k) = [a_L(k) \quad \tilde{v}_L(k) \quad \tilde{v}(k) \quad \tilde{F}_x(k) \quad \tilde{R}_L(k)]^T$

$$\mathbf{A} = \begin{bmatrix} h_1 & h_2 & 0 & 0 & 0 \\ T_s & 1 & 0 & 0 & 0 \\ 0 & 0 & -d_v & n_v & 0 \\ q_1 & q_2 & q_3 & q_4 & q_5 \\ 0 & T_s & -T_s & 0 & 1 \end{bmatrix}$$

$$\mathbf{B} = [1 \quad 0 \quad 0 \quad 0 \quad 0]^T, \mathbf{C} = [0 \quad 0 \quad 0 \quad 0 \quad 1]$$

with initial condition $\mathbf{X}(1) = [0 \quad 0 \quad 0 \quad 0 \quad 0]^T$ and physical constraints

$$\mathbf{X}_{min} \leq \mathbf{X}(k) \leq \mathbf{X}_{max}$$

where $\mathbf{X}_{min} = [a_L^{Min}, v_L^{Min} - v_0, v^{Min} - v_0, F_x^{Min} - F_{x0}, R_L^{Min} - R_L^{desire}]^T$ and $\mathbf{X}_{max} = [a_L^{Max}, v_L^{Max} - v_0, v^{Max} - v_0, F_x^{Max} - F_{x0}, R_L^{Max} - R_L^{desire}]^T$.

5.3.2 Accelerated Evaluation

In the following, we will describe the four steps of the Accelerated Evaluation procedure: i) calculate the optimal $\beta(k)$, ii) randomize the termination time, iii) run the accelerated tests, and iv) calculate the likelihood and estimate the real world benefits. The same procedure can be applied to estimate all three metrics: crash, injury, and conflict. For narrative simplicity, during the derivation, we use the term “crash” to represent all the three types of events.

5.3.2.1 Calculation of the optimal mean shift

We will first calculate $u^*(k)$ - the optimal realization of $u(k)$. Second, $\beta^*(k)$, the optimal value of $\beta(k)$, is calculated to maximize the likelihood for $u(k)$ to be $u^*(k)$ in the accelerated tests.

From Eq. (5.22), under the naturalistic driving conditions, we have

$$u(k) \sim f_{u_k}(u(k)) = \mathcal{N}(\mu_u, \sigma_u^2) \quad (5.32)$$

where $\mu_u = h_0 + h_2 v_0$. The simulation ends when either a crash happens or the maximum time step is reached. Define the termination time step

$$k_T = \min\{\min(k | R_L(k) < 0), K\} \quad (5.33)$$

where k_T is an integer $\in \{1, \dots, K\}$. K is the maximum step number in a car-following event. Because the lead HV is modeled as a Markov Chain, the probability density for a car-following event (from time step 1 to k_T) can be calculated from

$$f_u(u(1:k_T - 1)) = \prod_{k=1}^{k_T-1} f_{u_k}(u(k)). \quad (5.34)$$

Substituting Eq. (5.32) into Eq.(5.34), we have

$$f_u(u(1:k_T - 1)) = \left(\frac{1}{\sqrt{2\pi}\sigma_u}\right)^{k_T-1} \exp\left(-\frac{\|u(1:k_T - 1) - \mu_u \mathbf{1}\|_2^2}{2\sigma_u^2}\right) \quad (5.35)$$

where $u(1:k_T - 1) = [u(1), u(2), \dots, u(k_T - 1)]^T$, $\|\cdot\|_2^2$ represents the Euclidean two-norm and $\mathbf{1} = [1, 1, \dots, 1]^T \in \mathbb{R}^{(k_T-1) \times 1}$.

In the accelerated tests, from Eq. (5.18) and Eq. (5.22), we have

$$u(k) \sim \tilde{f}_{u_k}(u(k)) = \mathcal{N}(\mu_u + \vartheta(k), \sigma_u^2). \quad (5.36)$$

The modified probabilistic density distribution is calculated from

$$\tilde{f}_u(u(1:k_T - 1)) = \prod_{k=1}^{k_T-1} \tilde{f}_{u_k}(u(k)). \quad (5.37)$$

Substituting (5.36) into (5.37), we have

$$\begin{aligned} & \tilde{f}_u(u(1:k_T - 1)) \\ &= \left(\frac{1}{\sqrt{2\pi}\sigma_u} \right)^{k_T-1} \exp \left(-\frac{\|u(1:k_T - 1) - \mathcal{B}(1:k_T - 1) - \mu_u \mathbf{1}\|_2^2}{2\sigma_u^2} \right) \end{aligned} \quad (5.38)$$

The optimal realization of $u(k)$ is then calculated to achieve two goals

- i) *To make a crash happen at a specific time k_T^**
- ii) *To maximize the likelihood of the crash event happening*

We need i) to calculate the crash rate. We need ii) to focus on the events with a high probability of occurring. A crash happening at an extremely low probability (e.g. the surrounding vehicles are all Lamborghinis that cut in and accelerate/decelerate crazily) does not play a significant role in calculating the average crash rate. The two goals can be expressed as an optimization problem as follows.

$$u_{k_T^*}(1:k_T^* - 1) = \arg \max_{u(1:k_T^*-1)} f(u(1:k_T^* - 1))$$

subject to

$$R_L(k_T^*) \leq R_\varepsilon \quad (5.39)$$

$$X_{min} \leq X(k) \leq X_{max}$$

$$u_{min} \leq u(k) \leq u_{max}$$

for $k = 1, 2, \dots, k_T^* - 1$, where R_ε is the critical distance. For crash and injury, $R_\varepsilon = 0$. For conflict, according to Eq. (4.38), $R_\varepsilon = 30$ feet.

Substituting Eqs. (5.34) and (5.31) into Eq. (5.39) and rewriting Eq. (5.39) in the quadratic form, we have

$$\begin{aligned} & u_{k_T^*}(1:k_T^* - 1) \\ &= \arg \min_{u(1:k_T^*-1)} \left[\frac{1}{2} u(1:k_T^* - 1)^T u(1:k_T^* - 1) - \mu_u \mathbf{1}^T u(1:k_T^* - 1) \right] \end{aligned} \quad (5.40)$$

subject to

$$\mathbf{A}_{k_T^*} u_{k_T^*}(1:k_T^* - 1) \leq \mathbf{b}_{k_T^*}$$

where

$$\mathbf{A}_{k_T^*} = \begin{bmatrix} \mathbf{CA}^{(k_T^*-2)}\mathbf{B} & \mathbf{CA}^{(k_T^*-3)}\mathbf{B} & \cdots & \mathbf{CB} \\ \mathbf{B} & 0 & \cdots & 0 \\ \mathbf{AB} & \mathbf{B} & \cdots & 0 \\ \vdots & \vdots & \ddots & \vdots \\ \mathbf{A}^{(k_T^*-3)}\mathbf{B} & \mathbf{A}^{(k_T^*-4)}\mathbf{B} & \cdots & 0 \\ -\mathbf{B} & 0 & \cdots & 0 \\ -\mathbf{AB} & -\mathbf{B} & \cdots & 0 \\ \vdots & \vdots & \ddots & \vdots \\ -\mathbf{A}^{(k_T^*-3)}\mathbf{B} & -\mathbf{A}^{(k_T^*-4)}\mathbf{B} & \cdots & 0 \\ 1 & 0 & \cdots & 0 \\ 0 & 1 & \cdots & 0 \\ \vdots & \vdots & \ddots & \vdots \\ 0 & 0 & \cdots & 1 \\ -1 & 0 & \cdots & 0 \\ 0 & -1 & \cdots & 0 \\ \vdots & \vdots & \ddots & \vdots \\ 0 & 0 & \cdots & -1 \end{bmatrix}, \quad \mathbf{b}_{k_T^*} = \begin{bmatrix} R_{\varepsilon} - \mathbf{CA}^{(k_T^*-1)}\mathbf{X}(1) \\ \mathbf{X}_{max} - \mathbf{AX}(1) \\ \mathbf{X}_{max} - \mathbf{A}^2\mathbf{X}(1) \\ \vdots \\ \mathbf{X}_{max} - \mathbf{A}^{(k_T^*-2)}\mathbf{X}(1) \\ -\mathbf{X}_{min} + \mathbf{AX}(1) \\ -\mathbf{X}_{min} + \mathbf{A}^2\mathbf{X}(1) \\ \vdots \\ -\mathbf{X}_{min} + -\mathbf{A}^{(k_T^*-2)}\mathbf{X}(1) \\ u_{max} \\ u_{max} \\ \vdots \\ u_{max} \\ -u_{min} \\ -u_{min} \\ \vdots \\ -u_{min} \end{bmatrix}.$$

The optimal shift parameters $\boldsymbol{\theta}_{k_T^*}(1:K)$ are calculated to maximize the likelihood for $u_{k_T^*}(1:K)$ to be realized in the accelerated test. For a specific k_T^* , $\boldsymbol{\theta}_{k_T^*}(1:K)$ can be calculated from

$$\boldsymbol{\theta}_{k_T^*}(1:k_T^*) = \arg \max_{\boldsymbol{\theta}(1:K)} \tilde{f}\left(u_{k_T^*}(1:k_T^*), \boldsymbol{\theta}(1:k_T^*)\right). \quad (5.41)$$

Substituting (5.38) into (5.41), we have

$$\begin{aligned} & \boldsymbol{\theta}_{k_T^*}(1:k_T^*) \\ &= \arg \max_{\boldsymbol{\theta}(1:k_T^*)} \left(\frac{1}{\sqrt{2\pi}\sigma_u} \right)^{k_T^*} \exp \left(-\frac{\|u(1:k_T^*) - \boldsymbol{\theta}(1:k_T^*) - \mu_u \mathbf{1}\|_2^2}{2\sigma_u^2} \right). \end{aligned} \quad (5.42)$$

Taking out the constant terms from the $\arg \max$ function, we have

$$\boldsymbol{\theta}_{k_T^*}(1:k_T^*) = \arg \max_{\boldsymbol{\theta}(1:k_T^*)} \exp(-\|u(1:k_T^*) - \boldsymbol{\theta}(1:k_T^*) - \mu_u \mathbf{1}\|_2^2). \quad (5.43)$$

Because the exponential function is a monotonically increasing function, it will not affect the solution of the $\arg \max$ function. $\mathcal{B}_{k_T^*}(1:k_T^*)$ can be calculated from

$$\mathcal{B}_{k_T^*}(1:k_T^*) = \arg \min_{\mathcal{B}(1:k_T^*)} \|u(1:k_T^*) - \mathcal{B}(1:k_T^*) - \mu_u \mathbf{1}\|_2^2. \quad (5.44)$$

Since $\|u(1:k_T^*) - \mathcal{B}(1:k_T^*) - \mu_u \mathbf{1}\|_2^2 \geq 0$, to achieve the minimum value, we have

$$\|u(1:k_T^*) - \mathcal{B}(1:k_T^*) - \mu_u \mathbf{1}\|_2^2 = 0. \quad (5.45)$$

Therefore, the optimal mean shift is calculated from

$$\mathcal{B}_{k_T^*}(1:k_T^*) = u_{k_T^*}(1:k_T^*) - \mu_u \quad (5.46)$$

$\mathcal{B}_{k_T^*}(1:K)$ for each $k_T^* = 1, \dots, K$ will be calculated offline. We will use these $\mathcal{B}_{k_T^*}$ in the stochastic process during the evaluation.

5.3.2.2 Randomization of termination time

The termination time k_T^* is fixed in the previous section. However, crash can happen at any moment before time step K . k_T^* needs to be randomized to reflect all the crash scenarios.

We first set the boundary of k_T^* . When k_T^* is small, it may fail to find a feasible solution to the optimization problem in Eq. (5.40). This is because no HV motion will lead to a crash when the allowed time duration is very short (e.g. 0.1 s). Let $k_{T\min}^*$ be the minimum value of k_T^* that has a feasible solution in Eq. (5.40) calculated from the initial vehicle speed and maximum allowed deceleration, that is

$$k_{T\min}^* = \min k_T^* \text{ such that } \exists u_{k_T^*}(1:k_T^* - 1) \text{ that makes} \quad (5.47)$$

$$\mathbf{A}_{k_T^*} u_{k_T^*}(1:k_T^* - 1) \leq \mathbf{b}_{k_T^*}$$

k_T^* is randomized using a discrete uniform distribution

$$k_{\mathcal{T}}^* \sim f_{k_{\mathcal{T}}^*}(k_{\mathcal{T}}^*) = \frac{1}{K - k_{\mathcal{T}min}^* + 1} \quad (5.48)$$

where $k_{\mathcal{T}}^* = k_{\mathcal{T}min}^*, k_{\mathcal{T}min}^* + 1, \dots, K - 1, K$

It should be noted that $k_{\mathcal{T}}^*$ is different from $k_{\mathcal{T}}$. $k_{\mathcal{T}}$ is the real termination time in the simulation, while $k_{\mathcal{T}}^*$ is a computed value that is used to randomize termination time in calculating the optimal shift $\boldsymbol{\delta}_{k_{\mathcal{T}}^*}(1:k_{\mathcal{T}}^* - 1)$.

5.3.2.3 Conducting the accelerated tests

The car-following simulation is executed in the following steps:

- i) Sample a $k_{\mathcal{T}}^*$ from Eq.(5.48)
- ii) Obtain the corresponding optimal shift vector $\boldsymbol{\delta}_{k_{\mathcal{T}}^*}(1:K)$ calculated from Eq. (5.44)
- iii) Run an accelerated test with the acceleration of the lead HV following the distribution.

$$a_L(k+1) \sim \mathcal{N}(h_0 + h_1 a_L(k) + h_2 v_L(k) + \boldsymbol{\delta}_{k_{\mathcal{T}}^*}(k), \sigma_u^2) \quad (5.49)$$

- iv) Record crash indicator and the termination time

Define the crash event \mathcal{E} as

$$\mathcal{E} = \{\min(R_L(k)) < 0 | 1 \leq k \leq K\}. \quad (5.50)$$

The crash indicator function is defined as

$$I_{\mathcal{E}}(n) = \begin{cases} 1, & \text{crash} \\ 0, & \text{no crash} \end{cases} \quad (5.51)$$

where n is the index of the car-following test.

The termination time can be calculated from Eq. (5.33), which will be used in calculating the likelihood ratio in the next section.

5.3.2.4 Calculation of crash rate

The crash rate is calculated based on the Importance Sampling techniques introduced in Section 3.2.2. Based on Eq. (3.15), the crash rate in the real world can be estimated from

$$\hat{\gamma}(n) = \frac{1}{n} \sum_{i=0}^n I_{\varepsilon}(n) L(n) \quad (5.52)$$

where $L(n)$ is the likelihood ratio in the n^{th} car-following test, defined in Eq. (3.12), which is the ratio between $f(\cdot)$ the likelihood of in naturalistic driving condition over $f^*(\cdot)$ the likelihood in an accelerated test.

$$L(n) = \frac{f(a_L(1:k_T - 1))}{f^*(a_L(1:k_T - 1))} \quad (5.53)$$

Based on Eq. (5.17) $f(a_L(1:k_T - 1))$ can be calculated from

$$\begin{aligned} & f(a_L(1:k_T - 1)) \\ &= \prod_{k=1}^{k_T-1} \frac{1}{\sigma_u \sqrt{2\pi}} \exp \left\{ -\frac{(a_L(k+1) - h_1 a_L(k) - h_2 v_L(k) - h_0)^2}{2\sigma_u^2} \right\}. \end{aligned} \quad (5.54)$$

$f^*(\cdot)$ is calculated considering both the likelihood of the uncertainty of the dynamic procedure and the randomness of the termination time:

$$f^*(a_L(1:k_T - 1)) = \sum_{k_T^* = k_{T \min}^*}^K \tilde{f}(a_L(1:k_T - 1)|k_T^*) f_{k_T^*}(k_T^*) \quad (5.55)$$

where $\tilde{f}(a_L(1:k_T - 1)|k_T^*)$ is calculated from

$$\begin{aligned} & \tilde{f}(a_L(1:k_T - 1)|k_T^*) \\ &= \prod_{k=1}^{k_T-1} \frac{1}{\sigma_u \sqrt{2\pi}} \exp \left\{ -\frac{(a_L(k+1) - h_1 a_L(k) - h_2 v_L(k) - h_0 - \beta_{k_T^*}(k))^2}{2\sigma_u^2} \right\} \end{aligned} \quad (5.56)$$

Keep running the car-following tests until $\hat{\gamma}(n)$ converges. The convergence is reached when the relative half-width l_r (defined in Eq. (3.7)) is below β with $100(1 - \alpha)\%$ confidence level. β and α are small constant chosen by the tester.

5.3.2.5 Summary

The procedure of the accelerated test is summarized in Figure 5.5.

Before simulations:

- i) Calculate the optimal mean shift vector $\boldsymbol{\theta}_{k_{\mathcal{T}}^*}(1:K)$ for each $k_{\mathcal{T}}^*$ from Eq. (5.46)
- ii) $k_{\mathcal{T}min}^*$ is found from Eq. (5.47). Generate distribution $f_{k_{\mathcal{T}}^*}(\cdot)$ in Eq. (5.48) using $k_{\mathcal{T}min}^*$

During simulations:

- iii) Sample a $k_{\mathcal{T}}^*$ from Eq.(5.48)
- iv) Run the accelerated tests with AE distribution in Eq. (5.49). After each test record whether a crash happens (represented by $I_{\mathcal{E}}$) and the termination time $k_{\mathcal{T}}$.
- v) Calculate the likelihood of each test from Eq. (5.53)
- vi) Calculate the crash rate from Eq. (5.52)
- vii) Calculate the relative half-width l_r defined in Eq. (3.7)
- viii) If $l_r < \beta$, output the crash rate. Otherwise, go back to step iii)

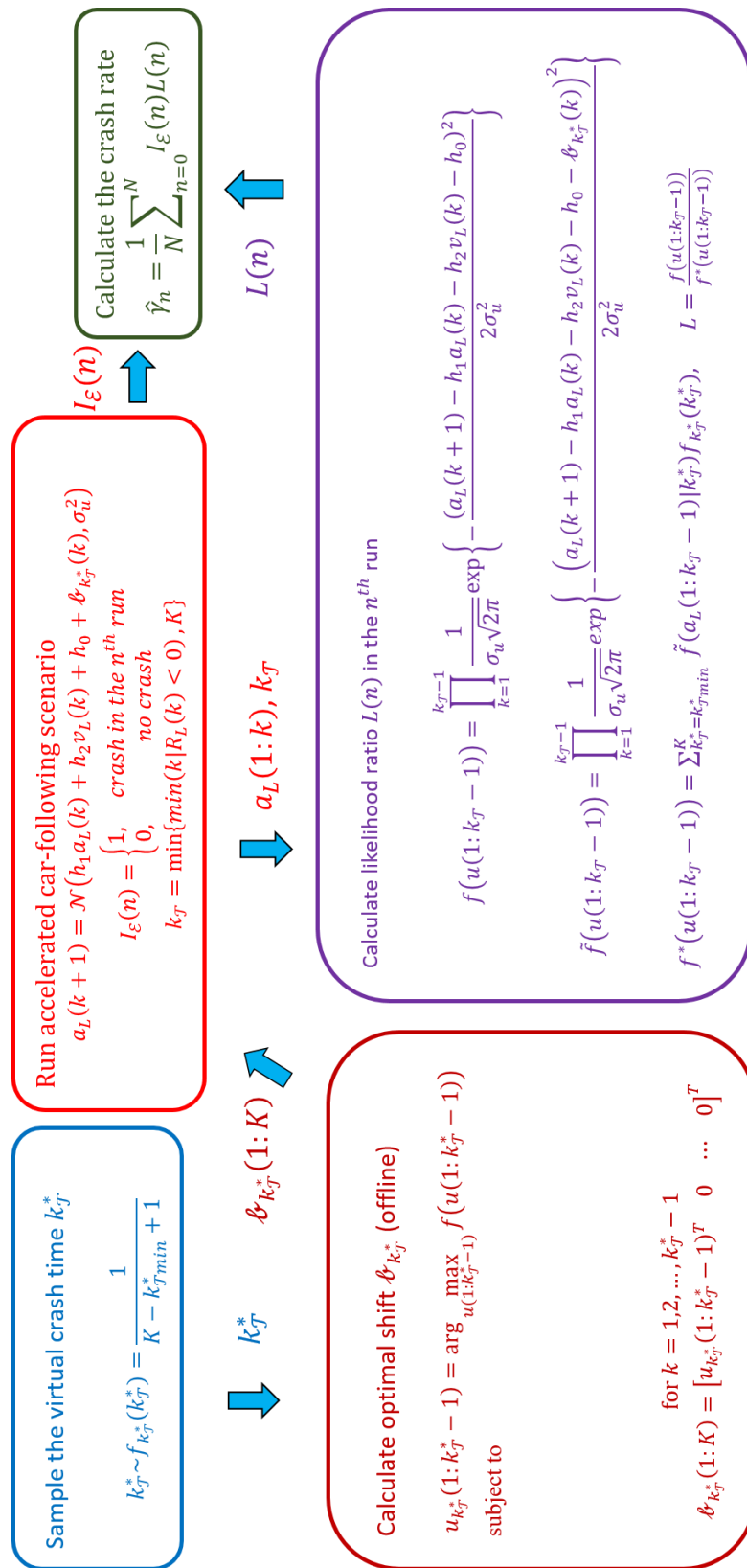


Figure 5.5 Procedure to calculate crash rate in the car-following scenario

5.4 Simulation Analysis

In this section, numerical examples are presented to demonstrate the performance and validity of the proposed approach. First, the uniform distribution is used as a baseline AE distribution to evaluate the dynamic interaction between AVs and HVs. The acceleration of the HV is amplified, but the evaluation is not accelerated. This result shows that the correlation between samples must be considered to effectively accelerate the evaluation of AVs, in the dynamic sampling environment, where the transition statistics are changing with states, such as in the car-following scenario. Second, the proposed approach is implemented to accelerate the evaluation procedure. Three metrics, cash, injury, and conflict rates, are calculated. In each case, both accelerated and naturalistic simulations were conducted to examine the accuracy and the accelerated rate of the proposed method. Finally, the sensitivity of the metric estimation to the accuracy of the HV model is analyzed.

5.4.1 Simulation results with baseline accelerated methods

In this section, we use a uniform AE distribution in the car-following estimation. The HV acceleration is generated via Eq. (5.57).

$$\begin{aligned} a_L(k+1) &\sim \tilde{f}_{ud}(a_L(k), v_L(k)) \\ &= \mathcal{U}([1, a_L(k), v_L(k)]\mathbf{h} - \vartheta_{ud}/2, [1, a_L(k), v_L(k)]\mathbf{h} + \vartheta_{ud}/2) \end{aligned} \quad (5.57)$$

where \mathcal{U} represents the uniform distribution and parameter ϑ_{ud} is chosen to be $6\sigma_u$. The comparison between the original HV distribution and the uniform AE distribution is shown in Figure 5.6.

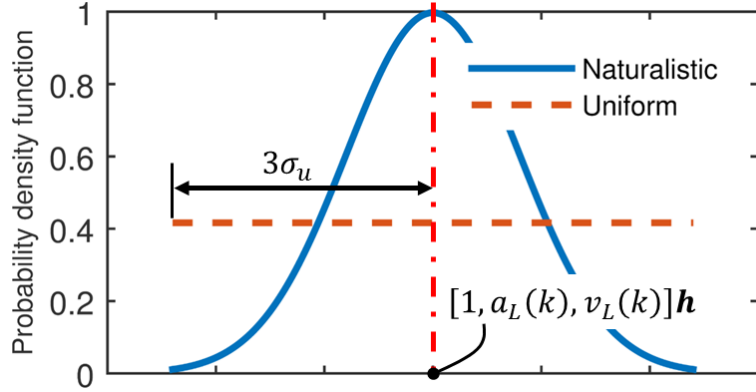


Figure 5.6 Original HV distribution and the uniform AE distribution

The HV model and AV model developed in Section 5.2 is used to demonstrate the performance of the method. Each simulation run starts with the same initial states. The likelihood ratio of the uniform distribution method can be calculated from

$$L(n) = \frac{f(a_L(1:k_T - 1))}{f_{ud}^*(a_L(1:k_T - 1))} \quad (5.58)$$

where k_T is the termination time defined in (5.33). $f(a_L(1:k_T - 1))$ is calculated from Eq. (5.54). $f_{ud}^*(\cdot)$ is calculated from

$$f_{ud}^*(a_L(1:k_T - 1)) = \prod_{k=1}^{k_T-1} \tilde{f}_{ud}(a_L(k)) = \vartheta_{ud}^{-k_T}. \quad (5.59)$$

The model parameters used in the simulation are listed in Table 5.2. One example of the accelerated test is shown in Figure 5.7. Although the lead HV acceleration surged up and down, most of the oscillations of the acceleration were canceled out in generating velocity, and crash did not happen.

Table 5.2 Parameters for the car-following simulations

Var.	Unit	Value	Var.	Unit	Value
a_{L_0}	m/s^2	0	K_p	-	62.63
a_0	m/s^2	0	M	Kg	1757
a_L^{Max}	m/s^2	9.81	R_L^{Max}	m	1e3
a_L^{Min}	m/s^2	-9.81	R_L^{Min}	m	0
a^{Max}	m/s^2	9.81	T_{CF}	s	114
a^{Min}	m/s^2	-9.81	t_{HW}^{desire}	s	2
A_v	m^2	2.2	T_s	s	0.3
C_d	-	0.32	u_{max}	m/s^2	1.2
F_x^{Max}	N	17236	u_{min}	m/s^2	-1.2
F_x^{Min}	N	-17236	v^{Max}	m/s	50
g	m/s^2	9.81	v^{Min}	m/s	1
h_0	-	3.395e-2	v_L^{Max}	m/s	50
h_1	-	0.8516	v_L^{Min}	m/s	1
h_2	-	-1.406e-3	v_0	m/s	20
K	-	119	v_{L_0}	m/s	20
K_d	-	882.7	ρ_{air}	kg/m^3	1.202
K_i	-	1.111	σ_u	-	0.3949

The crash rate was calculated from Eq. (5.52). Due to the misconnection between each sampling and the oversimplified AE distribution, most of the crashes had very small likelihood ratio. The estimated crash rate is shown in Figure 5.8. A million simulation runs have been conducted, but because the convergence is very weak, not much can be told about the crash rate. The uniform distribution cannot effectively accelerate crash evaluation in the car-following scenario.

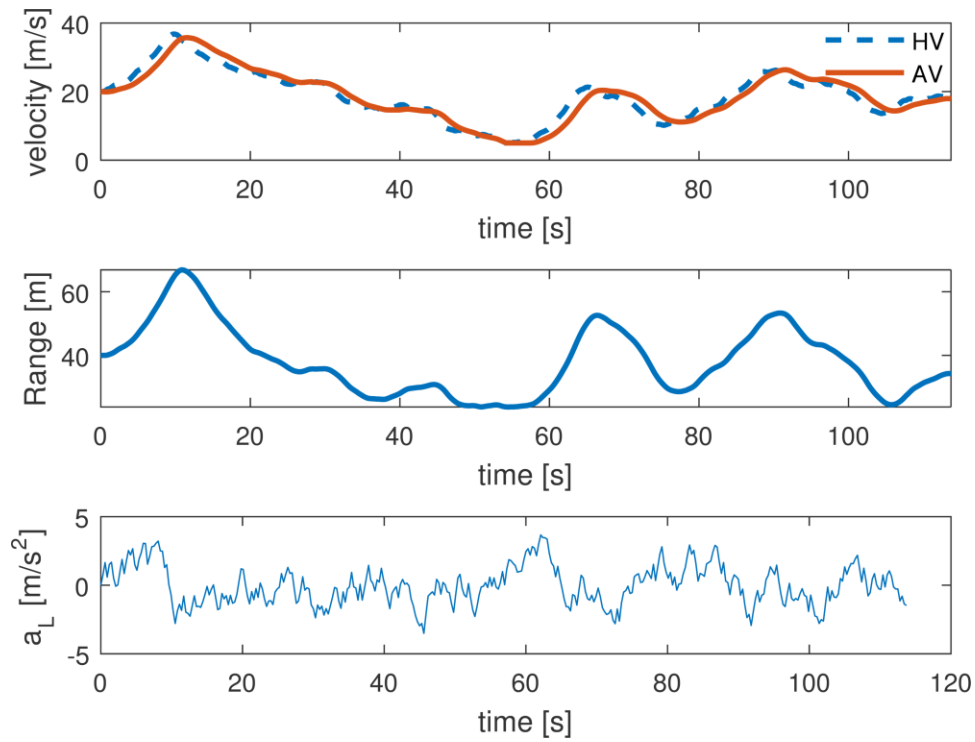


Figure 5.7 An example maneuver generated by the baseline accelerated evaluation approach with uniform distribution

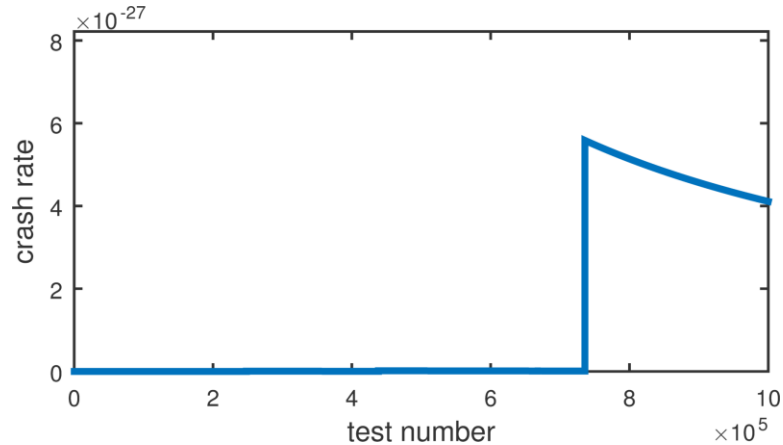


Figure 5.8 Estimation of the crash rate using uniform distribution as the AE distribution

5.4.2 Simulation results with proposed accelerated evaluation method

In this section, we applied the proposed Accelerated Evaluation approach on three types of events: the crash, injury, and conflict event to examine the accuracy, robustness, and the accelerated rate of the method.

5.4.2.1 Estimation of the crash rate

Both accelerated and naturalistic simulations were conducted. Selected examples of the lead HV speed in both cases are shown in Figure 5.9. In the accelerated tests, the vehicle tends to accelerate and decelerate at significant levels. In the naturalistic tests, the vehicle speed is obtained through direct Monte Carlo sampling and while the vehicle speed also fluctuates, it is much more mild.

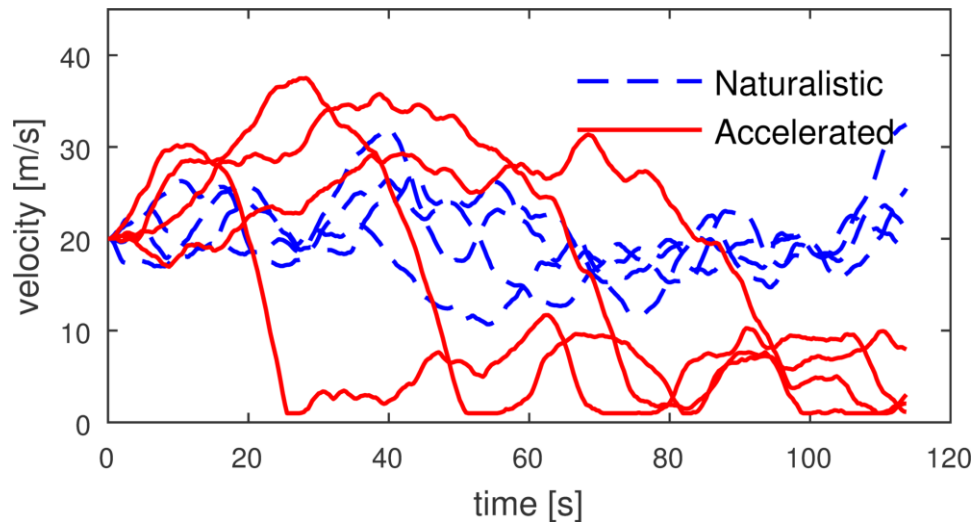


Figure 5.9 Comparison of lead vehicle speed profiles in accelerated and non-accelerated (naturalistic) driving conditions

Figure 5.10 shows an example in an accelerated test that leads to a crash. It can be seen that the crash is caused by frequent acceleration and deceleration, and in this case a “final blow” through a severe braking from a high speed. When the lead HV accelerates, it creates a larger R_L . The AV then accelerates to catch up. If HV conduct a harsh brake at the moment when AV overshoots, it may lead to a crash. This tactic is frequently observed in the proposed tests, but not in the current Euro-NCAP test protocols and ISO standards. In other words, the proposed accelerated evaluation method automatically generated high risk maneuvers, some of which might be considered in the future government certification process.

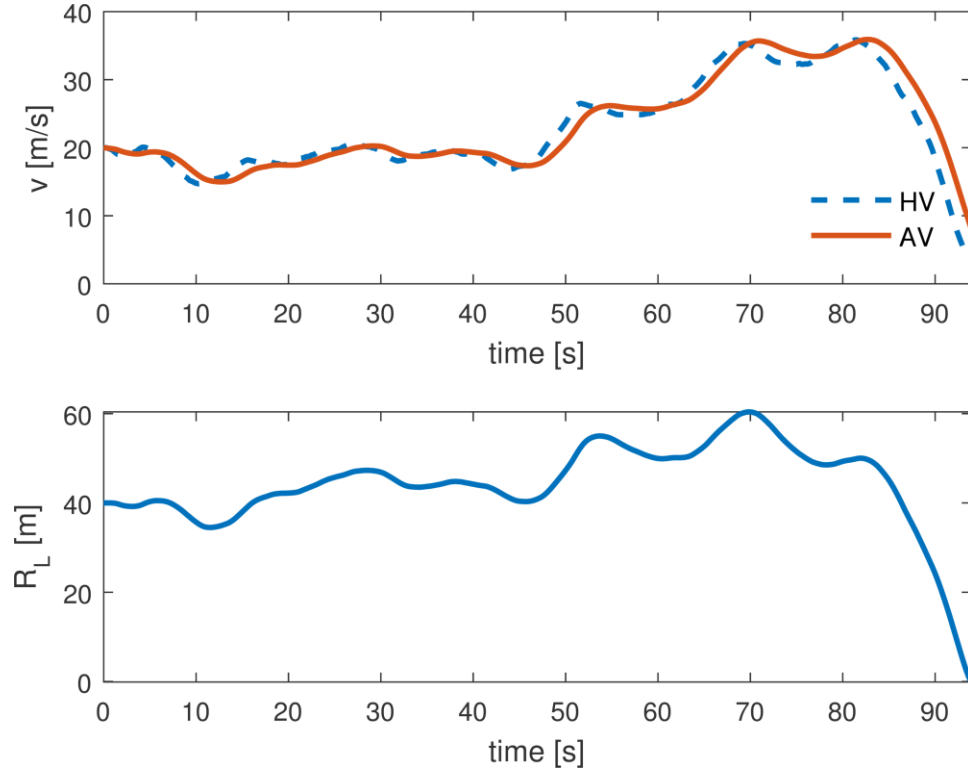


Figure 5.10 An example maneuver generated by the accelerated evaluation approach leading to a crash

Both accelerated and naturalistic tests were conducted until the crash rate converged with 80 % confidence level and $\beta = 0.2$. Figure 5.11 shows that the estimation of the crash rate calculated by the accelerated tests converges to the naturalistic driving estimation, which shows that the Accelerated Evaluation is unbiased.

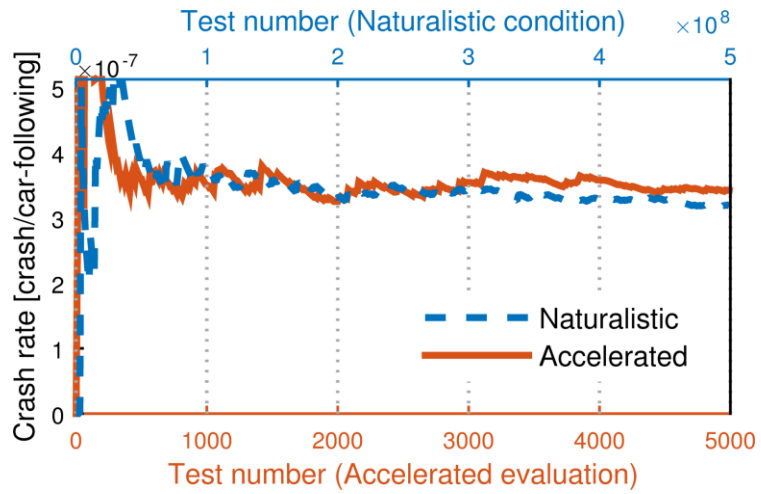


Figure 5.11 Estimation of the crash rate in the car-following scenario

Figure 5.12 shows that accelerated tests achieve the confidence level β after $N_{acc} = 3.84e3$ simulations, while the naturalistic (crude Monte Carlo) method took $N_{nature} = 4.30e8$ simulations.

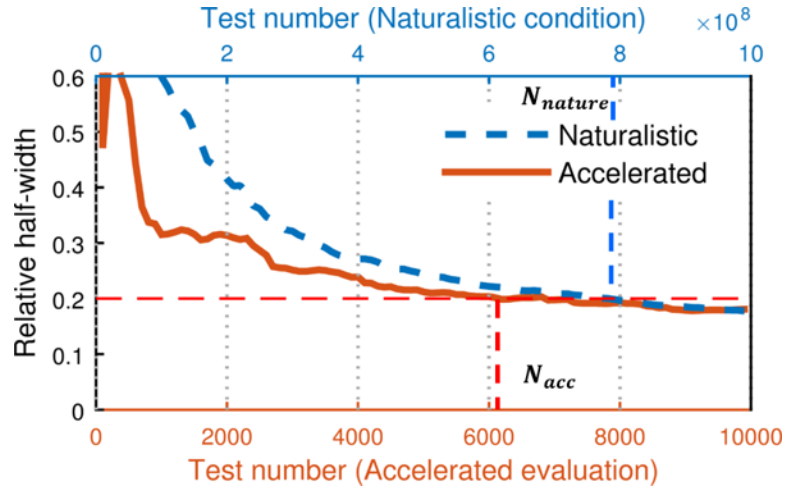


Figure 5.12 Convergence of crash rate estimation in the car-following scenario

5.4.2.2 Estimation of the injury rate

We also estimate the injury rate using the proposed Accelerated Evaluation method. The probability of moderate-to-fatal injuries for the AV passengers is defined in Eq. (3.38). The estimated injury rate can be calculated from Eq. (3.39). Both accelerated and naturalistic tests were conducted until the injury rate converged with 80 % confidence level and $\beta = 0.2$. Figure 3.15 shows that estimated injury rate in the accelerated test converges to the result under naturalistic driving conditions.

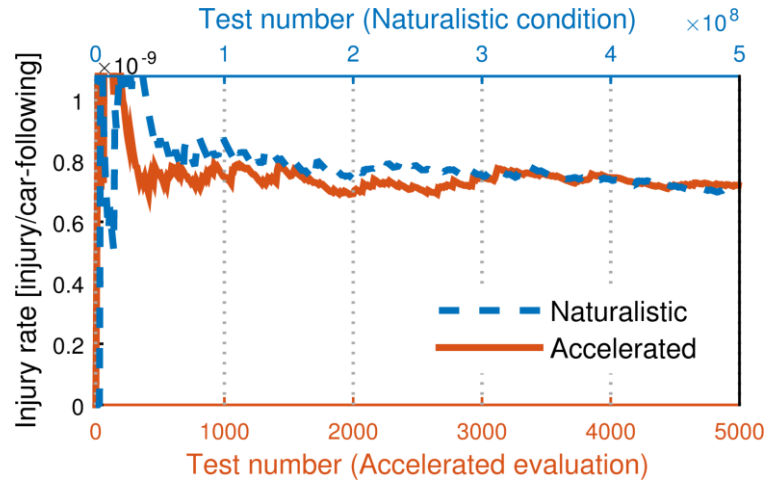


Figure 5.13 Estimation of the injury rate in the car-following scenario

Figure 5.12 shows that accelerated tests achieve the confidence level β after $N_{acc} = 3.10e3$ simulations, while the naturalistic (crude Monte Carlo) method took $N_{nature} = 4.20e8$ simulations.

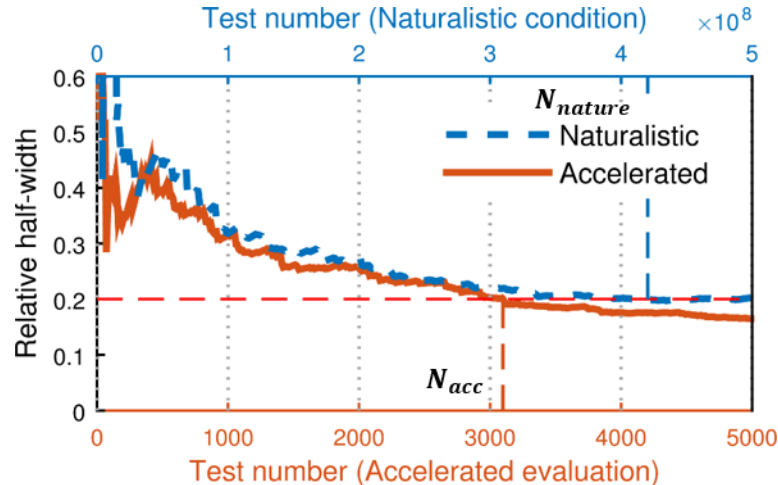


Figure 5.14 Convergence of injury rate estimation in the car-following scenario

5.4.2.3 Estimation of the conflict rate

Finally, we examine the conflict event, which is defined in Eq. (4.38). The conflict rate can be calculated from Eq. (3.39). Figure 5.15 shows that estimated conflict rate in the accelerated test converges to the result under naturalistic driving conditions.

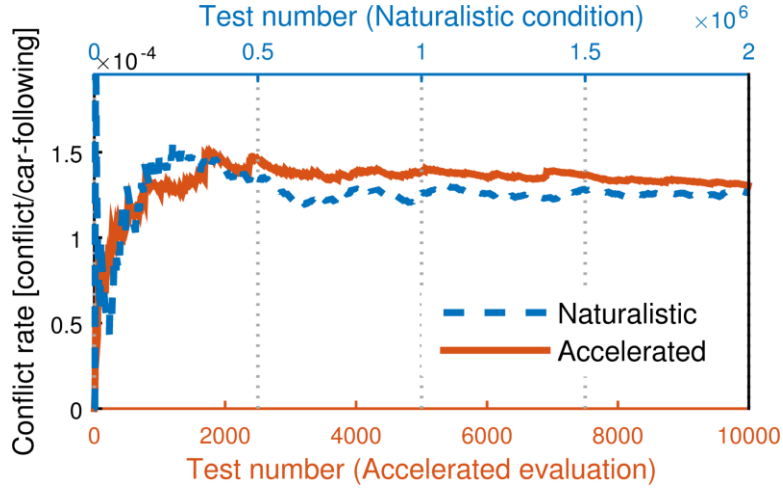


Figure 5.15 Estimation of the conflict rate in the car-following scenario

Figure 5.16 shows that accelerated tests achieve the confidence level β after $N_{acc} = 3.26e3$ simulations, while the naturalistic (crude Monte Carlo) method took $N_{nature} = 1.07e6$ simulations.

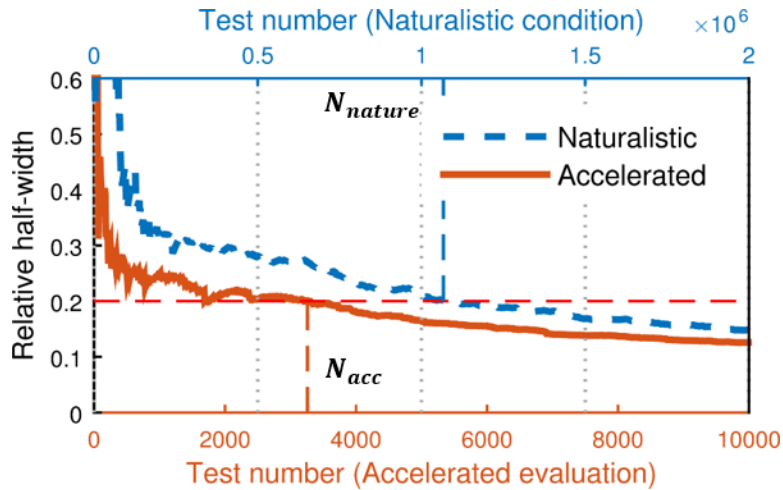


Figure 5.16 Convergence of conflict rate estimation in the car-following scenario

5.4.2.4 Summary

Table 5.3 summarizes the performance of the Accelerated Evaluation in estimating the three metrics of the AV. The accelerated rate is defined as N_{nature}/N_{acc} . It is shown that in the crash and injury cases, the proposed method successfully accelerates the evaluation by five orders of magnitude. In the conflict case, the AE method achieves over

a hundred times acceleration. In general, the IS techniques provide larger accelerated rate when target events are rarer. Since crashes and injuries occur with much lower probabilities than conflicts, we get higher accelerated rates when estimating them.

Table 5.3 Summary of performance of the Accelerated Evaluation in estimating the crash rate, injury rate, and the conflict rate in the car-following scenario

	N_{nature}	N_{acc}	N_{nature}/N_{acc}
Crash	4.30e8	3.84e3	1.12e5
Injury	4.20e8	3.10e3	1.35e5
Conflict	1.07e6	3.26e3	3.28e2

5.4.3 Sensitivity analysis of the human-controlled vehicle model

The Accelerated Evaluation is a HV model-based approach. The accuracy of the HV models can significantly affect the estimation of the benefits of AVs. In this section, we applied the Accelerated Evaluation to efficiently analyze the sensitivity of the estimation results to the HV models.

The lead HV models have two sets of parameters. $[h_0, h_1, h_2]$ represents the general principle of the driving behaviors of the drivers. σ_u represents the stochastic feature of the driving. A smaller σ_u means the driver accelerate/decelerate with a small increment thus drives more cautiously, while a larger σ_u means the driver drives more aggressively. In the SMPD database, we used driving data of 100 drivers in Ann Arbor whose cars were equipped Mobileye®. It may reflect the local driver behaviors but not necessary for drivers in other places in the U.S. By using the accelerated techniques proposed in this chapter, we studied the sensitivity of the estimated crash rate to the parameter σ_u .

Figure 5.17 shows the estimation of crash rate with different σ_u varying between ± 10 . It can be seen that the Accelerated Evaluation approach can quickly converge even when the HV parameter changes. In Figure 5.18, the crash rate is plotted in a logarithmic

scale. We can see that the crash rate varies exponentially with σ_u , which demonstrates that accurate HV behavior is crucial to understand the safety impact of AV.

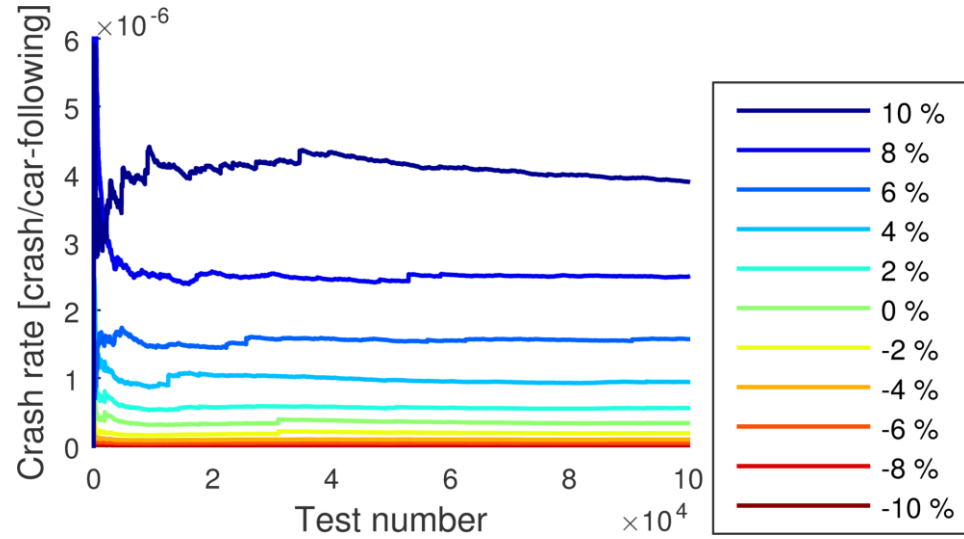


Figure 5.17 Calculation of crash rate using the Accelerated Evaluation approach with the varying HV parameter σ_u

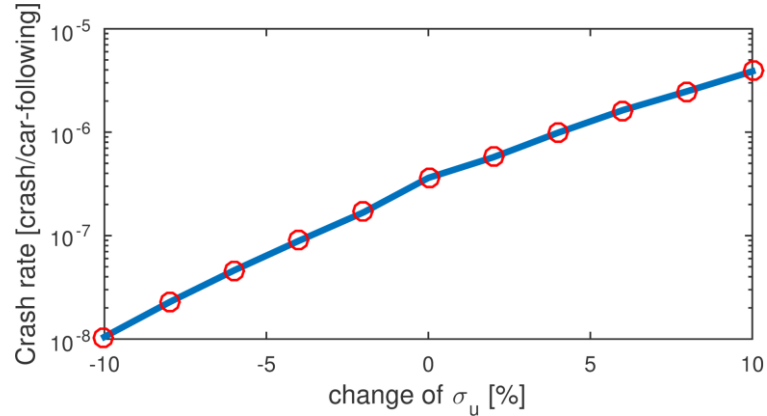


Figure 5.18 Crash rate varying with the HV parameter σ_u

5.5 Summary

In this section, we developed the accelerated evaluation approaches for the car-following scenario. The modified statistics of the lead HV were calculated based on analysis using stochastic optimization methods to maximize the likelihood for a crash to

happen. Simulations of the accelerated tests and the non-accelerated naturalistic driving were conducted to verify the credibility of the Accelerated Evaluation. Results show that the proposed Accelerated Evaluation approaches give unbiased estimation of the conflict, crash and injury rate of the AV, and can reduce simulation/testing time by a factor of 300 to 100,000.

CHAPTER 6

CONCLUSIONS AND FUTURE WORK

6.1 Conclusions

It is critical to evaluate AVs thoroughly before their release and deployment to the general public. Because most trips are not safety-critical in the naturalistic driving, testing AVs on public roads is extremely time-consuming, inefficient, and expensive.

In this dissertation, we proposed an “Accelerated Evaluation” approach as an alternative approach to evaluating AVs. The core idea is to modify the statistics of the naturalistic driving so that the safety-critical events are emphasized. Four approaches were proposed to implement this concept. In CHAPTER 2, we accelerated the evaluation by removing the relatively safe events with a high likelihood of occurring. As a result, the critical events happen more frequent in the accelerated test. A three-car car-following scenario was used to demonstrate the idea, in which the motion of the vehicle in front of the AV was modeled as a stochastic Markov Chain and the vehicle trailing the AV was simulated as an errorable driver model. Rear-end crashes were studied for two AVs simulating current production automated vehicles.

In CHAPTER 3, the Importance Sampling techniques were used to develop an Accelerated Evaluation method. This method provides a rigorous mathematical basis for calculating the real-world benefits from the accelerated test results. First, the fundamental limitation of the crude Monte Carlo method was analyzed. Then a statistical framework for the Accelerated Evaluation was established based on the Importance Sampling techniques and compared to the crude Monte Carlo method. Frontal collision due to unsafe cut-ins was used as the target crash scenario to demonstrate the proposed approach.

In CHAPTER 4, the “Adaptive Accelerated Evaluation” approach was developed to find the optimal modified statistics of HV in a systematic way. The optimal AE statistics was searched iteratively based on the Cross Entropy method. A comparison of the

accelerated performance between the non-optimized AE distribution and the Adaptive Accelerated Evaluation was conducted to demonstrate effectiveness of the proposed method.

In CHAPTER 5, we developed a new method to capture the dynamic interactions between the lead HV and the AV in the car-following scenario. The optimal way to modify the statistics was calculated by maximizing the likelihood of occurring of the events of interests. Three different types of events, crash, injury, and conflict were used to examine the performance of the method.

The Accelerated Evaluation approaches can be used to design AV evaluation procedure for field tests, Hardware-in-the-Loop (HIL), driving simulator, and computer simulation as shown in Figure 6.1. Since the proposed Accelerated Evaluation methods can accelerate the evaluation of the rare event including conflict, crash and injury events by 300 to 100,000 times, there is great potential to reduce the development and validation time for AVs significantly.

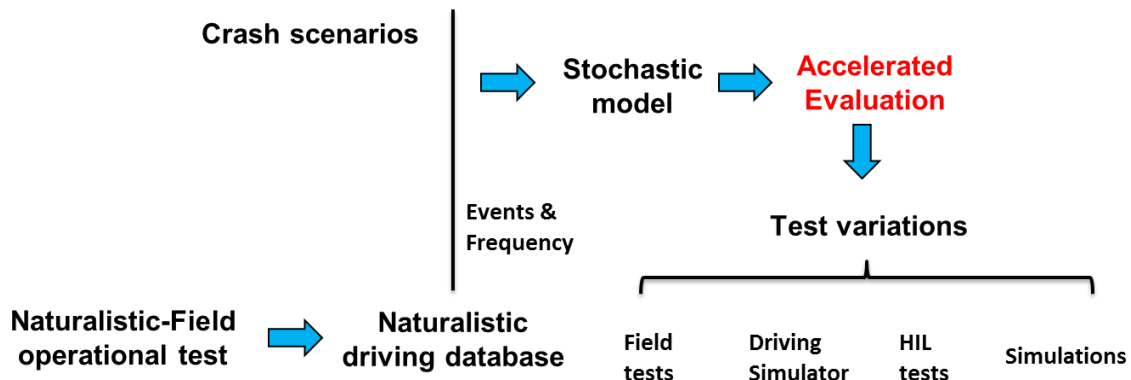


Figure 6.1 Procedure of the AV evaluation using the Accelerated Evaluation

6.2 Future Research Directions

The Accelerated Evaluation methods proposed in this research provides a new path of AV evaluation. While we successfully applied them in lane change and car-following scenarios, more can be done to improve the accuracy of the estimation and extend the

methods to other scenarios. A few research directions that can be exploited in the future research are discussed as follows.

6.2.1 Improvement of the HV model accuracy

The Accelerated Evaluation is an HV model-based approach. The HV models need to be accurate to estimate the performance of the AVs and their safety benefits. The naturalistic driving data used in this research recorded in Ann Arbor, MI, reflect the local driving behaviors but not necessarily the behaviors in other areas. Moreover, even though the current N-FOT database contains millions of miles of driving, it is still a challenge to accurately model the human behaviors under emergent conditions. More data and new analysis tools are of great benefits to improve the HV model accuracy.

6.2.2 Accelerated Evaluation of other AV scenarios

New Accelerated Evaluation approaches need to be developed for more scenarios to give a thorough evaluation of AVs. The full failure modes of AVs have not been fully understood by the community to design a complete list of test scenarios, but possible factors include:

- i) Challenge in sensing/detection (e.g., fog, snow, low light)
- ii) Challenge in perception (e.g., hand gesture, eye contact, blinking lights)
- iii) Aggression of surrounding vehicles/pedestrians/pedal-cyclists (e.g., running red light, cut-in, jaywalk)
- iv) Challenge in making decisions (e.g., low confidence, multiple threats)
- v) Challenge due to lower (than normal) control authorities (e.g., slippery roads, heavy vehicle load)

In this dissertation, we focus on the third category by taking the interaction with other HVs as the major disturbance to the control of the AV. Two fundamental driving scenarios - car-following and lane change, were studied. However, there are other scenarios that needs to fully consider vehicle to vehicle interactions. Based on the analysis of the crash data, research [75] shows that the top five scenarios to be considered are: car-

following, lane change, left turn, crossing, and opposite direction (illustrated in Figure 1.7). AV should first excel human drivers in these scenarios in order to become a safer alternative to human drivers. We studied the Accelerated Evaluation approaches for the first two scenarios, but more efforts are needed to cover the other three scenarios, and to gain deeper understanding of the first two.

There are scenarios that may not be covered well by HV crash data. As shown in Figure 6.2, crash scenarios are divided into three categories: scenarios that are challenging only for HV (e.g. drowsy driving), scenarios that are challenging only for AVs (e.g. software bugs), and scenarios that are challenging for both AVs and HVs (e.g. fail to response to an aggressive cut-in). Due to the different causations, the existing database should not be used as the sole source to design the evaluation protocol for AVs. Four possible approaches can be used in the future to find test scenarios for AVs: i) Brainstorming, ii) Crowdsourcing, iii) Analysis of existing crash databases, iv) Analysis of naturalistic driving databases.

Besides the V-V crash types, there are crashes involved the host vehicle only (single vehicle crash, denoted as V) or with pedestrians (V-P). These scenarios should also be studied and included in the AV evaluation process.

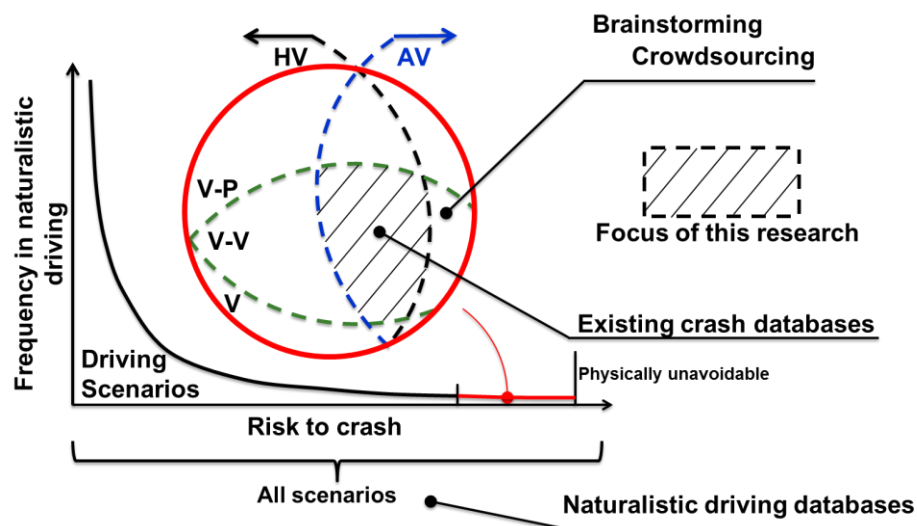


Figure 6.2 Approaches to identify AV evaluation scenarios

6.2.3 Accelerated Evaluation of other systems

In this research, we focus on AV evaluation. However, this approach may also be adopted in other systems such as the navigation systems of ships, auto pilot of airplane, drones, or other Cyber-Physical-Systems [151]. A common feature of these systems is that the dynamic system is controlled by intelligent algorithms and operate in an environment with disturbances. The proposed approaches could offer a new direction in evaluating these systems and obtaining better designs.

APPENDICES

APPENDIX A

SAE SIX LEVELS OF AUTOMATED VEHICLES [14]

Summary of Levels of Driving Automation for On-Road Vehicles

This table summarizes SAE International's levels of driving automation for on-road vehicles. Information Report J3016 provides full definitions for these levels and for the italicized terms used therein. The levels are descriptive rather than normative and technical rather than legal. Elements indicate minimum rather than maximum capabilities for each level.

"System" refers to the driver assistance system, combination of driver assistance systems, or automated driving system, as appropriate.

The table also shows how SAE's levels definitively correspond to those developed by the Germany Federal Highway Research Institute (BASt) and approximately correspond to those described by the US National Highway Traffic Safety Administration (NHTSA) in its "Preliminary Statement of Policy Concerning Automated Vehicles" of May 30, 2013.

Level	Name	Narrative definition	Execution of steering and acceleration/deceleration	Monitoring of driving environment	Fallback performance of dynamic driving task	System capability (driving modes)	Driver only	BASt level	NHTSA level
Human driver monitors the driving environment									
0	No Automation	the full-time performance by the <i>human driver</i> of all aspects of the <i>dynamic driving task</i> , even when enhanced by warning or intervention systems	Human driver	Human driver	Human driver	n/a	Assisted	0	
1	Driver Assistance	the <i>driving mode-specific execution</i> by a driver assistance system of either steering or acceleration/deceleration using information about the driving environment and with the expectation that the <i>human driver</i> perform all remaining aspects of the <i>dynamic driving task</i>	Human driver and system	Human driver	Human driver	Some driving modes	Assisted	1	
2	Partial Automation	the <i>driving mode-specific execution</i> by one or more driver assistance systems of both steering and acceleration/deceleration using information about the driving environment and with the expectation that the <i>human driver</i> perform all remaining aspects of the <i>dynamic driving task</i>	System	Human driver	Human driver	Some driving modes	Partially automated	2	
Automated driving system ("system") monitors the driving environment									
3	Conditional Automation	the <i>driving mode-specific performance</i> by an automated driving system of all aspects of the <i>dynamic driving task</i> with the expectation that the <i>human driver</i> will respond appropriately to a request to intervene	System	System	Human driver	Some driving modes	Automated	3	
4	High Automation	the <i>driving mode-specific performance</i> by an automated driving system of all aspects of the <i>dynamic driving task</i> , even if a <i>human driver</i> does not respond appropriately to a request to intervene	System	System	System	Some driving modes	Automated	4	
5	Full Automation	the full-time performance by an automated driving system of all aspects of the <i>dynamic driving task</i> under all roadway and environmental conditions that can be managed by a <i>human driver</i>	System	System	System	All driving modes	Automated	5	

APPENDIX B

CRASH DATABASES IN THE U.S. AND E.U.

(Databases with larger than 5000 crashes)

	Full name	Country	Crashes	Data years	Owner
NASS-CDS [78]	National Automotive Sampling system - Crashworthiness Data System	US	~3300-5000 per year	1988-present	NHTSA
NASS-GES [77]	National Automotive Sampling System - General Estimated System	US	~50,000 per year	1988-present	NHTSA
FARS [152]	Fatal Accidents Recording System	US	~33,000 per year	1975-present	NHTSA
NMVCCS [153]	National Motor Vehicle Crash Causation Survey	US	5,470	2005-2007	NHTSA
CARE [154]	Community Road Accident Database	EU & CH, IS, NO	1,000,000+	1991-present	European Commission
GIDAS [155]	German In- Depth Accident Study	DE	22000	1999-present	BASt and several manufacturers
ADAC [156]	ADAC Accident Investigation Study	DE	11456	2015-present	ADAC
CCIS [157]	Co-operative Crash Injury Study	UK	15000	1983-2010	Department for Transport
VOIESUR [158]	Vehicule Occupant Infrastructure Etudes de la Sécurité des Usagers de la Route	FR	9000	2011	CEESAR, CETE NC, IFSTTAR, LAB

BIBLIOGRAPHY

BIBLIOGRAPHY

- [1] C. Lewis, “The Economic Benefits of Driverless Cars,” *Morgan Stanley*, 2014. .
- [2] J. Anderson, K. Nidhi, K. Stanley, P. Sorensen, C. Samaras, and O. A. Oluwatola, “Autonomous Vehicle Technology: A Guide for Policymakers,” 2014.
- [3] CIS, “Automated Driving: Legislative and Regulatory Action,” *Stanford University*, 2014. [Online]. Available: http://cyberlaw.stanford.edu/wiki/index.php/Automated_Driving:_Legislative_and_Regulatory_Action. [Accessed: 01-Dec-2015].
- [4] J. Ironmonger, “UK to Allow Driverless Cars on Public Roads in January,” *BBC News*. [Online]. Available: <http://www.bbc.com/news/technology-28551069>. [Accessed: 22-Aug-2014].
- [5] The Department for Transport of the United Kingdom, “The Pathway to Driverless Cars Summary Report and Action Plan.” [Online]. Available: https://www.gov.uk/government/uploads/system/uploads/attachment_data/file/401562/pathway-driverless-cars-summary.pdf. [Accessed: 21-Dec-2015].
- [6] E.U.CORDIS Research Program, “Driverless Cars Take to the Road.” [Online]. Available: http://cordis.europa.eu/result/rcn/90263_en.html. [Accessed: 23-Aug-2014].
- [7] Wikipedia, “Autonomous Car.” [Online]. Available: http://en.wikipedia.org/wiki/Autonomous_car. [Accessed: 22-Aug-2014].
- [8] Volvo, “Autonomous Driving according to Volvo Car Group: Benefits for Society and Consumers Alike.” [Online]. Available: <http://www.volvocars.com/us/top/about/news-awards/pages/default.aspx?itemid=68>. [Accessed: 23-Aug-2014].
- [9] P. Natarajan and N. Ford, “Future of Autonomous Driving,” *Frost and Sullivan*. [Online]. Available: <http://www.slideshare.net/FrostandSullivan/future-of-autonomous-driving-28642051>. [Accessed: 03-Dec-2015].
- [10] “Strategic Analysis of the European and North American Market for Automated Driving,” M92C-18, 2014.
- [11] “Your Autopilot Has Arrived | Tesla Motors.” [Online]. Available: <https://www.teslamotors.com/blog/your-autopilot-has-arrived>. [Accessed: 14-Dec-2015].
- [12] “Model S Software Version 7.0 | Tesla Motors.” [Online]. Available: <https://www.teslamotors.com/presskit/autopilot>. [Accessed: 14-Dec-2015].
- [13] “Autonomous | Self-Driving Vehicles Legislation,” *National Conference of State Legislatures*, 2015. [Online]. Available:

- <http://www.ncsl.org/research/transportation/autonomous-vehicles-legislation.aspx>. [Accessed: 06-Jan-2016].
- [14] SAE J3016, “Taxonomy and Definitions for Terms Related to On-Road Motor Vehicle Automated Driving Systems,” 2014.
 - [15] “LEVELS OF DRIVING AUTOMATION ARE DEFINED IN NEW SAE INTERNATIONAL STANDARD J3016,” *SAE International*. [Online]. Available: http://www.sae.org/misc/pdfs/automated_driving.pdf. [Accessed: 28-Jan-2016].
 - [16] Information Is Beautiful, “Million Lines of Code,” 2014. [Online]. Available: <http://www.informationisbeautiful.net/visualizations/million-lines-of-code/>. [Accessed: 05-Sep-2014].
 - [17] NHTSA, “Preliminary Statement of Policy Concerning Automated Vehicles,” 2013.
 - [18] “Recalls & Defects,” *National Highway Traffic Safety Administration (NHTSA)*. [Online]. Available: <http://www.nhtsa.gov/Vehicle+Safety/Recalls+&+Defects>. [Accessed: 05-Sep-2014].
 - [19] “2009–11 Toyota Vehicle Recalls,” *Wikipedia*. [Online]. Available: http://en.wikipedia.org/wiki/2009–11_Toyota_vehicle_recalls.
 - [20] National Highway Traffic Safety Administration (NHTSA), “Department of Transportation Releases Policy on Automated Vehicle Development,” 2013. [Online]. Available: <http://www.nhtsa.gov/About+NHTSA/Press+Releases/U.S.+Department+of+Transportation+Releases+Policy+on+Automated+Vehicle+Development>. [Accessed: 21-Aug-2014].
 - [21] FESTA-Consortium, “FESTA Handbook Version 2 Deliverable T6.4 of the Field Operational Test support Action,” Brussels: European Commission, 2008.
 - [22] M. Aust, “Evaluation Process for Active Safety Functions: Addressing Key Challenges in Functional, Formative Evaluation of Advanced Driver Assistance Systems,” Chalmers University of Technology, 2012.
 - [23] V. L. Neale, T. A. Dingus, S. G. Klauer, and M. Goodman, “An Overview of the 100-Car Naturalistic Study and Findings,” *Traffic Safety*, pp. 1–10, 2005.
 - [24] T. A. Dingus, S. G. Klauer, V. L. Neale, A. Petersen, S. E. Lee, J. Sudweeks, M. A. Perez, J. Hankey, D. Ramsey, S. Gupta, C. Bucher, Z. R. Doerzaph, J. Jermeland, and R. Knippling, “The 100-Car Naturalistic Driving Study Phase II – Results of the 100-Car Field Experiment,” NHTSA, DOT HS 810 593, 2006.
 - [25] S. Klauer, T. Dingus, and V. Neale, “The Impact of Driver Inattention on near-Crash/crash Risk: An Analysis Using the 100-Car Naturalistic Driving Study Data,” no. April, 2006.
 - [26] G. M. Fitch and J. M. Hankey, “Investigating Improper Lane Changes: Driver Performance Contributing to Lane Change Near-Crashes,” *Proceedings of the Human Factors and Ergonomics Society Annual Meeting*, vol. 56, no. 1, pp. 2231–2235, Oct. 2012.

- [27] G. M. Fitch, S. E. Lee, S. Klauer, J. Hankey, J. Sudweeks, and T. Dingus, “Analysis of Lane-Change Crashes and near-Crashes,” *US Department of Transportation, National Highway Traffic Safety Administration*, 2009.
- [28] R. Ervin, J. Sayer, D. LeBlanc, S. Bogard, M. Mefford, M. Hagan, Z. Bareket, and C. Winkler, “Automotive Collision Avoidance System Field Operational Test Report: Methodology and Results.”
- [29] D. LeBlanc, J. Sayer, C. Winkler, R. Ervin, S. Bogard, M. Devonshire, J. Mefford, M. Hagan, Z. Bareket, R. Goodsell, and T. Gordon, “Road Departure Crash Warning System Field Operational Test : Methodology and Results,” UMTRI-2006-9-2, 2006.
- [30] T. Victor, J. Bärgman, M. Hjälmdahl, and K. Kircher, “Sweden-Michigan Naturalistic Field Operational Test (SeMiFOT) Phase 1 : Final Report,” 2010.
- [31] J. Sayer, D. LeBlanc, S. Bogard, D. Funkhouser, B. D., B. S., and A. M. L., Blankespoor, “Integrated Vehicle-Based Safety Systems Field Operational Test Final Program Report,” NHTSA, DOT HS 811 482, 2011.
- [32] D. J. Leblanc, J. R. Sayer, S. Bao, S. Bogard, M. L. Buonarosa, A. Blankespoor, and D. Funkhouser, “Driver Acceptance and Behavioral Changes with an Integrated Warning System: Key Findings from the IVBSS FOT,” *22nd ESV*, pp. 1–10, 2011.
- [33] UMTRI, “Safety Pilot Model Deployment.” [Online]. Available: <http://safetypilot.umtri.umich.edu/>. [Accessed: 22-Aug-2014].
- [34] D. LeBlanc, “Data from the Safety Pilot Model Deployment.” [Online]. Available: <http://assets.conferencespot.org/fileserver/file/46778/filename/39ftvo.pdf>. [Accessed: 22-Aug-2014].
- [35] RITA, “Connected Vehicle Project,” *U.S. Department of Transportation*. [Online]. Available: http://www.its.dot.gov/safety_pilot/. [Accessed: 22-Aug-2014].
- [36] D. LeBlanc, S. E. Bogard, and R. Goodsel, “Connected Commercial Vehicles — Integrated Truck Project Model Deployment Operational Analysis Report,” 2014.
- [37] “Google Self-Driving Car Project.” [Online]. Available: <https://www.google.com/selfdrivingcar/>.
- [38] “Velodyne LiDAR.” [Online]. Available: <http://velodynelidar.com/>. [Accessed: 14-Dec-2015].
- [39] “Google Gets License to Operate Driverless Cars in Nevada,” *CNN*, 2012. [Online]. Available: <http://www.cnn.com/2012/05/07/tech/nevada-driveless-car/>. [Accessed: 05-Jan-2016].
- [40] Wikipedia, “Google Driverless Car.” [Online]. Available: http://en.wikipedia.org/wiki/Google_driverless_car.
- [41] “Google Self-Driving Car Project Monthly Report - November 2015.” [Online]. Available: <https://static.googleusercontent.com/media/www.google.com/en//selfdrivingcar/files/reports/report-1115.pdf>. [Accessed: 14-Dec-2015].

- [42] NHTSA, “Traffic Safety Facts 2013.”
- [43] M. Akamatsu, P. Green, and K. Bengler, “Automotive Technology and Human Factors Research: Past, Present, and Future,” *International Journal of Vehicular Technology*, vol. 2013, pp. 1–27, 2013.
- [44] E. D. Dickmanns, “The Development of Machine Vision for Road Vehicles in the Last Decade,” in *Intelligent Vehicle Symposium, 2002. IEEE*, 2002, vol. 1, pp. 268–281.
- [45] M. Campbell, M. Egerstedt, J. P. How, and R. M. Murray, “Autonomous Driving in Urban Environments: Approaches, Lessons and Challenges.,” *Philosophical Transactions. Series A, Mathematical, physical, and engineering sciences*, vol. 368, no. 1928, pp. 4649–72, Oct. 2010.
- [46] J. Scholliers, K. Heinig, J. Blosseville, M. Netto, V. Anttila, and S. Leanderson, “D16.3 Proposal of Procedures for Assessment of Preventive and Active Safety Functions,” 2007.
- [47] K. Deering, Richard, “Crash Avoidance Metrics Partnership Annual Report, April 2001 - March 2002,” DOT HS 809 531, 2002.
- [48] M. Shulman and R. K. Deering, “Second Annual Report of the Crash Avoidance Metrics Partnership,” DOT HS 809 663, 2003.
- [49] M. Shulman and R. K. Deering, “Third Annual Report of the Crash Avoidance Metrics Partnership,” DOT HS 809 837, 2005.
- [50] R. Kiefer, D. LeBlanc, M. Palmer, and J. Salinger, “Development and Validation of Functional Definitions and Evaluation Procedures for Collision Warning/avoidance Systems,” DOT HS 808 964, 1999.
- [51] R. J. Kiefer, M. T. Cassar, C. A. Flannagan, D. J. LeBlanc, M. D. Palmer, R. K. Deering, and M. A. Shulman, “Forward Collision Warning Requirements Project Final Report - Task 1,” DOT HS 809 574, 2003.
- [52] R. J. Kiefer, M. T. Cassar, C. A. Flannagan, C. J. Jerome, and M. D. Palmer, “Forward Collision Warning Requirements Project Tasks 2 and 3a Final Report,” DOT HS 809 902, 2005.
- [53] “Cooperative Intersection Collision Avoidance Systems (CICAS),” U.S. Department of Transportation Research and Innovative Technology Administration. [Online]. Available: <http://www.its.dot.gov/cicas/>. [Accessed: 04-Sep-2014].
- [54] M. Maile, V. Neale, F. Ahmed-Zaid, C. Basnyake, L. Caminiti, and Z. Doerzaph, “Cooperative Intersection Collision Avoidance System Limited to Stop Sign and Traffic Signal Violations (CICAS-V) – Concept of Operations.,” DTFH61-01-X-00014, 2007.
- [55] S. E. Shladover, “Effects of Traffic Density on Communication Requirements for Cooperative Intersection Collision Avoidance Systems (CICAS),” California Partners for Advanced Transit and Highways (PATH), Mar. 2005.
- [56] David J. LeBlanc, “Development of Performance Evaluation Procedures for

- Active Safety Systems,” *University of Michigan Transportation Research Institute*, 2013. [Online]. Available: <http://www.umtri.umich.edu/our-results/projects/development-performance-evaluation-procedures-active-safety-systems>. [Accessed: 02-Sep-2014].
- [57] European Commission, “Human Machine Interaction and the Safety of Traffic in Europe.” [Online]. Available: http://www.transport-research.info/web/projects/project_details.cfm?id=13634. [Accessed: 04-Sep-2014].
- [58] O. Carsten, N. Merat, W. H. Janssen, E. Johansson, M. Fowkes, and K. A. Brookhuis, “Human Machine Interaction and the Safety of Traffic in Europe Final Report,” 2005.
- [59] H. Kussmann, H. Modler, J. Engstrom, A. Agnvall, P. Piamonte, G. Markkula’s, A. Amditis, A. Bolovinou, L. Andreone, E. Deregbus, and P. Kompfner, “Requirements for AIDE HMI and Safety Functions,” D3.2.1, 2004.
- [60] M. Rimini-Döring, A. Keinath, E. Nodari, F. Palma, A. Toffetti, N. Floudas, E. Bekiaris, V. Portouli, and M. Panou, “Considerations on Test Scenarios,” 2005.
- [61] V. Karabatsou, M. Pappas, P. van Elslande, K. Fouquet, and M. Stanzel, “A-Priori Evaluation of Safety Functions Effectiveness - Methodologies Table of Contents,” D4.1.3, 2007.
- [62] APROSYS, “Research Database: APROSYS - Advanced Protection Systems (CIC).” Department for Transport, Great Minster House, 33 Horseferry Road, London SW1P 4DR, 05-May-2011.
- [63] T. Wohllebe, J. Vetter, C. Mayer, M. McCarthy, and R. de Lange, “Integrated Project on Advanced Protection Systems,” AP-SP13-0035 Project, 2004.
- [64] “APROSYS - Advanced Protection Systems.” [Online]. Available: http://www.transport-research.info/web/projects/project_details.cfm?id=35419. [Accessed: 03-Sep-2014].
- [65] D. Gavrla, M. P., and M. M. Meinecke, “Deliverable 1-A: Vulnerable Road User Scenario Selection,” IST-2001-34040, 2003.
- [66] “PReVENT | ITS Europe.” [Online]. Available: <http://www.ertico.com/prevent>. [Accessed: 04-Sep-2014].
- [67] ERSO, “National Databases | European Road Safety Observatory.” [Online]. Available: http://ec.europa.eu/transport/wcm/road_safety/erso/data/Content/national_database_s.htm. [Accessed: 04-Sep-2014].
- [68] T. Bakri, R. Blanco, F. Fahrenkrog, S. Koskinen, A. Larsson, K. Malone, M. Saéz, D. Sánchez, A. Várhelyi, D. Willemsen, and A. Zlocki, “Deliverable 7 . 1 | Requirements for the Evaluation Framework,” 2011.
- [69] J.-A. Bühne, A. Lüdeke, S. Schönebeck, J. Dobberstein, H. Fagerlind, A. Bálint, and M. McCarthy, “Assessment of Integrated Vehicle Safety Systems for Improved Vehicle,” ASSESS D2.2 (2/2) Socio-economic, 2012.

- [70] J. Lenard and R. Danton, “Accident Data Study in Support of Development of Autonomous Emergency Braking (AEB) Test Procedures Insurance Institute of Highway Safety,” LUEL 5989/6175, 2010.
- [71] Euro NCAP, “Autonomous Emergency Braking.” [Online]. Available: <http://www.euroncap.com/rewards/technologies/brake.aspx>. [Accessed: 04-Sep-2014].
- [72] C. J. Wiacek and W. G. Najm, “Driver/Vehicle Characteristics in Rear-End Precrash Scenarios Based on the General Estimates System (GES),” *SAE Technical Paper*, Mar. 1999.
- [73] W. G. Najm, J. D. Smith, and M. Yanagisawa, “Pre-Crash Scenario Typology for Crash Avoidance Research,” DOT HS 810 767, 2007.
- [74] W. G. Najm and J. D. Smith, “Development of Crash Imminent Test Scenarios for Integrated Vehicle-Based Safety Systems,” DOT HS 810 757, 2007.
- [75] W. G. Najm, S. Toma, and J. Brewer, “Depiction of Priority Light-Vehicle Pre-Crash Scenarios for Safety Applications Based on Vehicle-to-Vehicle Communications,” DOT HS 811 732, 2013.
- [76] W. G. Najm, R. Ranganathan, G. Srinivasan, J. D. Smith, S. Toma, E. Swanson, and A. Burgett, “Description of Light-Vehicle Pre-Crash Scenarios for Safety Applications Based On Vehicle-to-Vehicle Communications,” DOT HS 811 731, 2013.
- [77] “NASS General Estimates System.” [Online]. Available: [http://www.nhtsa.gov/Data/National+Automotive+Sampling+System+\(NASS\)/NA%20SS+General+Estimates+System](http://www.nhtsa.gov/Data/National+Automotive+Sampling+System+(NASS)/NA%20SS+General+Estimates+System). [Accessed: 04-Sep-2014].
- [78] “Crashworthiness Data System,” *National Highway Traffic Safety Administration (NHTSA)*. [Online]. Available: [http://www.nhtsa.gov/Data/National+Automotive+Sampling+System+\(NASS\)/NA%20SS+Crashworthiness+Data+System](http://www.nhtsa.gov/Data/National+Automotive+Sampling+System+(NASS)/NA%20SS+Crashworthiness+Data+System). [Accessed: 22-Dec-2015].
- [79] “NCSA Publications & Data Requests.” [Online]. Available: <http://www-nrd.nhtsa.dot.gov/Cats/listpublications.aspx?Id=227&ShowBy=Category>. [Accessed: 04-Sep-2014].
- [80] “Event Data Recorder (EDR) | National Highway Traffic Safety Administration (NHTSA).” [Online]. Available: <http://www.nhtsa.gov/EDR>. [Accessed: 04-Sep-2014].
- [81] C. A. Flannagan, P. E. Green, K. D. Klinich, M. A. Manary, A. Bálant, U. Sanders, B. Sui, P. Sandqvist, and C. Selpi, Howard, “Mutual Recognition Methodology Development,” UMTRI-2014-32, 2014.
- [82] H. Peng and D. Leblanc, “Evaluation of the Performance and Safety of Automated Vehicles,” *White paper for NSF Transportation CPS Workshop*, 2012.
- [83] W. Ma, “Worst-Case Evaluation Methods for Vehicles and Vehicle Control Systems,” 1998.
- [84] W.-H. Ma and H. Peng, “A Worst-Case Evaluation Method for Dynamic

- Systems," *Journal of Dynamic Systems, Measurement, and Control*, vol. 121, no. 2, p. 191, 1999.
- [85] A. Ungoren and H. Peng, "An Adaptive Lateral Preview Driver Model," *Vehicle System Dynamics*, vol. 43, no. 4, pp. 245–259, Apr. 2005.
- [86] Y. Kou, "Development and Evaluation of Integrated Chassis Control Systems," The University of Michigan, 2010.
- [87] S. Jayasuriya, "On the Determination of the Worst Allowable Persistent Bounded Disturbance for a System With Constraints," *Journal of Dynamic Systems, Measurement, and Control*, vol. 117, no. 2, p. 126, Jun. 1995.
- [88] I. Fialho and T. Georgiou, "Worst Case Analysis of Nonlinear Systems," *Automatic Control, IEEE Transactions on Automatic Control*, vol. 44, no. 6, pp. 11180–1196, 1999.
- [89] Y. Fujii and R. Shiobara, "The Analysis of Traffic Accidents," *Journal of Navigation*, vol. 24, no. 04, p. 534, Jan. 2010.
- [90] F. Goerlandt and P. Kujala, "Traffic Simulation Based Ship Collision Probability Modeling," *Reliability Engineering & System Safety*, vol. 96, no. 1, pp. 91–107, Jan. 2011.
- [91] P. Angelov, D. Filev, and N. Kasabov, *Evolving Intelligent Systems: Methodology and Applications*. Wiley, 2010.
- [92] H.-H. Yang and H. Peng, "Development and Evaluation of Collision Warning/collision Avoidance Algorithms Using an Errable Driver Model," *Vehicle System Dynamics*, vol. 48, no. sup1, pp. 525–535, Dec. 2010.
- [93] J. Woodrooffe, D. Blower, S. Bao, S. Bogard, C. Flannagan, P. E. Green, and D. LeBlanc, "Performance Characterization and Safety Effectiveness Estimates of Forward Collision Avoidance and Mitigation Systems for Medium/Heavy Commercial Vehicles," UMTRI-2011-36, 2014.
- [94] E. Ackerman, "CMU's Autonomous Car Doesn't Look like a Robot," *IEEE Spectrum*, 2013. [Online]. Available: [http://spectrum.ieee.org/automaton/robotics/artificial-intelligence/cmu-autonomous-car-doesnt-looks-like-a-robot?utm_source=feedburner&utm_medium=feed&utm_campaign=Feed%3A+IeeeSpectrum+\(IEEE+Spectrum\)](http://spectrum.ieee.org/automaton/robotics/artificial-intelligence/cmu-autonomous-car-doesnt-looks-like-a-robot?utm_source=feedburner&utm_medium=feed&utm_campaign=Feed%3A+IeeeSpectrum+(IEEE+Spectrum)). [Accessed: 09-Sep-2014].
- [95] Euro NCAP, "Euro NCAP Test Protocol – AEB Systems," 2013.
- [96] K. Lee, "Longitudinal Driver Model and Collision Warning and Avoidance Algorithms Based on Human Driving Databases," University of Michigan., 2004.
- [97] H. Yang, "Driver Models to Emulate Human Anomalous Behaviors Leading to Vehicle Lateral and Longitudinal Accidents," Ph.D Dissertaion, University of Michigan, Ann Arbor, 2010.
- [98] J. Sayer, D. LeBlanc, S. Bogard, D. Funkhouser, J. Sayer, D. LeBlanc, S. Bogard, D. Funkhouser, B. D., B. S., and A. M. L., Blankespoor, "Integrated Vehicle-Based Safety Systems Field Operational Test Final Program Report," no. October,

2011.

- [99] D. Reynolds, “Gaussian Mixture Models,” in *Encyclopedia of Biometric Recognition*, Heidelberg: Springer, 2009, pp. 659–663.
- [100] A. Dempster, N. Laird, and D. Rubin, “Maximum Likelihood from Incomplete Data via the EM Algorithm,” *Journal of the royal statistical society. ...*, 1977.
- [101] L. A. Pipes, “An Operational Analysis of Traffic Dynamics,” *Applied Physics*, vol. 24, pp. 271–281, 1953.
- [102] D. C. Gazis, R. Herman, and R. W. Rothery, “Nonlinear Follow-The-Leader Models of Traffic Flow,” *Operations Research*, vol. 9, no. 4, pp. 545–567, 1961.
- [103] J. Tyler Jr., “The Characteristic of Model-Following Systems as Synthesized by Optimal Control,” *IEEE Transactions on Automatic Control*, vol. 9, no. 4, pp. 485–498, 1964.
- [104] H. Yang and H. Peng, “Development of an Errorable Car-Following Driver Model,” *Vehicle System Dynamics*, vol. 48, no. 6, pp. 751–773, Jun. 2010.
- [105] M. Brackstone and M. McDonald, “Car-Following: A Histori- Cal Review,” *Transportation Research Part F: Traffic Psychology and Behaviour*, vol. 2, pp. 181–196, 1999.
- [106] H. Ozaki, “Reaction and Anticipation in the Car Following Behaviour,” in *13th International Symposium on Traffic and Transportation Theory*, 1993, pp. 349–366.
- [107] G. Markkula, O. Benderius, K. Wolff, and M. Wahde, “A Review of Near-Collision Driver Behavior Models,” *Human Factors: The Journal of the Human Factors and Ergonomics Society*, vol. 54, no. 6, pp. 1117–1143, Jun. 2012.
- [108] P. G. Gipps, “A Behavioural Car-Following Model for Computer Simulation,” vol. I, no. 2, 1981.
- [109] J. Treat, N. Tumbas, and S. McDonald, “Tri-Level Study of the Causes of Traffic Accidents: Final Report,” DOT HS 034 3 535, 1979.
- [110] L. Blincoe, T. R. Miller, E. Zaloshnja, and B. A. Lawrence, “The Economic and Societal Impact Of Motor Vehicle Crashes, 2010 (Revised),” NHTSA, DOT HS 812 013, 2015.
- [111] H. Yang, H. Peng, T. J. Gordon, and D. Leblanc, “Development and Validation of an Errorable Car-Following Driver Model,” *2008 American Control Conference*, pp. 3927–3932, Jun. 2008.
- [112] T. Tang, C. Li, H. Huang, and H. Shang, “A New Fundamental Diagram Theory with the Individual Difference of the Driver’s Perception Ability,” *Nonlinear Dynamics*, vol. 67, no. 3, pp. 2255–2265, Jul. 2011.
- [113] J. Przybyla, J. Taylor, J. Jupe, and X. Zhou, “Simplified, Data-Driven, Errorable Car-Following Model to Predict the Safety Effects of Distracted Driving,” *2012 15th International IEEE Conference on Intelligent Transportation Systems*, pp. 1149–1154, Sep. 2012.
- [114] L. Bi, G. Gan, J. Shang, and Y. Liu, “Queuing Network Modeling of Driver

Lateral Control With or Without a Cognitive Distraction Task,” *IEEE Transactions on Intelligent Transportation Systems*, vol. 13, no. 4, pp. 1810–1820, Dec. 2012.

- [115] A. G. Ulsoy, H. Peng, and M. Çakmakci, *Automotive Control Systems*. Cambridge University Press, 2012.
- [116] ADAC, “Comparative Test of Advanced Emergency Braking Systems,” 2011.
- [117] T. I. Gorman, “Prospects for the Collision-Free Car : The Effectiveness of Five Competing Forward Collision Avoidance Systems,” Virginia Polytechnic Institute and State University, 2013.
- [118] “Mechanical Simulation Corporation.” [Online]. Available: <http://carsim.com/>.
- [119] S. Ross, *Introductory Statistics*. 2010.
- [120] J. Bucklew, *Introduction to Rare Event Simulation*. Springer Science & Business Media, 2010.
- [121] J. Blanchet and H. Lam, “State-Dependent Importance Sampling for Rare-Event Simulation: An Overview and Recent Advances,” *Surveys in Operations Research and Management Science*, vol. 17, pp. 38–59, 2012.
- [122] S. Juneja and P. Shahabuddin, “Chapter 11 Rare-Event Simulation Techniques: An Introduction and Recent Advances,” *Handbooks in Operations Research and Management Science*, vol. 13, no. 06, pp. 291–350, 2006.
- [123] S. Asmussen and P. W. Glynn, *Stochastic Simulation: Algorithms and Analysis*. 2012.
- [124] P. Heidelberger, “Fast Simulation of Rare Events in Queueing and Reliability Models,” *ACM Transactions on Modeling and Computer Simulation*, vol. 5, no. 1, pp. 43–85, Jan. 1995.
- [125] P. Glasserman and J. Li, “Importance Sampling for Portfolio Credit Risk,” *Management Science*, Nov. 2005.
- [126] S. Asmussen and H. Albrecher, *Ruin Probabilities*, 2nd ed. World Scientific, 2010.
- [127] M. Macke and C. Bucher, “Importance Sampling for Randomly Excited Dynamical Systems,” *Journal of Sound and Vibration*, vol. 268, no. 2, pp. 269–290, 2003.
- [128] C.-S. Chang, P. Heidelberger, S. Juneja, and P. Shahabuddin, “Effective Bandwidth and Fast Simulation of ATM Intree Networks,” *Performance Evaluation*, vol. 20, no. 1–3, pp. 45–65, May 1994.
- [129] H. L. Royden, *Real Analysis*. New York: Prentice Hall, 1948.
- [130] D. Shinar, *Psychology on the Road: The Human Factor in Traffic Safety*. Wiley, 1978.
- [131] S. E. Lee, C. B. E. Olsen, and W. W. Wierwille, “A Comprehensive Examination of Naturalistic Lane-Changes,” NHTSA, DOT HS 809 702, 2004.
- [132] D. Zhao, H. Peng, K. Nobukawa, S. Bao, D. J. LeBlanc, and C. S. Pan, “Analysis of Mandatory and Discretionary Lane Change Behaviors for Heavy Trucks,” in

- 12th International Symposium on Advanced Vehciel Control*, 2014.
- [133] J. Harding, G. Powell, R. Yoon, and J. Fikentscher, “Vehicle-to-Vehicle Communications: Readiness of v2v Technology for Application,” 2014.
 - [134] G. P. Stein, O. Mano, and A. Shashua, “Vision-Based ACC with a Single Camera: Bounds on Range and Range Rate Accuracy,” in *IEEE Intelligent Vehicles Symposium*, 2003, pp. 120–125.
 - [135] SAE J2944, “Operational Definitions of Driving Performance Measures and Statistics.” [Online]. Available: http://standards.sae.org/j2944_201506/. [Accessed: 22-Dec-2015].
 - [136] T. Gennarelli, *Abbreviated Injury Scale 2005 : Update 2008*. Barrington Ill.: Association for the Advancement of Automative Medicine, 2008.
 - [137] K. D. Kusano and H. C. Gabler, “Safety Benefits of Forward Collision Warning, Brake Assist, and Autonomous Braking Systems in Rear-End Collisions,” *IEEE Transactions on Intelligent Transportation Systems*, vol. 13, no. 4, pp. 1546–1555, Dec. 2012.
 - [138] R. Y. Rubinstein, “Optimization of Computer Simulation Models with Rare Events,” *European Journal of Operational Research*, vol. 99, no. 1, pp. 89–112, 1997.
 - [139] R. Y. Rubinstein, “Rare Event Simulation via Cross-Entropy and Importance Sampling,” in *Second International Workshop on Rare Event Simulation*, 1999, pp. 1–17.
 - [140] P.-T. de Boer, D. P. Kroese, S. Mannor, and R. Y. Rubinstein, “A Tutorial on the Cross-Entropy Method,” *Annals of Operations Research*, vol. 134, no. 1, pp. 19–67, 2005.
 - [141] F. B. Hildebrand, *Introduction to Numerical Analysis*. Courier Corporation, 1987.
 - [142] P. W. Holland and R. E. Welsch, “Robust Regression Using Iteratively Reweighted Least-Squares,” *Communications in Statistics - Theory and Methods*, vol. 6, no. 9, pp. 813–827, 1977.
 - [143] “Robust Regression - MATLAB Robustfit.” [Online]. Available: <http://www.mathworks.com/help/stats/robustfit.html>. [Accessed: 04-Mar-2016].
 - [144] W. Dumouchel and F. O’Brien, “Integrating a Robust Option into a Multiple Regression Computing Environment,” *Institute for Mathematics and Its Applications*, 1991.
 - [145] P. a. Ioannou and C. C. Chien, “Autonomous Intelligent Cruise Control,” *IEEE Transactions on Vehicular Technology*, vol. 42, no. 4, pp. 657–672, 1993.
 - [146] Katsuhiko Ogata, *Modern Control Engineering*, 5th ed. Prentice Hall.
 - [147] “V60 | Specifications | Volvo Cars.” [Online]. Available: <http://www.volvocars.com/intl/cars/new-models/v60/specifications>. [Accessed: 12-Feb-2016].
 - [148] H. B. Pacejka, *Tyre and Vehicle Dynamics*, 3rd ed. Butterworth-Heinemann, 2012.

- [149] R. Rajamani, “Vehicle Dynamics and Control,” *Dynamics and Control*, 2011.
- [150] K. Ogata, *Discrete-Time Control Systems*, 2nd ed. Prentice Hall, 1995.
- [151] “DARPA AVM Program .” [Online]. Available: <http://cps-vo.org/group/avm/meta-overview>. [Accessed: 20-Jun-2015].
- [152] “Fatality Analysis Reporting System,” *National Highway Traffic Safety Administration (NHTSA)*. [Online]. Available: <http://www.nhtsa.gov/FARS>. [Accessed: 22-Dec-2015].
- [153] “National Motor Vehicle Crash Causation Study,” *National Highway Traffic Safety Administration (NHTSA)*. [Online]. Available: [http://www.nhtsa.gov/Data/Special+Crash+Investigations+\(SCI\)/NASS+National+Motor+Vehicle+Crash+Causation+Study](http://www.nhtsa.gov/Data/Special+Crash+Investigations+(SCI)/NASS+National+Motor+Vehicle+Crash+Causation+Study). [Accessed: 22-Dec-2015].
- [154] “Community Road Accident Database,” *European Commission*. [Online]. Available: http://ec.europa.eu/transport/road_safety/specialist/statistics/index_en.htm. [Accessed: 22-Dec-2015].
- [155] “German In- Depth Accident Study,” *VUFO*. [Online]. Available: <http://www.vufo.de/forschung-und-entwicklung/gidas/?L=1>. [Accessed: 22-Dec-2015].
- [156] “ADAC Accident Investigation Study,” *ADAC*. [Online]. Available: <https://www.adac.de/infotestrat/unfall-schaeden-und-panne/Unfallforschung/default.aspx>. [Accessed: 22-Dec-2015].
- [157] “Cooperative Crash Injury Study (CCIS) - Datasets,” *Department for Transport of the United Kingdom*. [Online]. Available: <https://data.gov.uk/dataset/cooperative-crash-injury-study-ccis>. [Accessed: 22-Dec-2015].
- [158] “VOIESUR (Vehicle Occupant Infrastructure Road User Safety Study),” *The French National Research Agency*. [Online]. Available: http://www.agence-nationale-recherche.fr/en/anr-funded-project/?tx_lwmsuivibilan_pi2%255bCODE%255d=ANR-11-VPTT-0007. [Accessed: 22-Dec-2015].
- [159] S. P. Wood, J. Chang, T. Healy, and J. Wood, “The Potential Regulatory Challenges of Increasingly Autonomous Motor Vehicles,” *52nd Santa Clara Law Review*, vol. 4, no. 9, pp. 1423–1502, 2012.